

ANTICIPATORY LOCOMOTOR ADJUSTMENTS DURING WALKING OVER
UNILATERAL OBSTACLES IN ABLE-BODIED PARTICIPANTS

by

Gary Ohanessian

Submitted in partial fulfillment of the requirements
for the degree of Master of Science

at

Dalhousie University
Halifax, Nova Scotia
April 2025

Dalhousie University is located in Mi'kma'ki, the
ancestral and unceded territory of the Mi'kmaq.
We are all Treaty people.

© Copyright by Gary Ohanessian, 2025

Table of Contents

List of Tables	v
List of Figures	vi
Abstract	viii
List of Abbreviations Used	ix
Acknowledgements	x
Chapter 1: Introduction	1
1.1 Statement of the problem	1
1.2 Purpose and significance of the study.....	6
1.3 Specific aims of the study.....	7
1.3.1 Hypotheses.....	7
Chapter 2: Literature Review	10
2.1 Energy as a link between biomechanics and motor control.....	11
2.2 The walking cycle.....	12
2.2.1 Net joint moment and net joint power during walking.....	13
2.2.2 Complementarity of the lower limbs during walking.....	18
2.3 Changes in the walking pattern during obstructed walking.....	20
2.3.1 Strategies to cross over the obstacle	24
2.3.2 Kinematic adaptations during obstructed walking.....	27
2.3.3 Modular organization of muscle activity patterns during obstructed walking	29
2.3.4 Mechanical adaptations during obstructed walking.....	31
2.4 Gaps in the literature.....	34
Chapter 3: Methodology	35
3.1 Ethics.....	35
3.2 Study location	35
3.3 Participants.....	35
3.3.1 Sample size	35
3.3.2 Recruitment.....	35
3.3.3 Inclusion and exclusion criteria	36
3.4 Research design	36
3.4.1 Outcome measures	37

3.4.2	Experimental protocol.....	38
3.5	Measurement and calculations of the outcome variables	42
3.5.1	Kinematic measurements	42
3.5.2	Kinetic measurements	46
3.5.3	Statistical analysis.....	50
Chapter 4: Results.....		51
4.1	Demographic characteristics.....	51
4.2	Total number of trials.....	52
4.3	Crossing leg adaptations to obstructed walking.....	52
4.3.1	Crossing leg average duration.....	52
4.3.2	Crossing leg lower limb joint angles during obstructed walking	53
4.3.3	Crossing leg lower limb joint moments during obstructed walking	56
4.3.4	Crossing leg lower limb joint powers during obstructed walking	58
4.3.5	Crossing leg anticipatory locomotor adjustments.....	60
4.4	Supporting leg adaptations to obstructed walking.....	64
4.4.1	Supporting leg average duration	64
4.4.2	Supporting leg lower limb joint angles during obstructed walking	65
4.4.3	Supporting leg lower limb joint moments during obstructed walking	67
4.4.4	Supporting leg lower limb joint powers during obstructed walking.....	69
4.4.5	Supporting leg anticipatory locomotor adjustments	71
Chapter 5: Discussion		76
5.1	Able-bodied participants' adaptations to obstructed walking.....	77
5.1.1	Mechanisms of elevating the foot higher.....	77
5.1.2	Mechanisms of upward bias of the swing limb	82
5.1.3	Unilateral obstructed walking as a bilateral behaviour.....	88
5.1.4	ALAs complementarity in able-bodied participants.....	90
5.2	Limitations	93
5.3	Future directions	95
Chapter 6: Conclusion		96
References		97
Appendix A: Informed consent form		108
Appendix B: Participant's characteristics form		119

Appendix C: Lysholm Knee Questionnaire	120
Appendix D: Tegner Activity Scale.....	121
Appendix E: Waterloo Footedness Questionnaire-Revised (WFQ-R).....	122
Appendix F: Supplementary material for the methodology section	123
Appendix G: Breakdown of the number of trials	133
Appendix H: ALAs during walking over unilateral obstacles following anterior cruciate ligament reconstruction	134

List of Tables

Table 1. Primary outcome measures.....	37
Table 2. 6 DOF marker set	40
Table 3. Able-bodied participants demographics	51
Table 4. Total and average number of trials	52
Table 5. Summary of the crossing leg energy burst changes observed during the unobstructed and obstructed walking conditions	77
Table 6. Summary of the supporting leg energy burst change observed during the unobstructed and obstructed walking conditions	83
Table 7. Summary of energy bursts complementarity between during unobstructed and obstructed walking conditions	90

List of Figures

Figure 1. Mean net joint power and timing of each muscle power burst during the gait cycle	9
Figure 2. Net joint moment curves and joint power curves of the hip, knee, and ankle during a stride cycle of walking.....	17
Figure 3. Visualization of bilateral and unilateral obstacle placement	23
Figure 4. Toe elevation, greater trochanter (GT) elevation and lower limb flexion as a function of unilateral obstacle heights	27
Figure 5. Changes in angle at the hip, knee and ankle joints as a function of unilateral obstacle height.	29
Figure 6. Net joint powers in the sagittal plane for the trail limb knee joint.	32
Figure 7. Net joint powers in the frontal plane for the trail limb hip joint.	32
Figure 8. Changes in the muscle kinetics during obstructed walking.....	34
Figure 9. 6 DOF markerset	39
Figure 10. Experimental procedure.....	41
Figure 11. Lower body local coordinate systems.....	43
Figure 12. Calculating the CoM and Mass-moment of Inertia of the segments	45
Figure 13. Average duration of the crossing leg gait cycle as a function of unilateral obstacle height.	53
Figure 14. The ensemble average of the joint angles of the crossing legs during unobstructed and unilateral obstacles walking conditions.....	55
Figure 15. The ensemble average of the net joint moments of the crossing legs during unobstructed and unilateral obstacles walking conditions.....	57
Figure 16. The ensemble average of the net joint powers of the crossing legs during unobstructed and unilateral obstacles walking conditions.....	59
Figure 17. Mean selected muscle power bursts of the crossing leg as a function of unilateral obstacle height	60
Figure 18. Average duration of the supporting leg gait cycle as a function of unilateral obstacle height	64

Figure 19. The ensemble average of the joint angles of the supporting legs during unobstructed and obstructed walking conditions	66
Figure 20. The ensemble average of the net joint moments of the supporting legs during unobstructed and obstructed walking conditions	68
Figure 21. The ensemble average of the net joint powers of the supporting legs during unobstructed and obstructed walking conditions	70
Figure 22. Mean selected muscle power bursts of the supporting legs as a function of unilateral obstacle height	71
Figure 23. Mean selected ankle muscle power bursts of the supporting legs as a function of unilateral obstacle height	75

Abstract

Walking control was assessed by investigating the changes in net joint power while going over unilateral obstacles placed in the plane of progression. Participants performed obstructed walking trials across seven different obstacle heights (0 to 60 cm) while kinematic and kinetic data were collected. Anticipatory locomotor adjustments (ALA) were observed in both crossing and supporting legs. Notably, there were significant adjustments in the supporting leg with the emergence of a plantar flexor energy generation phase, accompanied by an increase in hip extensors energy generation at the onset of the stance phase for higher obstacles. Furthermore, a complementarity in the power bursts of the crossing leg muscles was noted. Specifically, the left leg exhibited a greater pulling motion at the knee due to an enhanced knee flexor energy generation. This thesis contributes to a greater characterization of ALA to unilateral obstacles and provides some evidence about the complementarity of these adjustments.

List of Abbreviations Used

HAT	Head, arms and trunk
GC	Gait cycle
ALA	Anticipatory locomotor adjustments
H1	Hip extensors energy generation
H2	Hip flexors energy absorption
H3	Hip flexors energy generation
H1F	Hip abductors energy absorption
H2F	Hip abductors energy generation
H3F	Hip abductors energy generation
H4F	Hip adductors energy absorption, hip abductors energy generation
K1	Knee extensors energy absorption
K2	Knee extensors energy generation
K3	Knee extensors energy absorption
K4	Knee flexors energy absorption
K5	Knee flexors energy generation
A1	Ankle plantar flexors energy absorption
A1G	Ankle plantar flexors energy generation
A1A	Ankle plantar flexors energy absorption
A2	Ankle plantar flexors energy generation
ACL	Anterior cruciate ligament
ACLR	Anterior cruciate ligament reconstruction
ADL	Activities of the daily living
RTS	Return to sports
CNS	Central nervous system
BOS	Base of support
CoM	Center of mass
GRF	Ground reaction forces
GT	Greater trochanter
95% CI	95% confidence interval
SL	Supporting leg
CL	Crossing leg
L/RSL	Left/right supporting leg
L/RCL	Left/right crossing leg
cm	Centimeter
m	Meter
OA	Osteoarthritis
EMG	Electromyography

Acknowledgements

I would like to express my deepest gratitude to my supervisor, Dr. Michel Ladouceur, for his invaluable guidance, unwavering support, and insightful feedback throughout this journey. His expertise, patience, and encouragement have been instrumental in shaping this work, and I am truly grateful for the opportunity to learn under his supervision.

I would like to sincerely thank my committee members sincerely, Dr. Scott Landry, Dr. Derek Rutherford, and Dr. Christopher MacLean, as well as my external reader, Dr. David Westwood, for their valuable time, thoughtful feedback, and constructive suggestions. Their diverse perspectives and academic insights have greatly enriched my research and contributed significantly to the quality of this work.

My thanks go to everyone in the BENlab at Dalhousie for their support and accommodation. I am grateful to my lab mates, Dylan Sutherland, Connor Stadnyk and Afarin Kebritchi, for their unwavering support and shared experiences that helped us navigate this journey together. Their kindness, collaboration, and positive energy were crucial in getting me through this challenging time

To my family and friends back home, thank you for your endless love, encouragement, and emotional support. Even from afar, your presence has been a constant source of strength and comfort throughout this journey. Your calls, messages, and thoughtful check-ins reminded me I was never alone, even in the toughest moments. I am deeply grateful for your sacrifices, understanding, and unwavering belief in me. I would also like to extend a heartfelt thank you to my aunt, Rihab Saad, whose kindness,

wisdom, and quiet strength have been a guiding light. Khalto, your words of encouragement and genuine care have meant the world to me, and your support has brought me comfort in so many ways. I would also like to acknowledge my uncle, Joe Saad, whose constant support and comforting presence made my life in Canada much easier. His generosity, encouragement, and steady help have meant more than words can express.

To my wonderful mother, Rhea Saad, my supportive father, Hovig Ohanessian, and my loving partner, Patil Agopian, thank you all for being my greatest sources of strength throughout this journey. Mom, your unconditional love, prayers, and constant support have been a guiding light; I carry your strength with me every day. Dad, your quiet strength and belief in me have always been a foundation of stability. Pat, your patience, encouragement, and unwavering belief in me helped me stay grounded through the toughest moments. I am endlessly grateful for your love and understanding. This accomplishment reflects the support, sacrifices, and faith you all have given me, and I share it wholeheartedly with you.

Lastly, a slightly exasperated thanks to Manchester United FC for consistently making this journey even more stressful than needed. Supporting you through this thesis may have been the toughest challenge of all.

Chapter 1: Introduction

1.1 Statement of the problem

Walking is a common human movement that is characterized by coordinated motion of the limbs in order to go from one place to another (Winter, 1987). Furthermore, the purpose of gait analysis is to record a person's walking pattern, interpret and assess these biomechanical measurements, as well as report the presence of any gait dysfunction (D'Août et al., 2022; Kharb et al., 2011). Four major components are being controlled during gait: a) supporting the body weight; b) maintaining balance of the head, arms and trunk (HAT); c) generating and absorbing energy during different stages of the gait cycle; and d) controlling the foot's trajectory during the swing phase (Barbeau et al., 1999; Nashner, 1980, 1982; Winter, 1983a, 1983b, 1987).

Human gait is a cyclical movement, where the cycle is delineated by the start and end points of foot contact with the ground. This cycle is characterized by two phases: the stance phase, during which the leg is in contact with the floor, and the swing phase, during which the foot moves forward to prepare for the next ground contact. While joint moments have traditionally been emphasized in walking research, joint power offers a more comprehensive and additional evaluation of gait mechanics as it refers to the energy flow of muscle groups (Zajac et al., 2002, 2003) providing information on how the nervous system adapts to external constraints (Latash, 2016). Stereotypical patterns of energy generation and absorption have been demonstrated during walking (Allard et al., 1996; Eng and Winter, 1995; Sadeghi et al., 1997). A brief description of the pattern, sorted by lower limb joint and its labels, follows.

From the sagittal plane point of view, during the stance phase, an initial generation of energy by the hip extensors (miometric contraction, H1) manages the forward motion of the leg (Winter, 1987). It is followed by a pliometric contraction of the hip flexors (absorption of energy, H2) to control the backward motion of the thigh (Winter, 1987). Lastly, a miometric contraction of the hip flexors (generation of energy, H3) propels the lower limb forward at the initiation of the swing phase (Sloot and van der Krogt, 2018; Winter, 1987). In the frontal plane, the hip abductors would initially absorb energy through a pliometric contraction (absorption of energy, H1F) to support and control the slight drop of the contralateral limb (Eng and Winter, 1995). This is followed by two miometric contractions of the hip abductors (generation of energy, H2F and H3F) that serve to control and raise the pelvis (Eng and Winter, 1995). Lastly, there is a pliometric contraction of the hip adductors (absorption of energy, H4F) that is speculated to control the lower limb advancement during the swing phase since this variable has not been reviewed in the literature.

At the knee, an initial absorption of energy by the knee extensors (pliometric contraction, K1) is present to control knee collapse (Winter, 1987). This is followed by the only generation of energy by the knee extensors (miometric, K2) during walking (Winter, 1987). There is an absorption of energy by the knee extensor at the end of the stance phase/early swing phase (pliometric contraction, K3) to control the knee flexion during the swing phase (Winter, 1987). Furthermore, there is a pliometric contraction of the knee flexors at the end of the swing phase (absorption of energy, K4) to control the lower leg velocity in anticipation of the next foot contact (Winter, 1987).

At the ankle, during the first part of the stance phase, there is an absorption of energy by the plantar flexors (pliomeric contraction, A1) to control the velocity of the centre of mass (Winter, 1987). This is followed by a plantar flexor generation of energy (miometric contraction, A2) at the end of stance to propel the body forward (Sloot and van der Krogt, 2018; Winter, 1987).

The four control variables in walking consist of generating and absorbing energy during key phases of the gait cycle, controlling the foot trajectory during the swing phase, and balancing the HAT and supporting the body weight (Barbeau et al., 1999; Nashner, 1980, 1982; Winter, 1983a, 1983b, 1987) can be assessed through different tasks. An example could be placing an obstacle in the walking path, which challenges walking control by altering the foot trajectory during the swing phase (Barbeau et al., 1999; McFadyen and Winter, 1991; Patla et al., 1991). Additionally, this adaptation of the foot trajectory requires a change in the energy flow during the gait cycle and may necessitate adjustments to maintain the balance of the HAT (McFadyen and Winter, 1991). These crucial changes during walking, associated with adaptations to the environment, have been labeled anticipatory locomotor adjustments (ALA) (McFadyen et al., 1993). Unilateral and bilateral obstacles have been used to elicit ALAs, with bilateral obstacles being more common in the literature (McFadyen et al., 1993; McFadyen and Prince, 2002; Patla et al., 1991; Patla and Rietdyk, 1993). Even though the objective is similar for both types (cross over the obstacle), there are differences in their ALAs (Ladouceur et al., 2005; McFadyen et al., 1993; McFadyen and Prince, 2002; Winter et al., 1991).

Previous studies (McFadyen et al., 1993; Winter et al., 1991) using low-height (0.1m) unilateral obstacles have shown ALAs occurring at the end of the stance/early

swing phase of the leg going over the obstacle (crossing leg in contrast to the supporting leg that is contacting the ground) consisting of: a) reduced energy absorption by the knee extensors (pliometric contraction, K3) at the end of the stance phase, b) a reduced energy generation by the hip flexors (miometric contraction, H3), and c) the emergence of a new generation of energy by the knee flexors (miometric contraction, K5) during the swing phase (McFadyen et al., 1993; Winter et al., 1991). A study using obstacles of greater heights (up to 0.6m) has shown that in addition to the ALAs presented above, there was an increase in the height of the greater trochanter while going over the obstacles (Ladouceur, 2025).

A study (McFadyen and Prince, 2002) using low-height (0.1m) bilateral obstacles showed similar unilateral obstacle ALAs for the leading limb (first leg over the obstacle) with: a) the emergence of a knee flexors energy generation (K5) and b) a decrease of the knee extensors energy absorption (K3). However, in contrast to unilateral obstacles, the hip flexors generation of power (H3) was increased. In addition, the hip abductor absorption of energy at the end of the stance phase (H3F) remained constant, but there was increased greater trochanter elevation (“hip hiking”) due to increased vertical hip power (McFadyen and Prince, 2002). This study also reported on the trailing limb (second leg over the obstacle) and showed: a) the emergence of a knee flexors energy generation (K5) that was more prominent than for the leading limb, b) a decrease of the knee extensors energy absorption (K3), c) a tendency to decrease for the hip flexors energy generation (H3), d) a reduction of the hip abductors energy generation (H3F) and e) more “hip hiking”. In contrast to the leading limb, there was a decrease in the hip abductors energy absorption at the start of the stance phase (H1F) (McFadyen and Prince,

2002). Furthermore, it has been suggested that bilateral obstacles require greater modifications of the energy generation and absorption pattern, greater foot trajectory, body weight support and upper body postural control adjustments (Barbeau et al., 1999; Ladouceur et al., 2005). As such, a unilateral obstacle may provide a better assessment of the control strategies during the adaptation of the foot trajectory during the swing phase.

For such a complex task as going over unilateral obstacles that separate the right and left legs, a common concern could be the complementarity and the presence of lateralization (preferential use of one limb in voluntary motor acts (Boucher, 1993; DeVita et al., 1991; Engsberg et al., 1991; Peters, 1988; Sadeghi et al., 2000)) of the lower limbs in contributing to the success of this task. In the past, gait symmetry was assumed as a means of simplifying data collection and analysis, with researchers acquiring data for one limb or using the average of both (Eng and Winter, 1995; Hannah et al., 1984; Milner et al., 1971; Ounpuu et al., 1991; Yang and Winter, 1985). A spectrum of results have been reported when symmetry was specifically tested. Some studies found no ground reaction forces and energy efficiency asymmetries (Chou et al., 1995; Hamill et al., 1984; Hesse et al., 1997; Wall and Turnbull, 1986), while other studies revealed spatiotemporal (Allard et al., 1996; Chodera, 1974; Chodera and Levell, 1973), muscular activations (soleus and rectus femoris), and kinetic measurements (such as ground reaction forces) difference (Arsenault et al., 1986; Dickey and Winter, 1992; Ounpuu et al., 1991; Sadeghi et al., 2000). To investigate the complementarity of the lower limbs during walking, a review of these findings has resulted in the suggestion that one limb is responsible for propulsion and forward movement while the other is responsible for support and control during gait (Hirsawa, 1981 referenced in Hirokawa, 1989; Sadeghi et

al., 1997). The limb with a propulsion function was characterized by strong hip powers at the end of the stance phase (i.e. the hip flexors energy generation (H3S) and the hip abductors energy generation (H3F)). This would contrast with the limb responsible for support and control, which would be characterized by power bursts spread throughout the stance phase (i.e. the hip extensors energy generation (H1), the knee extensors energy generation (K2), and the knee extensors energy absorption (K3)) (Sadeghi et al., 1997).

1.2 Purpose and significance of the study

The purpose of this study was to analyze how able-bodied participants adapt to an external constraint, such as the addition of a unilateral obstacle on the walking pathway. This constraint increases the body's demand to maintain control while going over the obstacle (Barbeau et al., 1999; McFadyen and Winter, 1991; Patla et al., 1991). To better understand how the nervous system interacts with, and adapts to such a constraint, the study included a detailed analysis of joint power during unilateral obstructed walking in able-bodied participants. Though this topic has been assessed in bilateral (MacLellan, 2017; McFadyen et al., 1993; McFadyen and Prince, 2002; Niang and McFadyen, 2004) and unilateral obstacles (Ladouceur et al., 2005; McFadyen et al., 1993; McFadyen and Winter, 1991), the present study investigated kinematic and kinetic adaptations occurring on both the supporting and crossing legs during unilateral obstructed walking at heights as high as 60 centimeters (cm). In addition to evaluating how able-bodied individuals adapt to obstructed walking, the complementarity of the lower limbs during this task is also assessed. Obstructed walking offers a challenge that requires a modification of the normal walking pattern (MacLellan, 2017; MacLellan and McFadyen, 2013; McFadyen et al., 1993; McFadyen and Carnahan, 1997; McFadyen and Prince, 2002; McFadyen and

Winter, 1991; Niang and McFadyen, 2004; Patla et al., 1991; Patla and Prentice, 1995; Patla and Rietdyk, 1993). Using unilateral obstacles provides an experimental situation where the control of the foot trajectory and the associated control of the balance of the HAT can be decoupled (McFadyen et al., 1993; McFadyen and Winter, 1991; Patla et al., 1991; Patla and Rietdyk, 1993; Winter et al., 1991).

1.3 Specific aims of the study

This study aimed to perform a comprehensive analysis of ALAs during obstructed walking in able-bodied individuals.

The specific aims were:

- a) to identify the bilateral ALAs of able-bodied participants during walking over unilateral obstacles of increasing heights.
- b) to identify if there is a lateralization of the ALAs of able-bodied participants during walking over unilateral obstacles of increasing heights.

1.3.1 Hypotheses

The following hypotheses were tested to answer the first specific aim: to identify the bilateral ALAs of able-bodied participants during walking over unilateral obstacles of increasing height. Figure 1 summarizes the different muscle power bursts and their timing in relation to crossing the obstacle.

- a) The crossing leg muscle power bursts associated with the ALAs would be modulated as a function of obstacle heights in the following manner:
 - a. The knee flexor muscles generation of energy at the initiation of swing (K5) would increase with increasing obstacle heights.

- b. The knee extensor muscles absorption of energy at the initiation of swing (K3) would decrease with increasing obstacle heights.
 - c. The hip flexor muscles generation of energy at the initiation of swing (H3) would decrease with increasing obstacle heights.
 - d. The hip abductor muscles generation of energy at the end of the stance phase (H3F) would decrease with increasing obstacle heights.
- b) The supporting leg muscle power bursts associated with the ALAs would be modulated as a function of obstacle heights in the following manner:
- a. The hip abductor muscles absorption of energy at the start of the stance phase (H1F) would decrease with increasing obstacle heights.

The following hypotheses were tested to answer the second specific aim, which consists of identifying the lateralization of the bilateral ALAs of able-bodied participants during walking over unilateral obstacles of increasing height.

- a) There were no differences between the right and left leg ALAs of able-bodied participants walking over unilateral obstacles of increasing heights. The ALAs muscle burst are defined as:
- a. The crossing leg knee flexor muscles generation of energy at the initiation of swing (K5).
 - b. The crossing leg knee extensor muscles absorption of energy at the initiation of swing (K3).
 - c. The crossing leg hip flexor muscles generation of energy at the initiation of swing (H3).

- d. The crossing leg hip abductor muscles generation of energy at the end of the stance phase (H3F).
- e. The supporting leg hip abductor muscles absorption of energy at the start of the stance phase (H1F).

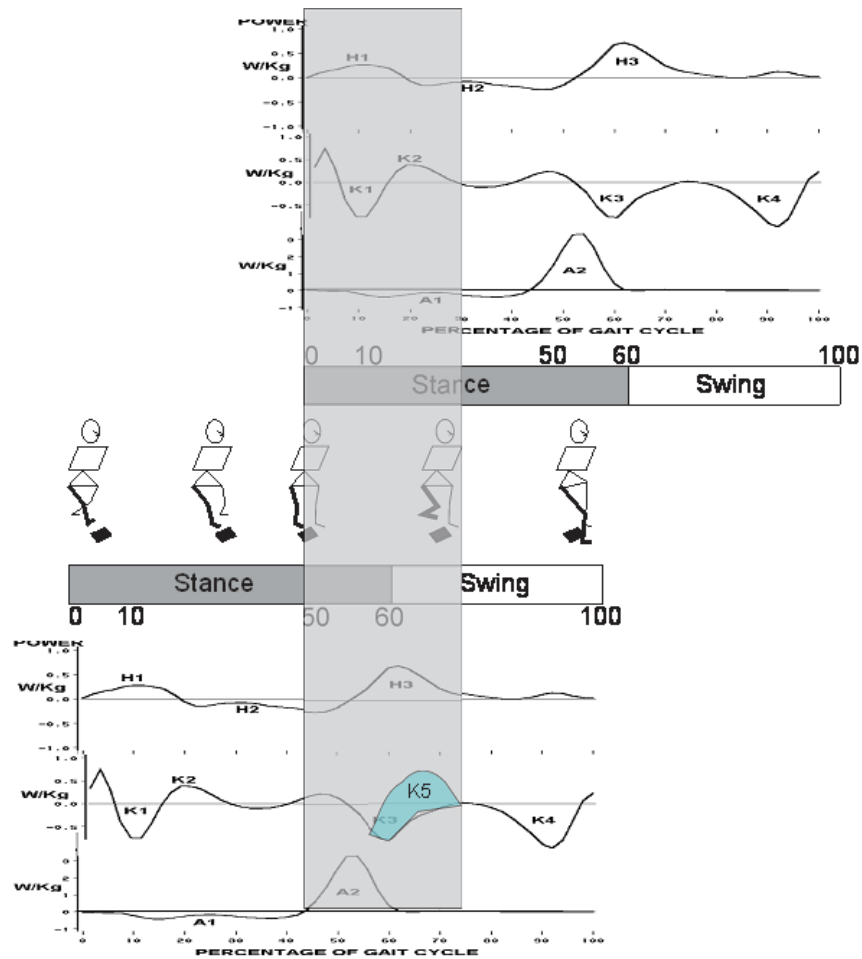


Figure 1. Mean net joint power and timing of each muscle power burst during the gait cycle (Adapted from (Winter, 1987)). The top figure represents the behaviour of the supporting leg, while the bottom figure depicts the behaviour of the crossing leg. Outcome measures in the sagittal plane of the supporting leg include H1, H2, K1, K2, and A1 muscle power bursts. Outcome measures in the sagittal plane of the crossing leg comprise H3, K3, K5, K4, and A2 muscle power bursts. The grey rectangle indicates the timing in which the task of obstructed walking is occurring.

Chapter 2: Literature Review

The study of walking control can be enhanced by introducing perturbations, such as unilateral obstacles, that challenge the body's ability to control the foot trajectory during the swing phase and maintain balance during the movement. By examining gait under such conditions, we gain insights into the body's dynamic responses to external disturbances and better understand the impact of these challenges on overall gait performance.

This literature review will consist of sections on energy as the link between biomechanics and motor control (section 2.1), the walking cycle (section 2.2), and adaptations to the walking cycle during obstructed walking (section 2.3).

Gait is a fundamental aspect of human movement that involves the coordinated movement of limbs during locomotion (D'Août et al., 2022; Kharb et al., 2011). Barbeau et al. (1999) proposed that the body must simultaneously control multiple variables and tasks while walking to ensure proper function. These tasks include a) supporting body weight, b) maintaining balance of the head, arms, and trunk (HAT), c) generating and absorbing energy during different stages of the gait cycle, and d) controlling the foot's trajectory during the swing phase (Barbeau et al., 1999). The central nervous system (CNS) controls these functions using three key neurological subsystems: a) one that generates the basic movement synergy, b) one that controls equilibrium during propulsive movement, and c) one associated with the adaptation to behavioural goals and external constraints, ensuring that each component of the gait cycle is appropriately executed (Barbeau et al., 1999; Forssberg, 1982). These factors are all critical for enabling smooth walking and maintaining stability, as these neurological subsystems integrate intended

motor commands with sensory feedback from the periphery, vestibular and visual inputs to produce the appropriate force patterns at each joint (Winter, 1987).

2.1 Energy as a link between biomechanics and motor control

Understanding the neural control of movement is complex (Latash, 2016). To better understand how the musculoskeletal system and the nervous system interact, biomechanics serves as an effective tool to bridge these two systems, as investigating the reasons behind our movement can shed light on how the CNS organizes motor control (Latash, 2016). Additionally, the concept of synergy has been studied to investigate motor coordination, which refers to the neural organization to maintain stability while performing tasks (Latash, 2016; Scholz and Schöner, 1999). This concept helps stabilize performance in the face of external constraints (Latash, 2016), that could be in the form of an obstacle during walking (McFadyen et al., 1993; McFadyen and Carnahan, 1997; McFadyen and Prince, 2002; McFadyen and Winter, 1991; Niang and McFadyen, 2004).

Walking is a cyclic motion of the body that requires coordinated action from multiple systems, like the musculoskeletal and central nervous system (Zajac et al., 2002). A key concept revolves around understanding muscle synergies, which are defined as patterns of muscle activity that work together to produce coordinated movement (Zajac et al., 2003). As part of a dynamic process and to minimize effort, muscles can redistribute energy between the segments to maintain forward movement (Zajac et al., 2002), a task unobtainable by one muscle alone (Zajac et al., 2002). Simulation models revealed that a uni-articulate muscle like the soleus, a muscle that aids in ankle plantar flexion, also plays a role in decelerating the thigh and accelerating the trunk, both segments to which the soleus does not attach (Zajac et al., 2002). As such, investigating

the net joint power, which is the derivative of energy, will expand the understanding of the behaviour of walking.

2.2 The walking cycle

Walking can be described using kinematic and/or kinetic variables. Kinematic variables focus on the spatiotemporal aspects of the motion of body segments like a) step and stride length, b) cadence and stride time, c) segment positions, velocities, and accelerations, and d) joint angles (Winter, 1987). Kinetic variables, on the other hand, provide a deeper insight into movement by considering the forces and moments responsible for its kinematics (Winter, 1987). Measuring and estimating/calculating kinetic variables, like net joint moment and net joint power, is crucial to understanding how the body controls walking (Barbeau et al., 1999; Latash, 2016; Winter, 1987; Zajac et al., 2002, 2003).

Net joint moment refers to the rotational forces generated by muscles, ligaments, and connective tissues around a joint (Sloot and van der Krogt, 2018). These moments are responsible for causing the rotation of body segments during walking. On the other hand, net joint power refers to the energy flow between muscle groups around the joint, which is essential for all movement (Winter, 1987). Without energy flow, motion would not occur (Winter, 1987). Net joint power is a more comprehensive measure of gait mechanics, offering more profound insight into how energy is managed and transferred during walking (Latash, 2016; Zajac et al., 2002, 2003). Net joint power is characterized by three key energy states: a) positive power, where energy is generated as muscles shorten, b) negative power, where energy is absorbed as muscles lengthen, and c) transfer of power, where energy is transferred as muscles do not change length (Robertson and

Winter, 1980). These energy states are critical for generating forward motion and maintaining stability during walking. Estimating energy flow by calculating the net joint power gives strong evidence of the mechanisms of energy transfer and conservation that our neural control recognizes and may be optimizing (Winter, 1987).

By analyzing the net joint moment and the net joint power, we can better understand how joint rotation changes affect overall walking behaviour, offering valuable insights into the underlying mechanics of gait (Winter, 1987). Kinetic variables such as net muscle moment and net joint power are critical in assessing and correcting steady and disturbed gait imbalances (McFadyen and Winter, 1991; Zajac et al., 2002, 2003). For example, net joint power is particularly valuable in assessing pathological gait, as it helps distinguish how energy flow is altered in individuals with gait abnormalities (Winter, 1987). This analysis can inform interventions to restore balance, improve gait, and enhance efficiency.

2.2.1 Net joint moment and net joint power during walking

A complete gait cycle consists of one stride and two steps (Winter, 1987). It is characterized by a stance phase, which makes up 60% of the cycle and is defined as the period when the leg is in contact with the ground. It is further divided into heel strike (initial stance phase), mid stance, and push-off phases (Winter, 1987). The remaining 40% is the swing phase, during which the leg is elevated and preparing for ground contact. It can be divided into early, mid-swing, and late swing phases (Winter, 1987).

Figure 2, and the description of the energy bursts during the walking cycle, is a collection of data from two different studies (Bovi et al., 2011; Eng and Winter, 1995). The net sagittal and frontal plane joint moments (first and third columns, respectively)

and the net sagittal plane joint powers (second column) were extracted from a normative dataset of 20 able-bodied adults (Bovi et al., 2011). Lastly, the net frontal plane hip joint power time history curve (fourth column) was extracted from a dataset of nine able-bodied subjects (Eng and Winter, 1995). The following sections will describe the net joint moment and net joint power during walking for each sub-phase of the gait cycle.

The initial contact and loading response phase begin when the heel touches the ground and continues until the foot is fully flat. Initially, the ankle starts in a neutral position and then moves into approximately 15 degrees of plantar flexion. This motion is controlled by a net dorsiflexion joint moment generated by the pliometric contraction of the ankle dorsiflexors, which counterbalances the plantar flexion caused by the ground reaction force and gravity (Winter, 1987). At the knee, a brief internal flexion moment occurs with the pliometric contraction of the knee extensors, helping to control the impact during weight acceptance as the heel strikes the ground. This results in the absorption of energy by the knee extensors (K1) (Winter, 1987). The hip joint generates power through a miometric contraction of the hip extensors, which aids in managing the forward motion of the thigh. This results in energy generation by the hip extensors (H1) (Winter, 1987). Concomitantly, in the frontal plane, the hip joint absorbs energy through a pliometric contraction of the hip abductors to maintain the pelvis level. This results in energy absorption by the hip abductors (H1F) (Eng and Winter, 1995).

The midstance phase begins when the foot is flat on the ground and continues until just before heel-off. At the ankle, the plantar flexors undergo pliometric contraction to control the acceleration of the shank. This results in the absorption of energy by the plantar flexors (A1) (Winter, 1987). At the knee, the knee extensors exert a miometric

contraction to initiate an extension moment. This results in the generation of energy by the knee extensors (K2) (Winter, 1987). At the hip, the joint continues to extend until just before push-off, at this point, the hip flexors undergo a pliometric contraction, creating a flexion moment. This helps control the backward motion of the thigh and results in the absorption of energy by the hip flexors (H2) (Winter, 1987). In the frontal plane, the hip abductor generates a pliometric contraction to help control the pelvis during this gait cycle phase. This results in the generation of energy by the hip abductors (H2F) (Eng and Winter, 1995).

The terminal stance and pre-swing phase spans from heel-off to toe-off. During this period, an ankle plantar flexion moment is generated by the miometric contraction of the ankle plantar flexors, propelling the body upward and forward (Sloot and van der Krogt, 2018; Winter, 1987). This results in the generation of energy by the ankle plantar flexors (A2) (Winter, 1987). At the knee, a pliometric contraction of the knee extensors creates a knee extension moment, preventing knee collapse. This results in the absorption of energy by the knee extensors (K3) (Winter, 1987). A miometric contraction from the hip flexors results in the generation of energy by the hip flexor (H3) and is considered the second-largest contribution of propulsive power during the gait cycle (Sloot and van der Krogt, 2018).

Small moments are exerted at all three joints during the swing phase (see Figure 2) except toward the terminal swing phase. At this point, a net knee flexion moment is generated through a pliometric contraction of the knee flexors to help control the forward acceleration of the shank. This results in the absorption of energy by the knee flexors (K4) (Winter, 1987). Additionally, a net hip extension moment is produced through a

plometric contraction to control the forward acceleration of the thigh. This results in a slight energy absorption by the hip extensors (no labels). In the frontal plane, a net abductor muscles joint moment is generated at the hip and knee joints to help stabilize the joints. This results in the generation of energy by the hip abductors (H3F) (Eng and Winter, 1995). In addition, a net adductor muscle joint moment is generated at the hip to control the pelvis during the swing phase. This results in the absorption of energy by the hip adductors, which were not labelled in Eng and Winter (1995) but will be labelled as H4F in this thesis.

Maintaining pelvic control during walking is crucial for overall balance, as it supports the weight of the head and trunk (Neumann, 2016). When the heel strikes the ground, the pelvis on that side rotates forward, causing internal thigh rotation, which is counterbalanced by the hip external rotators to keep the foot aligned (Neumann, 2016). As the body transitions into a single-leg stance, the pelvis on the swing side tends to drop due to gravity, a movement the hip abductors control to stabilize the pelvis and trunk (MacKinnon and Winter, 1993; Neumann, 2016). If these muscles are weak, the trunk may lean toward the stance side to reduce the load on the hip abductors (Neumann, 2016). Additional muscles, such as the quadratus lumborum and hip extensors, assist in maintaining pelvic and trunk stability (Neumann, 2016). These coordinated movements help limit excessive vertical and lateral shifts in the body's center of mass.

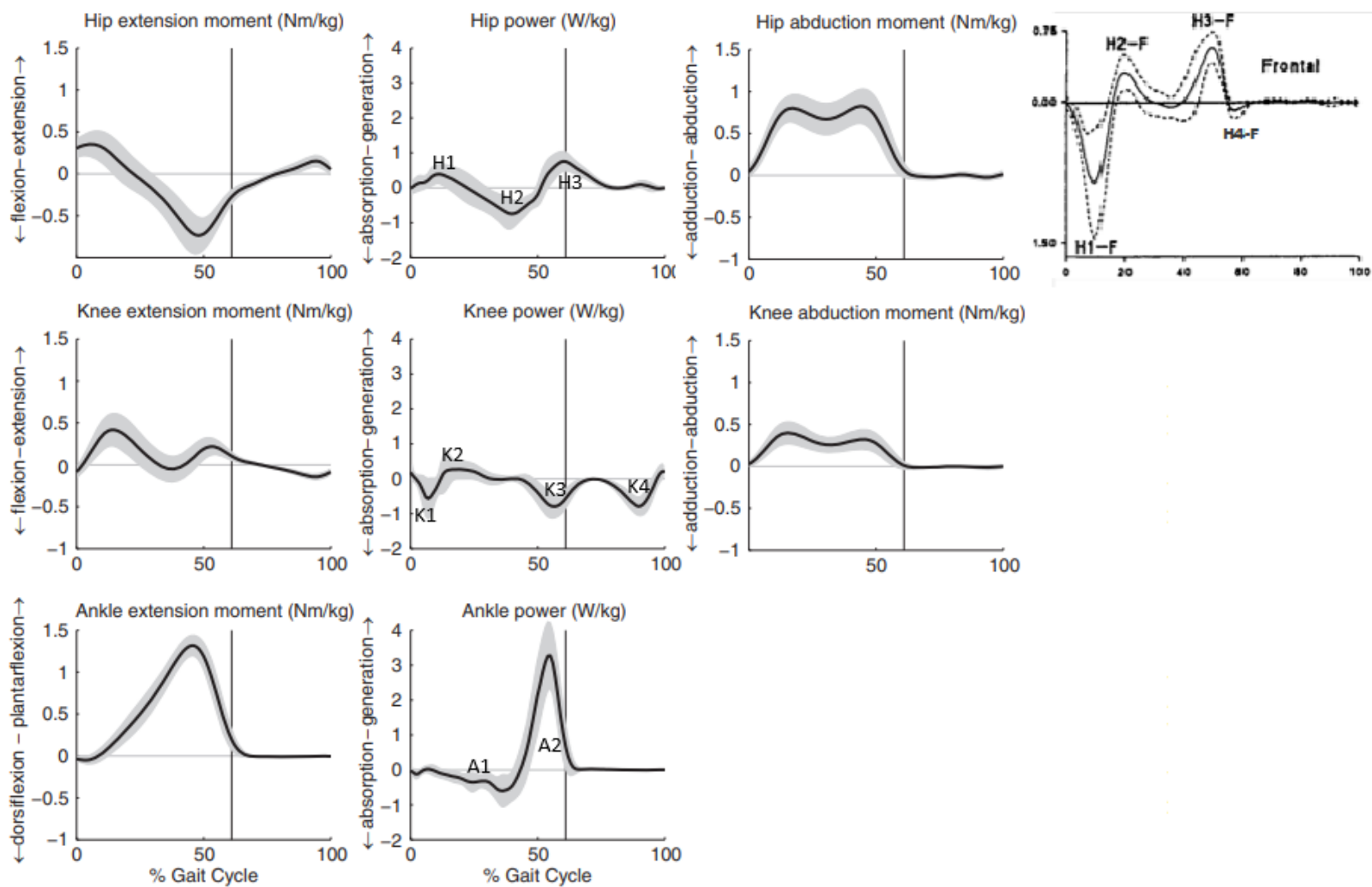


Figure 2. Net joint moment curves and joint power curves of the hip, knee, and ankle during a stride cycle of walking. From a normative dataset of 9, 13 and 20 able-bodied adults (Adapted from (Bovi et al., 2011; Eng and Winter, 1995)). The solid line represents the mean value, the band/dashed lines represent the standard deviation.

2.2.2 Complementarity of the lower limbs during walking

In the past, researchers assumed gait symmetry to simplify data collection and analyses of walking. As a result, many gait studies relied on data from single leg or averaged data from both lower limbs (Eng and Winter, 1995; Hannah et al., 1984; Milner et al., 1971; Ounpuu et al., 1991; Yang and Winter, 1985).

Studies that investigated lower limb asymmetries during walking found that temporal and kinematic factors, such as velocity (Baker and Hewison, 1990), joint motion during walking among all three planes of the hips and the sagittal plane of the knees (Hannah et al., 1984), the three components of the ground reaction forces (Hamill et al., 1984), the energy efficiency between both limbs were reported to be symmetrical (Chou et al., 1995). These studies supported the notion that limbs had symmetrical actions during gait (Hesse et al., 1997; Wall and Turnbull, 1986).

In contrast, other studies revealed asymmetries in some spatiotemporal variables (step and stride length, foot placement angle), maximum knee flexion (Allard et al., 1996; Chodera, 1974; Chodera and Levell, 1973), ground reaction forces (Herzog et al., 1988, 1989), and hip joint work (Dickey and Winter, 1992). Furthermore, the electromyography (EMG) of selected muscles have also been reported to be asymmetrical (Ounpuu and Winter, 1989). More specifically, the EMG amplitude profiles of the soleus and rectus femoris showed differences between limbs (Arsenault et al., 1986).

Furthermore, the complementarity of the functional actions of the lower limb has been suggested as locomotion aims to propel the body forward while supporting it against gravity (Winter, 1991). It has been suggested that the right leg was primarily responsible for propulsion and forward movement, while the left leg provided support and control

(Hirasawa, 1981, as referenced in Hirokawa, 1989). By using a Principal Component Analysis to determine functional gait asymmetry, Sadeghi et al (1997) associated the hip flexors energy generation (H3S), the hip abductors energy generation (H3F), the hip external rotator energy generation (H2T)), and the knee extensors energy absorption (K1S) with propulsion during the push-off period (Sadeghi et al., 1997; Schache et al., 2007). Furthermore, the hip extensors energy generation (H1S), the hip internal rotators energy absorption (H1T), the knee extensors energy generation (K2S), the knee extensors energy absorption (K3S), the knee abductors energy generation (K1F), and the knee external rotators energy absorption (K2T) were associated with support throughout the stance phase (Sadeghi et al., 1997). Lastly, Sadeghi et al. (1997) identified five muscle energy bursts that differed between the two lower limbs in a sample of a right-footed participant. For the left limb, there were differences in hip abductors energy absorption (H1F) at heel strike, the knee abductors energy generation (K1F), the knee extensors energy generation (K2S) at mid-stance, and the knee extensors energy absorption (K3S) at push-off, suggesting a role in the control or stabilizing actions of the limb (Sadeghi et al., 1997). For the right limb, there was only a difference in the hip flexors energy generation (H3S) at push-off which could be linked to a propulsive function (Sadeghi et al., 1997). Sadeghi's study (Sadeghi et al., 1997) had two main issues with all the participants being classified as right footed and participants walked with crossed arms over their chest. This restriction in the movement of the upper limbs might affect results since asymmetrical arm action has the potential to contribute to asymmetry elsewhere in the body (Hinrichs, 1992).

One of the questions that arises from the lower limb complementarity during walking is whether the dominant leg is used for mobility and propulsion, while the non-dominant leg is used for postural control or stabilizing actions (Sadeghi et al., 2000). A study by Ounpuu and Winter (1989) has shown a higher neural drive to the plantar flexors of the dominant leg, as established by the Harris test of lateral dominance (Harris, 1955), which would be related to the propulsive role of the dominant leg (Ounpuu and Winter, 1989). Moreover, the dominant side contributed around 60% of the total positive work during walking, which was higher than the non-dominant side (DeVita et al., 1991).

2.3 Changes in the walking pattern during obstructed walking

The examination of fundamental locomotor patterns has progressed through investigations utilizing animal models, such as in cats (Drew, 1993; Forssberg et al., 1980). These investigations propose that the spinal cord encompasses essential circuits capable of generating locomotor-like activity, thereby coordinating muscle movements in the respective body segments. Although anecdotal evidence suggests the potential presence of analogous spinal networks in humans (Calancie et al., 1994; Minassian et al., 2017), direct evidence quantifying these circuits in the human population remains lacking. Nevertheless, it is plausible to suggest that such spinal networks may be conserved across species due to evolutionary continuity (McFadyen and Carnahan, 1997).

Understanding the control mechanisms involved in walking requires more than observing stereotypical locomotor patterns; it demands evaluative tasks that introduce perturbations to walking. These perturbations, such as changes in speed, direction, or surface slope, provide valuable insight into the body's ability to absorb and generate energy at key points in the gait cycle (Barbeau et al., 1999; Kuster et al., 1995; Winter,

1983). Another effective method to evaluate locomotor control is by introducing obstacles, which require controlling foot trajectory adjustments during the swing phase (McFadyen et al., 1993, 1994; McFadyen and Prince, 2002; McFadyen and Winter, 1991; Niang and McFadyen, 2004; Patla et al., 1991; Patla and Rietdyk, 1993).

These basic locomotor responses, also termed as ALAs, do not result in entirely new movement patterns. Instead, they reflect modifications of a basic locomotor pattern (McFadyen et al., 1993; McFadyen and Carnahan, 1997; Niang and McFadyen, 2004). Fundamental walking patterns themselves are regulated by central pattern generators (CPGs), intricate spinal neural networks responsible for producing rhythmic gait activity (Grillner, 2006; Kiehn, 2006). These CPGs are thought to consist of two layers: a rhythm generator network, which manages the timing of the gait cycle, and a pattern formation network, which organizes the spatiotemporal muscle activations (Aoi and Funato, 2016; Patla, 1985; Shevtsova and Rybak, 2016).

However, in the presence of perturbations, like obstacles, supraspinal structures are needed to modify the basic CPG-driven patterns. Animal studies have provided key insights into this process. In cats, for example, motor cortex activity increases when they step over obstacles, suggesting that the motor cortex contributes to limb trajectory adjustments in response to environmental demands (Drew, 1988). This implies that supraspinal structures overlay additional control on spinal circuits to achieve flexible locomotion (MacLellan, 2017).

Recent findings also suggest parallels between cortical circuits used for reaching and those used for modifying gait (Dyson et al., 2014; Yakovenko and Drew, 2015), indicating a shared cortical framework for motor adaptations. In humans, increased

activity in both the prefrontal and primary motor cortex during obstacle clearance supports the idea of a comparable supraspinal mechanism (Haefeli et al., 2011). However, a notable distinction is the lateralization of this activity in the right prefrontal cortex, suggesting species-specific differences in cortical involvement (Haefeli et al., 2011).

Altogether, these findings emphasize that while basic locomotor patterns are generated by spinal CPGs, adaptive gait modifications, especially in response to environmental challenges, require supraspinal input to fine-tune movement. This highlights the complex interplay between automatic spinal networks and higher-order brain regions in flexible locomotor control.

The ALAs are proactive adaptations made to accommodate changes in surroundings or movement goals (McFadyen et al., 1993). Visual guidance plays a key role in the programming of these ALAs (McFadyen et al., 2018). Since unexpected obstacles trigger faster reactions than voluntary stride adjustments, the involvement of the autonomic nervous system and subcortical structures has been suggested (Weerdesteyn et al., 2004). These adjustments are also reflected in how our muscles control the movement energy flow, influencing the kinematic movements (Latash, 2016; Zajac et al., 2002). The level of force, or moment of a force, produced offers insight into how muscles function together, while studying muscle mechanical power reveals the energy flow propelling movement (Robertson and Winter, 1980). This section of the literature review will focus on the changes in the locomotor pattern associated with modifying the foot trajectory while walking over obstacles.

Before reviewing the literature related to obstructed walking, an important point is that the obstacle can be unilateral or bilateral. This difference yields a different nomenclature of the legs. In bilateral obstacle conditions, the legs will be labelled based on which one goes over the obstacle first. The first one is labelled the “leading leg” and the second one is labelled the “trailing leg” (McFadyen and Prince, 2002) (Figure 3, left and right leg, respectively). When the experimental condition is a unilateral obstacle, the leg going over the obstacle is labelled the “crossing leg” and the leg on the ground during the obstacle clearance is labelled the “supporting leg” (Ladouceur et al., 2005) (Figure 3, right and left legs, respectively).

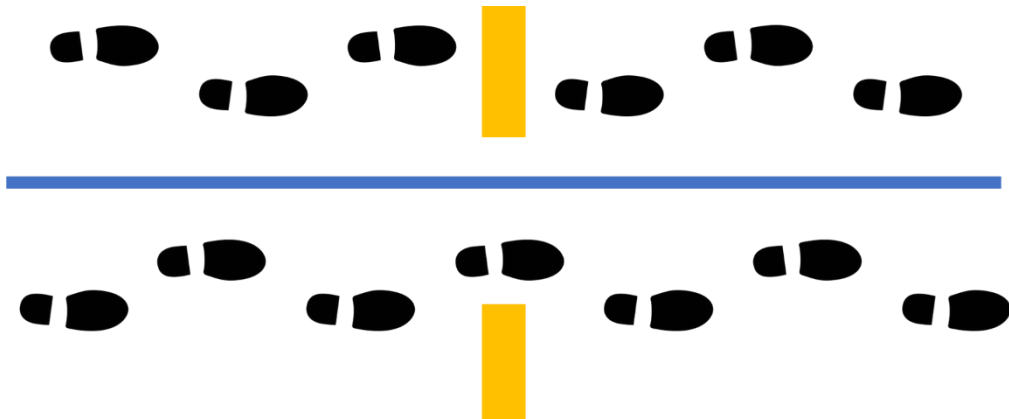


Figure 3. Visualization of bilateral and unilateral obstacle placement. Example of a bilateral obstacle (top) and a unilateral obstacle (bottom).

The next sections will highlight differences in the motor strategies used to cross the different obstacles. Briefly, bilateral obstacles seemed to demand a higher level of coordination due to the increased safety margin with the obstacle, the reduction in the horizontal impulse, and the smaller increase in greater trochanter height for unilateral obstacles placed at the location of mid-swing (Ladouceur et al., 2005).

2.3.1 Strategies to cross over the obstacle

When walking over obstacles, it is important to have proper pelvis control to manage the trajectory of the greater trochanter and alter muscle energy patterns. When encountering an obstacle on their path, individuals may opt to either navigate around it or cross over it (Patla et al., 1991). If the latter case is chosen, what modifications and adaptations must be made to their movement to guarantee a secure clearance of the obstacle without compromising their equilibrium or risking a stumble?

Strategies that ensure crossing over an obstacle are two-fold: a) generating an upward bias of the swing limb trajectory and b) elevating the foot higher (Patla et al., 1991). A third and safer adaptation that consists of decreasing the forward progression velocity to prevent a sudden brake when getting closer to the obstacle that may lead to tripping has also been mentioned (Patla et al., 1991). This third adaptation was supported by the increase in the braking antero-posterior GRF impulse of the supporting leg during the stance phase (Patla et al., 1991).

2.3.1.1 Upward bias of the swing limb

The strategy to increase the bias of the swing limb does not change the relative trajectory of the crossing leg, rather providing upward bias by the supporting leg (Patla et al., 1991). This strategy is used to elevate the CoM high enough. It requires a greater than normal vertical acceleration by generating a higher GRF under the stance limb (Patla et al., 1991). The bias in upward trajectory enhances limb clearance sufficiently to clear obstacles of increased height (Patla and Rietdyk, 1993). Vertical impulse during the initial double support phase, which reflected the weight transfer to the trailing leg, decreased as obstacle height increased, indicating greater reliance on the trailing leg for the initial

weight acceptance and stability during crossing over the obstacle (Patla and Rietdyk, 1993). Moreover, during weight acceptance on the trailing leg, greater knee flexion would further assist hip hiking in the leading leg, contributing to higher limb elevation (Patla and Rietdyk, 1993).

2.3.1.2 Higher foot elevation

The second strategy is to elevate the foot higher; this is done by increasing the joint angles of the lower body to ensure crossing over the obstacle. Patla et al (1991) presented five options.

The first two options would occur during the push-off phase of the crossing leg (Patla et al., 1991). They consist of increasing the knee flexion angle and knee angular velocity by activating the crossing leg's biceps femoris muscle. The second option consists of decreasing the ankle plantar flexion angle and angular velocity, which consequently increases the ankle's dorsiflexion by activating the crossing leg's tibialis anterior muscle (Patla et al., 1991).

The three other options would occur during the pre-swing phase (Patla et al., 1991). The first option consists of either increasing hip flexion angles or increasing the activation of the rectus femoris on the leg going over the obstacle. The second option consists of increasing knee and hip flexion by increasing the activation of the biceps femoris on the leg going over the obstacle (Patla et al., 1991). The third option consists of increasing ankle dorsiflexion by increasing the activation of the tibialis anterior muscle. It can also be noted that activating the biceps femoris, a bi-articulate muscle, when going over the obstacle would not only flex the knee but would also flex the hip and dorsiflex

the ankle through passive mechanical interaction between segments (Patla and Prentice, 1995).

2.3.1.3 The combined contribution of both strategies during obstructed walking

Patla and Rietdyk (1993) showed that for a small bilateral obstacle (approx. 10cm), the second strategy (higher foot elevation) contributed to 78% of the toe elevation, whereas the first strategy of increasing the bias of the swing limb contributed to 22% of the toe elevation. As such, this synergistic use of the two strategies would allow a rapid flexing of the limb that would also prevent any instability caused by the high reactive moments generated at the trunk (Patla and Rietdyk, 1993).

A more recent study (Ladouceur, 2025) of unilateral obstacles with a greater range of heights showed that both strategies are used with different magnitudes as a function of obstacle height. The relative use of the two strategies is presented in Figure 4. For lower obstacles, the higher foot elevation strategy is sufficient to ensure the clearance of the obstacle. As obstacle height increases, a blend of strategies becomes apparent when the higher foot elevation plateaus for obstacles of 30 cm, with an increase in the upward bias of the swing limb, then becomes prominent (Ladouceur, 2025).

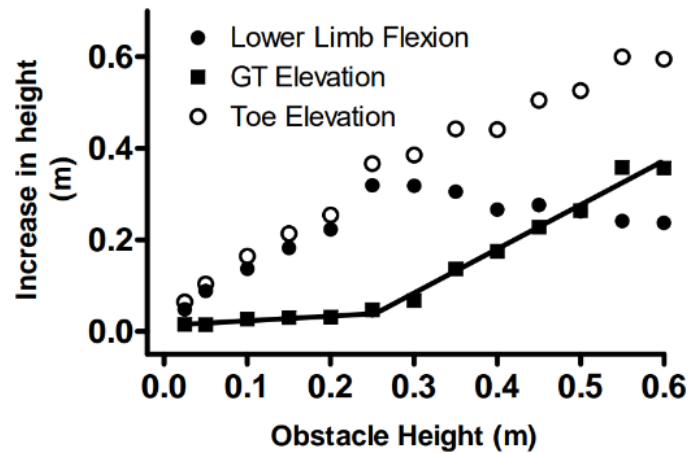


Figure 4. Toe elevation, greater trochanter (GT) elevation and lower limb flexion as a function of unilateral obstacle heights (Ladouceur, 2025).

2.3.2 Kinematic adaptations during obstructed walking

This section will review the kinematic changes occurring during obstructed walking. The main variables reviewed are toe clearance, toe velocity, hip position, and increased lower body joint angles. The obstacle conditions were unilateral (McFadyen et al., 1993) and bilateral (Patla et al., 1991; Patla and Rietdyk, 1993) obstacles.

Patla and Rietdyk (1993) calculated the safety margin while crossing the obstacle by subtracting toe height over the obstacle from the height of the obstacle. It was shown that the safety margin increased as obstacle height increased. Furthermore, there was a decrease in the horizontal toe velocity as obstacle height increased (Patla and Rietdyk, 1993). In addition to the toe kinematic changes, the hip location was situated further back from the edge of the obstacle as the height of the obstacle increased (Patla and Rietdyk, 1993). Moreover, hip velocity was also reduced (Patla and Rietdyk, 1993). It was suggested that the hip kinematic changes were done as a precaution to keep the CoM over the stance limb while ensuring the leading leg clears the obstacle (Patla and Rietdyk, 1993). In summary, these adjustments are made at the end of the stance phase and

actively during the swing phase to avoid tripping and ensure crossing over the obstacle (McFadyen and Carnahan, 1997; Patla and Rietdyk, 1993).

Studies of the relative joint angles of the lower limb show an increased flexion of all three relative joints that starts just prior to toe-off (McFadyen et al., 1993; McFadyen and Carnahan, 1997; Patla and Rietdyk, 1993). It was shown in a bilateral obstacle that the lower limb flexion increased with the obstacle height (Patla and Rietdyk, 1993). This relative joint angle adaptation was necessary as foot elevation is one of the two strategies to ensure clearance over the obstacle (McFadyen and Carnahan, 1997).

A study of the changes in relative joint angles as a function of unilateral obstacle heights showed that in this experimental condition, all three lower limb joints increased their flexion as a function of obstacle height (Ladouceur, 2025). Despite the increase across the three joints, each joint had a different adaptation function (Figure 5). The ankle joint adapted rapidly for lower obstacle heights and reached a plateau for an obstacle of 10% of their leg length (Ladouceur, 2025). The knee joint adapted for smaller obstacles but reached its plateau for an obstacle of 50% of the participant's leg length. Lastly, the hip joint increase in flexion did not reach a plateau and seemed to increase linearly with obstacle height increases (Ladouceur, 2025).

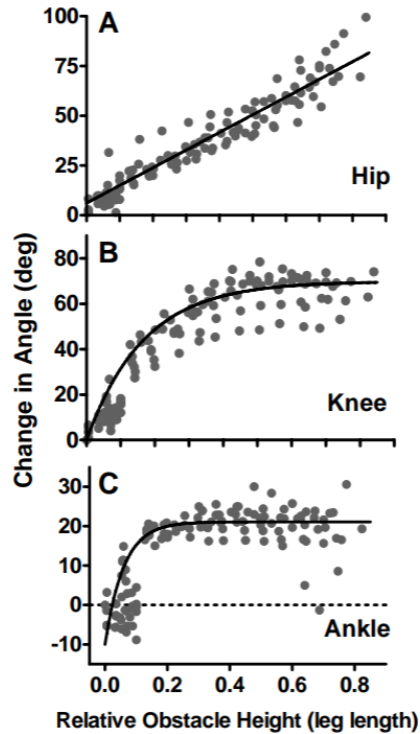


Figure 5. Changes in angle at the hip, knee and ankle joints as a function of unilateral obstacle height. Adapted from (Ladouceur, 2025).

2.3.3 Modular organization of muscle activity patterns during obstructed walking

Muscular activation studies were performed to investigate the patterns during obstructed walking and identify how the CNS implements its ALAs (Hahn et al., 2005; MacLellan, 2017; McFadyen and Winter, 1991; Patla et al., 1991; Patla and Rietdyk, 1993). They have revealed that on the leading limb, there was an increase in gluteus maximus (GM) and vastus lateralis (VL) activities during the stance phase (Hahn et al., 2005), and an increase in knee flexor and dorsiflexor activity in the swing phase (McFadyen and Winter, 1991; Patla et al., 1991). On the trailing leg, however, there was an increase in gastrocnemius, gluteus maximus and vastus lateralis activity during the stance and double support phase (Hahn et al., 2005), accompanied by an increase in hamstring activity during early swing to elevate the lower limb (Patla and Prentice,

1995). Although both the leading and trailing legs would increase their hamstrings activity, McFadyen and Niang (2004) revealed that the leading and trailing leg would adopt a different mechanical pattern, specifically the leading leg would flex the knee and the hip simultaneously, while the trailing leg would flex the knee then flex the hip to avoid tripping (Niang and McFadyen, 2004). Additionally, there was increased tensor fasciae latae (TFL) and vasti muscle activation during the late swing phase on the leading limb to stabilize the hip in preparation for ground contact (MacLellan, 2017).

Unlike during unobstructed walking, where temporal patterns are coordinated between the right and left lower limbs (Ivanenko et al., 2006; Olree and Vaughan, 1995), the leading and trailing legs would alter their temporal patterns in response to the obstacle. Specifically, during the initial swing phase, the observed patterns were associated with joint flexion. In mid-swing, the leading leg exhibited increased activation of the knee extensors, whereas the trailing leg showed greater activation of the knee flexors, hip adductors, and trunk muscles (MacLellan, 2017). These alterations suggest that there is a link between both legs in some phases of the gait cycle, but would differ in others to implement the locomotor adjustments rather than create an entirely new pattern (MacLellan, 2017). Additionally, the stance-swing transition would alter during obstructed walking as a shift in the temporal patterns of the gait cycle would occur. Similar to what has been reported in cat studies in obstructed walking (Krouchev and Drew, 2013), the leading leg would delay its activation to go over the obstacle, while the trailing leg would advance its activation to support the body and assist in going over the obstacle (Aoi and Funato, 2016; MacLellan, 2017).

In summary, a bilateral modular organization of the lower limbs occurs to maintain support while clearing an obstacle (MacLellan, 2017). This involves coordinated adjustments in the timing and activation of muscles in both the leading and trailing limbs, ensuring effective movement and stability during the task (Aoi and Funato, 2016; MacLellan, 2017). Timing shifts in the limb movements and coupling muscle activation patterns are crucial for successfully going over the obstacle.

2.3.4 Mechanical adaptations during obstructed walking

During obstructed walking, individuals modify lower limb energy distribution and muscle activation to cross obstacles. A shift from knee extensor activation in normal walking to increased hip and knee flexion through biarticular muscle activation is observed (Winter et al., 1991).

It has been shown that in both unilateral (crossing leg) and bilateral obstacles (leading/trailing legs), there is a reorganization of the lower body net joint power to ensure proper toe clearance (McFadyen et al., 1993; McFadyen and Carnahan, 1997; McFadyen and Prince, 2002; McFadyen and Winter, 1991; Niang and McFadyen, 2004). This reorganization consists of the emergence of the generation of power by the knee flexor muscles (K5) as well as a decrease in knee extensors energy absorption (K3) and the hip flexors energy generation (H3) (McFadyen and Winter, 1991). An example of this reorganization at the knee is presented in Figure 6.

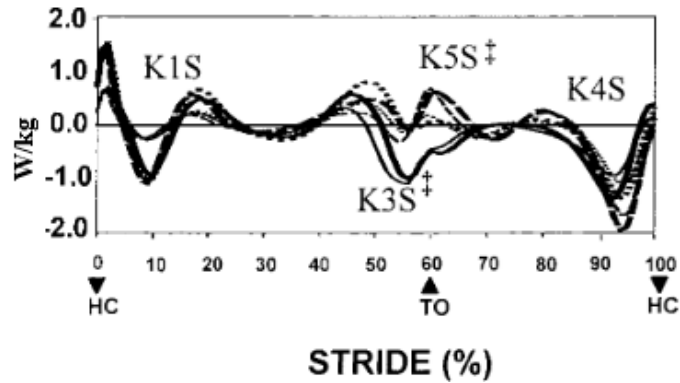


Figure 6. Net joint powers in the sagittal plane for the trail limb knee joint. Data are presented across the young (thick curves) and elderly (thin curves) subjects for the unobstructed (solid curve), obstacle (dashed curve), and platform (dotted curve) conditions. Main effects are shown for age (\dagger) and for environment (\ddagger). Positive power indicates generation and negative power indicates absorption (Adapted from McFadyen and Prince, 2002).

In addition to these adaptations, the trailing leg of bilateral obstacles has been shown to reduce energy absorption (H1F) and to increase energy generation (H2F) by the hip abductors (McFadyen and Prince, 2002). These ALAs aim to facilitate obstacle avoidance by modifying limb elevation and muscle power dynamics (McFadyen et al., 1994).

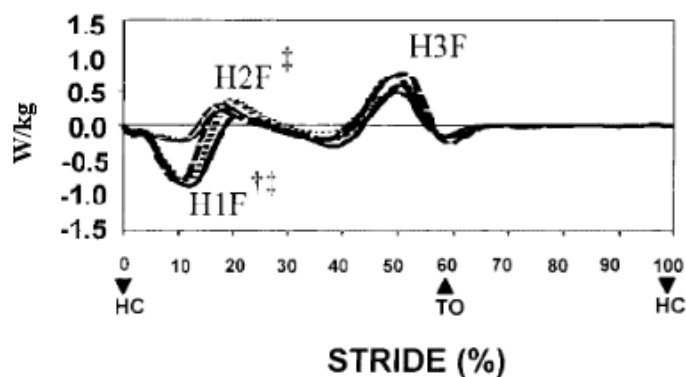


Figure 7. Net joint powers in the frontal plane for the trail limb hip joint. Data are presented across the young (thick curves) and elderly (thin curves) subjects for the unobstructed (solid curve), obstacle (dashed curve), and platform (dotted curve) conditions. Main effects are shown for age (\dagger) and for environment (\ddagger). Positive power indicates generation (Adapted from (McFadyen and Prince, 2002)).

The ALA presented above suggests that the motor control system selects a knee flexor strategy, resulting in combined hip and knee flexion with minimal muscular effort so that the hip joint drives the limb forward while the knee joint controls foot elevation (McFadyen and Winter, 1991; Niang and McFadyen, 2004). Furthermore, a study using the EMG of 14 muscles on each lower limb, including the erector spinae, gluteus medius, biceps femoris, and semitendinosus, for bilateral obstacles of lower heights ($< 0.2\text{m}$) provides evidence that obstacle clearance may be achieved not only with the addition of a new activation pattern in the leading limb, but with a temporal shift of a pattern present during unobstructed walking in both the leading and trailing limbs (MacLellan, 2017).

A study of unilateral obstacles showed (Figure 8) that in addition to the lower limb flexion changes in the energy flow, there was an increase in crossing hip joint vertical impulse (Ladouceur, 2025). As shown previously, the two strategies to either increase the bias of the crossing leg or elevate the foot are used during unilateral obstacle crossing. For obstacles of lower heights, adaptations occur only in the crossing leg. However, for obstacles of higher heights, there is a bilateral adaptation that takes place as both legs adjust to safely cross the obstacle (Ladouceur, 2025).

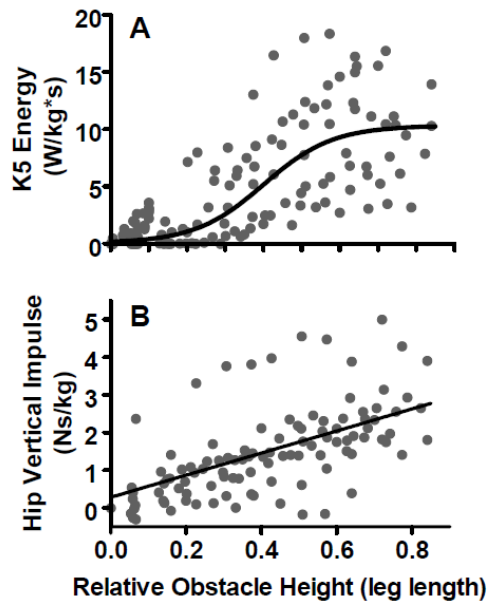


Figure 8. Changes in the muscle kinetics during obstructed walking. Adapted from (Ladouceur, 2025).

2.4 Gaps in the literature

Ladouceur et al. (2005) investigated the effects of various obstacle placements and found that lower bilateral obstacles (less than 30 cm) increased crossing complexity, while higher unilateral obstacles (greater than 40 cm) during mid-swing result in significantly greater elevation of the greater trochanter compared to bilateral ones, suggesting distinct adaptations at higher obstacle heights. Ladouceur (2025) further noted that successful toe clearance over high obstacles was largely due to increased elevation of the greater trochanter, commonly referred to as hip hiking. The current study addressed this gap by examining the adaptations in the supporting leg when crossing unilateral obstacles at 60 cm, aiming to deepen the understanding of control mechanisms required for elevated foot clearance.

Chapter 3: Methodology

3.1 Ethics

The study protocol received approval from Dalhousie's Research Ethics Board (REB: 2024-7253). All participants provided written informed consent prior to data collection.

3.2 Study location

The study was conducted in the Biodynamics, Ergonomics, and Neuroscience Laboratory, located in room 217 of the Dalplex facility at Dalhousie University.

3.3 Participants

3.3.1 Sample size

To determine an appropriate sample size, values of knee negative and positive work (DeVita et al., 1998) were imported into G*Power software (Faul et al., 2007) that revealed the need for a sample size of 10-15 participants, based on a power (beta) of 80% and an alpha value of 0.05. The sample size of the present study relied upon an article addressing the altered mechanics observed during gait in participants following anterior cruciate ligament reconstruction (ACLR) (DeVita et al., 1998). It was originally designed to investigate the effects of this injury in comparison to able-bodied participants. However, due to a lack of sufficient participants post-ACLR, the design of the study changed into a case study involving two individuals post-ACLR (see Appendix H).

3.3.2 Recruitment

Posters displayed throughout the Dalhousie premises, social media blurbs and posts, as well as word of mouth, served as recruitment strategies for this study. A contact

email for the primary researcher was included in the recruitment materials. Potential participants who contacted the primary researcher received a more detailed description of the study in an email response. This included information on the inclusion and exclusion criteria, allowing participants to assess their eligibility for the study. A letter of information and informed consent were also attached to the email; however, these were intended to provide further details about the research project and were not to be completed until the participant arrived in the lab.

3.3.3 Inclusion and exclusion criteria

The only inclusion criterion for the able-bodied participant group was age, with participants ranging from 18 to 35 years old. The reasoning behind this specific age group was based on a study that reported spatiotemporal variable differences during obstructed walking between three age groups, those being the young (18 to 35), middle-aged (50-64) and older adults (65-79) (Muir et al., 2019). The exclusion criteria included having undergone any surgery on the lower body, experiencing difficulties with unobstructed and obstructed walking, and having suffered a musculoskeletal injury in the past six months.

3.4 Research design

Using a quasi-experimental design, able-bodied participants were recruited based on the inclusion and exclusion criteria. Walking trials were conducted with obstacles of increasing height after unobstructed walking trials, manipulating height as a within-subjects factor. This study investigated the energy flow adaptations during unilateral obstructed walking in able-bodied individuals.

3.4.1 Outcome measures

Table 1. Primary outcome measures

Unobstructed and Obstructed Walking	Crossing Leg	Sagittal Plane	H3 K3, K5, K4 A2
		Frontal Plane	H3F, H4F
	Supporting Leg	Sagittal Plane	H1, H2 K1, K2 A1, A1A, A1G
		Frontal Plane	H1F, H2F
The bolded outcome measures (reviewed in the literature) were related to the specific hypotheses of the study			

Based on the specific aims and hypotheses of the study, the selected primary outcome measures are presented in Table 1. For the crossing leg, muscle power bursts of interest in the sagittal plane (flexion-extension) were the hip flexors energy generation (**H3**), the knee extensors energy absorption (**K3**), the knee flexors energy generation (**K5**), the knee flexors energy absorption (K4) and the ankle plantar flexors energy generation (A2); muscle power bursts of interest in the frontal plane (adduction-abduction) were the hip abductors energy generation (**H3F**) and the hip adductors energy absorption (H4F). For the supporting leg, muscle power bursts of interest in the sagittal plane (flexion-extension) were the hip extensors energy generation (H1), the hip flexors energy absorption (H2), the knee extensors energy absorption (K1), the knee extensors energy generation (K2), the ankle plantar flexors energy absorption (A1), the ankle plantar flexors energy absorption (A1A) and the ankle plantar flexors energy generation (A1G); muscle power bursts of interest in the frontal plane (adduction-abduction) were the hip abductors energy absorption (**H1F**) and the hip abductors energy generation (H2F). Other outcome measures, such as spatiotemporal data, joint angles, and joint moments, were also measured but were not considered primary outcomes for analysis.

3.4.2 Experimental protocol

Following their arrival at the Dalplex, participants were escorted to the laboratory. They had previously received a consent form via email and were given another opportunity to read it before their appointment. The lead researcher reviewed the informed consent form with each participant, asked questions to ensure their eligibility for the study, and then provided more information about the study and data collection process. Following the information period, the participants signed an informed consent letter (Appendix A).

All participants were requested to wear tight-fitting upper and lower body clothes to ensure accurate marker placement. Subsequently, mass and height were measured using a stadiometer and a scale while wearing the same clothing as during data collection and without shoes. They were then asked to fill out three questionnaires: the Lysholm Knee Questionnaire (LKQ), the Tegner Activity Scale (TAS) and the Waterloo Footedness Questionnaire-Revised (WFQ-R) (Appendices C, D and E, respectively). For the TAS, able-bodied participants were asked to fill out their current activity level. Furthermore, while the WFQ-R demonstrates high reliability (Aldaihan, 2023; Yang et al., 2018), its results should be viewed as subjective opinions rather than definitive measures of foot preference.

The retroreflective markers for the lower body were placed based on a full-body six degrees of freedom (6 DOF) marker set (Figure 9). Eight rigid bodies containing four non-collinear markers were strapped on the left and right upper arm, forearm, thigh, and shank. Thirty-six retroreflective markers were placed on the following anatomical landmarks on the left and right sides: posterior and anterior head, acromion process,

lateral and medial humeral epicondyles, radial and ulnar styloid processes, second and fifth metacarpal heads, anterior and posterior superior iliac spines (to define the pelvis segment), lateral and medial femoral epicondyles (to define the thigh segments), lateral and medial malleoli (to define the shank segments), calcaneal tuberosity, first and fifth metatarsal heads, and distal hallux (to define the foot segments). Five additional markers were placed on the spinous processes of the 7th cervical vertebrae and 8th thoracic vertebrae, sternal jugular notch, middle sternum, and xyphoid process.

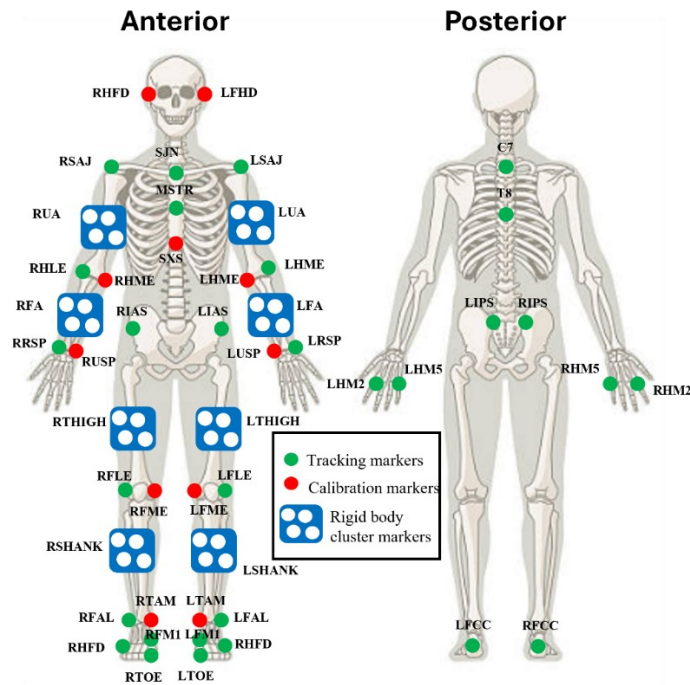


Figure 9. 6 DOF marker set. Tracking markers are in green, calibration markers are in red and blue rigid body marker clusters are in blue, square and white circles.

The table below (Table 2) provides each marker's description and role.

Anatomical markers were used for tracking and segment definition, calibration markers for segment definition, and cluster markers for tracking.

Table 2. 6 DOF marker set.

L/RFHD	Left and Right Front Head	Calibration Markers
L/RSAJ	Left and Right Acromion	Anatomical Markers
L/RUA	Rigid cluster of 4 markers, placed laterally	Tracking Markers
L/RHLE	Left and Right Humeral Lateral Epicondyles	Anatomical Markers
L/RHME	Left and Right Humeral Medial Epicondyles	Calibration Markers
L/RFA	Rigid cluster of 4 markers, placed laterally	Tracking Markers
L/RRSP	Left and Right Radial Styloid Processes	Anatomical Markers
L/RUSP	Left and Right Ulnar Styloid Processes	Anatomical Markers
L/RHM2	Left and Right 2 nd Metacarpal Head	Anatomical Markers
SJN	Jugular Notch of the Sternum	Anatomical Marker
MSTR	Middle sternum	Anatomical Marker
SXS	Xiphoid Process	Calibration Marker
C7	7 th Cervical vertebrae	Anatomical Marker
T8	8 th Thoracic vertebrae	Anatomical Marker
L/RHM5	Left and Right 5 th Metacarpal Head	Anatomical Markers
L/RIAS	Left and Right ASIS	Anatomical Markers
L/RIPS	Left and Right PSIS	Anatomical Markers
L/RTHIGH	Rigid cluster of 4 markers, placed laterally	Tracking Markers
L/RFLE	Left and Right Femoral Lateral Epicondyles	Anatomical Markers
L/RFME	Left and Right Femoral Medial Epicondyles	Calibration Markers
L/RSHANK	Rigid cluster of 4 markers, placed laterally	Tracking Markers
L/RFAL	Left and Right Lateral Malleoli	Anatomical Markers
L/RTAM	Left and Right Medial Malleoli	Calibration Markers
L/RFM5	Left and Right 5 th Metatarsal Head	Anatomical Markers
L/RFM1	Left and Right 1 st Metatarsal Head	Anatomical Markers
L/RTOE	Left and Right Toes	Anatomical Markers
L/RFCC	Left and Right Calcaneus	Anatomical Markers

Participants were familiarized with the process of data collection during walking and obstructed walking. A T-pose was performed for 10 seconds as a calibration trial with all markers and rigid bodies in place. The calibration markers (red in Figure 9) were removed for the walking trials. For both the unobstructed and obstructed walking trials, a member of the research team counted down, “three, two, one, and go,” to signal the participant to begin the task. The task started from a stationary position, followed by a few steps (four to six) before contacting the floor-embedded force plates. For the unobstructed walking trials, the right leg contacted the first force plate while the left leg

contacted the second. For the obstructed walking trials, an obstacle was placed in the middle of the second force plate, coinciding with the mid-swing phase for the crossing leg. For the obstructed walking trials, the legs that contacted the force plates were different. For instance, when the left leg was the crossing leg, it contacted the first force plate only, while the right leg contacted the second force plate only (and vice versa in the condition where the right leg is the crossing leg). Walking was tested across several experimental conditions: unobstructed and obstructed walking at six different heights (from 10 cm to 60 cm). For each obstructed walking condition, five valid trials were collected per leg as the supporting leg, resulting in 10 valid trials per condition. In total, 65 valid trials were collected per participant (Appendix G). One participant refused to perform the highest obstacle height; hence, 55 trials were collected for that participant. The trials were deemed valid if the participants had their foot land entirely on the force plate, safely crossed over the obstacle without touching it, looked straight ahead, and had a walking speed comparable to their unobstructed, comfortable walking speed.

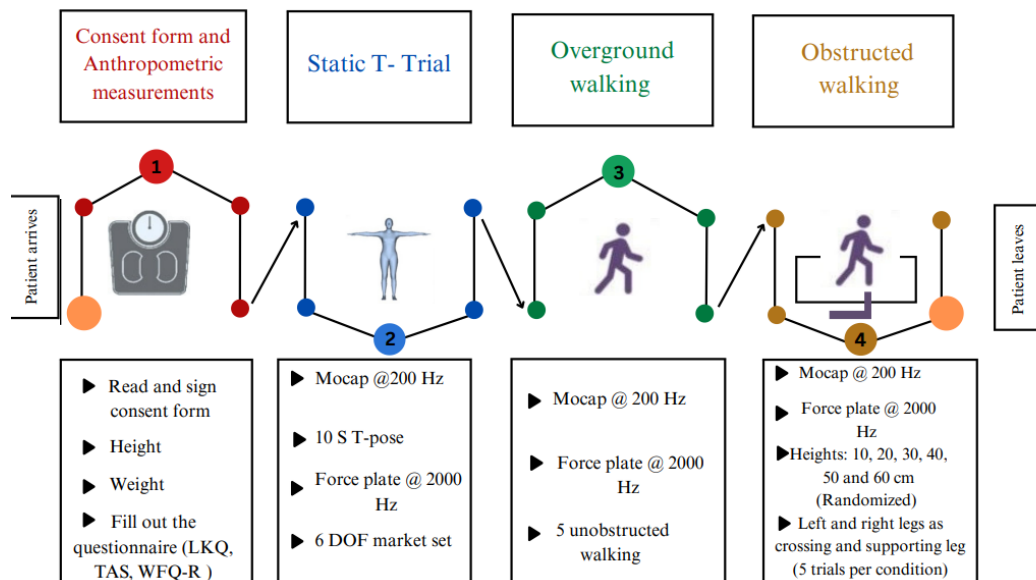


Figure 10. Experimental procedure.

3.5 Measurement and calculations of the outcome variables

3.5.1 Kinematic measurements

3.5.1.1 Motion capture system

Retroreflective markers were placed at specific bony landmarks on the participant (Figure 9). Marker locations were captured by a 14-camera Optitrack Motion Capture System (OptiTrack, NaturalPoint, Inc., OR USA), acquiring data at a sampling frequency of 200 Hz. All 14 cameras were used to collect marker position. Motive software (version 2.1.1, NaturalPoint, Inc., OR USA) was used for data acquisition and post-collection marker labelling. The system, which consisted of cameras, markers, and 3D reconstruction processing software, has shown to be valid and reliable (Aurand et al., 2017; Carse et al., 2013) (Check Appendix F for additional information).

Figure 9 displays the placement of the markers. Green markers were used for tracking and segment definition, red markers were calibration markers used only for segment definition (meaning that they were removed after the static T trial), and blue rigid bodies were used only for tracking. The rigid bodies were placed on the lateral side of the segment (Żuk and Pezowicz, 2015). Comparing the 6 DOF marker set to the traditional gait model marker set (Helen Hayes), studies revealed that the 6 DOF marker set has excellent reliability and equivalent accuracy (Collins et al., 2009; Żuk and Pezowicz, 2015). Furthermore, because the segments in the 6 DOF marker set were independent of one another and there were no joint constraints, the construct validity of this model was higher than that of the standard gait model (Collins et al., 2009).

Missing marker data points were interpolated via cubic spline in Visual3D. The marker trajectories were then filtered using a 4th order, 6 Hz, zero-phase lag, low-pass

Butterworth filter to attenuate noise at frequencies above 6 Hz in Visual3D (Winter, 1991). Based on the static trial, a 6 DOF full-body model was created and applied to the motion trials for calculations.

3.5.1.2 Lower body model

The lower body segments included the pelvis, thighs, shanks and feet (Figure 11). Coordinate systems were adjusted to follow the International Society of Biomechanics (ISB) recommendations (Wu et al., 2002, 2005) which was different from the Visual3D default coordinate system. The ISB recommends naming the axes in relation to the line of progression where the anteroposterior axis is labelled the X axis, the mediolateral axis is labelled the Z axis, and the vertical axis is labelled the Y axis.

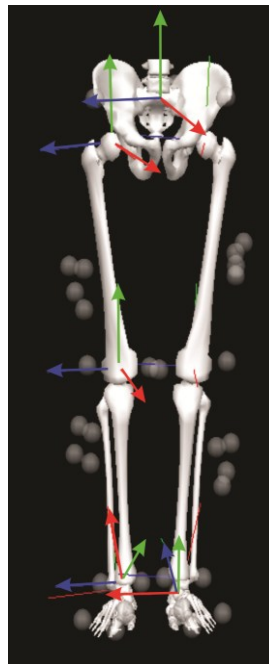


Figure 11. Lower body local coordinate systems (LCS, Z axis (blue), X axis (red) and Y axis (green)). The LCS on the right side correspond to the pelvis, hip, knee and ankle (kinetic) coordinate systems. The LCS on the left side corresponds to the ankle (kinematic) coordinate system. The right ankle (kinematic) coordinate system is represented on the left side, while the left ankle (kinematic) should be multiplied by -1 about the Y axis (green) to indicate inversion in the positive frontal plane.

To build the lower body model, the pelvis segment was initially defined using the CODA model (embedded in Visual3D) by the anterior superior iliac spine (ASIS) and posterior superior iliac spine (PSIS) markers. This computed the right and left hip joint centers, which were used to build the thigh segment along with half the distance between both ASIS and the medial and lateral femoral condyles. To build the shank segment, the medial and lateral femoral condyles as well as the medial and lateral malleoli were used. Two ankle segments were built; one that was used for kinetic purposes based on the medial and lateral malleoli, as well as the markers of the calcaneus, first and fifth metatarsals, and toe markers; and one that was used for kinematic purposes using the calcaneus as the origin and tracking the toe and fifth metatarsal markers. More information can be found in Appendix F.

3.5.1.3 Kinematics calculations

After the full-body model was built, three-dimensional joint angles for the hip, knee, and ankle were calculated based on the relative orientation of the proximal and distal segments with respect to one another. The ISB recommendations, a Z-X-Y rotation order (Flexion/Extension, Adduction/Abduction, Internal/External rotation), were used to calculate the Cardan angles of the relative joint (Wu et al., 2002, 2005). Positive values for both legs corresponded to hip flexion, adduction, and internal rotation; knee flexion, adduction, and internal rotation; and ankle dorsiflexion, inversion, and internal rotation. The proximal segment was utilized as the reference segment. Calculating joint angles involved transforming from one coordinate system to another while ensuring that both systems had identical origins. The ensemble average of the relative joint angles was performed and stored.

3.5.1.3.1 Segment's inertial properties (mass, location of their CoM, mass moment of inertia)

The inertial properties of each segment were determined. The mass of the segments in Visual3D is based on regression equations (Dempster, 1955). The center of mass location was calculated as the point at which the segment's mass can be considered to be concentrated (Robertson, 2014). The segments were represented by a frustum of a right circular cone (Figure 12), as outlined by Hanavan (1964). The segment was defined by its length (L), proximal radius ($R_{proximal}$) and the distal radius (R_{distal}). The CoM was positioned along the vector passing through the distal and proximal ends of the segment at a ratio distance c from the proximal end of the segment in the local coordinate system (LCS) (Robertson, 2014).

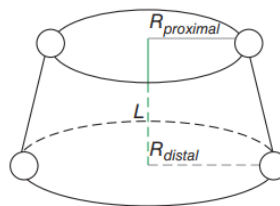


Figure 12. Calculating the CoM and Mass-moment of Inertia of the segments. A frustum of right cones is created by cutting the top of a cone such that the cut is parallel to the base of the cone (Robertson, 2014).

3.5.1.4 Joint angular velocity and acceleration

Joint angular velocity refers to the rate of change of one segment coordinate system relative to another. Although not directly calculated, determining joint angular velocity and acceleration was needed to calculate joint moments and power, respectively.

In Visual3D, joint angular velocities were expressed in terms of derivatives of Euler angles (see Appendix F). Joint angular accelerations were calculated as the derivatives of the above joint angular velocity calculations.

3.5.2 Kinetic measurements

3.5.2.1 Force plate system

An AMTI force plate system (6-Degree of Freedom dimensions; Watertown, MA) with two floor-embedded strain gauge force plates were used to collect kinetic data at a sampling frequency of 2000 Hz, which were synchronized with the motion capture system. The two force plate amplifiers (MiniAmp MSA-6, Advanced Mechanical Technology, Inc., MA, USA) provided ± 10 V excitation voltage to the force plates and 1000x gain to each force plate channel. Sampling frequencies had to be high enough to ensure precision of measurement and reduction of signal aliasing (Beckham et al., 2014).

Six channels were recorded, corresponding to the ground reaction forces in the x, y, and z directions (F_x , F_y , F_z) and the moments in the x, y, and z axes (M_x , M_y , M_z). The force plate analog-to-digital conversion data used a custom-written MATLAB script, which converted the variables to text files that were imported into Visual3D. In addition to these, the center of pressure (COP), which is the intersection of the force vector with the surface of the platform (Robertson, 2014), position was determined, such as that $COP_z=0$, and COP_x and COP_y were calculated by the following equations:

$$COP'_x = \frac{F_x d_z - M_y}{F_z}$$

$$COP'_y = \frac{F_y d_z + M_x}{F_z}$$

d_z is the distance from the force platform's electrical origin to the top surface's center.

3.5.2.2 Internal joint moment calculations

The ground reaction forces and moments about all three axes were combined with the kinematic data to calculate the net joint moments as well as the net joint powers through inverse dynamics using classical link segment calculations (Bresler and Frankel, 2022) in Visual3D. The right-hand rule was used to represent the calculations. The ensemble average of the gait cycle time, normalized net joint moments, was performed and stored. Detailed information can be found in Appendix F.

3.5.2.3 Joint power calculation

Joint powers describe the net rate, amount, and timing of energy generation and dissipation of all muscles and ligaments around a joint (Sloot and van der Krogt, 2018). Joint power is calculated as the dot product of the joint moment and the joint angular velocity. The joint forces, moments and powers calculations used a distal to proximal approach with the ankle being calculated first, followed by the knee, and lastly the hip.

3.5.2.4 Muscle power burst calculation

Data was processed in Visual3D, and text files containing angles, moments, and power around all three axes of the hip, knee, and ankle joints were generated. A custom-written MATLAB script was used to extract the primary outcomes for the supporting leg (H1, H2, H1F, H2F, K1, K2, A1, A1A, A1G) and crossing leg (H3, H3F, H4F, K3, K5, K4, A2).

To determine the energy bursts of each participant per condition, the mean net joint power, normalized to 100% of the gait cycle (GC), was plotted for the hip (sagittal and frontal), knee, and ankle joints. The start and end of each energy burst of interest

were defined manually using an iterative process based on the 'ginput' MATLAB function. Below is a description of each energy burst's start and end timing during the gait cycle.

At the hip in the sagittal plane, the hip extensors energy generation (H1) was assigned as the energy generation between the 0 and 20% periods of the gait cycle (GC), although it was not always present. The hip flexors energy absorption (H2) was assigned as the energy absorption between the 20 to 50% period of the GC. The hip flexors energy generation (H3) was assigned as the energy generation between the 50 to 70% period of the GC (Winter, 1987). In the frontal plane, the hip abductors energy absorption (H1F) was assigned as the energy absorption between the 0 to 20% period of the GC. The hip abductors energy generation (H2F) was assigned as the energy generation between the 20 to 35% period of the GC. The hip abductors energy generation (H3F) was assigned as the energy generation between the 40 to 60% period of the GC (Eng and Winter, 1995). For the same period, the H4F muscle power burst, for heights 0 to 40 cm, was assigned the power absorption between the 55 to 65% period of the GC, and H4F, for heights 50 and 60 cm, was assigned to the energy generation.

The knee extensors energy absorption (K1) was assigned as the energy absorption between the 5 to 15% period of the GC. The knee extensors energy generation (K2) was assigned as the energy generation between the 15 to 30% period of the GC. The knee extensors energy absorption (K3) was assigned as the energy absorption between the 50 to 70% period of the GC. The knee flexors energy absorption (K4) was assigned as the energy absorption between the 80 to 100% period of the GC (Winter, 1987). The knee

flexors energy generation (K5) (for obstructed walking only) was assigned as the energy generation between the 60 to 70% period of the GC.

The ankle plantar flexors energy absorption (A1) was assigned as the energy absorption between the 10 to 40% period of the GC. The ankle plantar flexors energy generation (A2) was assigned as the energy generation between the 45 to 60% period of the GC (Winter, 1987). The ankle plantar flexors energy generation (A1G) was assigned as the energy generation that potentially occurred for some obstacles between the 10 to 30% period of the GC. The ankle plantar flexors energy absorption (A1A) was assigned as the energy absorption that occurred between the 30 to 50% period of the GC.

The energy bursts were calculated by computing the area under the net joint power curve normalized to the gait cycle using numerical integration from the defined start to the end of each burst ($W * \%gaitcycle$). The numerical integration was done using the MATLAB 'trapz' function. The $W * \%gaitcycle$ values were transformed into absolute time by multiplying them with the average duration of the trials included in that experimental condition divided by 100. The result of this product expressed the values in $W*s$ (or J). This value was then normalized to the participant's mass to convert it to $W*s/kg$. The last step in establishing the energy burst values was a quality control process to determine if any of the trials were outliers. A custom-written MATLAB script computed each trial's energy burst, based on the timing of the burst timing established using the ensemble average. The value for each trial were compared with each other and the value extracted from the ensemble average. A decision to exclude specific trials was based on a qualitative decision that the trial result was different from the remaining part of the sample. This process was performed for each power burst, each obstacle height,

each leg, and for each participant. If a trial was removed, the mean energy burst was calculated based on the remaining trials and stored. The results from the able-bodied participants were collated and averaged for every outcome measure. If a participant did not perform a specific height, the ensemble average omitted that data from the calculations.

The ensemble average of the normalized net joint powers and net muscle joint power bursts was performed and stored.

3.5.3 Statistical analysis

Statistical analysis was performed using the R software package. Normality was assessed via Shapiro-Wilks test, histograms, QQ-plots, and homoscedasticity was examined using Levene's test.

A mixed-effects linear model (using the lmerTest package) was used to assess each outcome measure. The model included the interaction between the fixed effects (leg and obstacle height) and a random intercept for participants to account for individual variability. This approach was chosen because the data involved repeated measures, and therefore, within-subject observations are not independent, requiring a model that accounts for participant-level variability. A Type III Analysis of Variance with Satterthwaite's method was used to evaluate the significance of the fixed effects. Type III ANOVA tests each main effect and interaction while controlling for the influence of the others, and Satterthwaite's method provides an estimate of the degrees of freedom necessary for accurate p-value calculation in mixed models. In the event of a significant effect, post hoc comparisons were performed using the Tukey HSD test to identify specific group differences. The alpha level for statistical significance was set at 0.05.

Chapter 4: Results

4.1 Demographic characteristics

Data were collected and analyzed from 12 able-bodied participants. Table 3 displays the characteristics of the able-bodied group. Of the 12 participants, seven were female and the group had an average age of 24.6 ± 3.0 y, an average height of 1.68 ± 0.07 m, and an average mass of 71.2 ± 12.0 kg.

The Lysholm Knee Questionnaire (LKQ) had an average of 99.2 ± 1.8 . The Tegner Activity Scale (TAS) revealed their current activity level of 4.7 ± 1.9 . Lastly, the Waterloo Footedness Questionnaire-Revised (WFQ-R) revealed that 11 of the 12 participants had a preference for the right foot, with only one participant considered ambidextrous.

Table 3. Able-bodied participants demographics.

Participant	Age (y)	Gender	Height (m)	Mass (kg)	LKQ	TAS	WFQ-R
1	30	F	1.68	63.5	100	3	Right
2	21	F	1.65	93.4	100	5	Right
3	25	F	1.67	55.7	100	3	Right
4*	28	F	1.59	48	100	3	Right
5	21	F	1.58	78.4	100	6	Right
6	24	F	1.68	75	100	3	Right
7	25	M	1.78	68.3	100	5	Amb.
8	23	M	1.71	80.7	95	7	Right
9	26	F	1.61	73	96	3	Right
10	25	M	1.82	76	100	4	Right
11	20	M	1.75	73.5	100	5	Right
12	27	M	1.63	69.4	100	9	Right
Average (\pm 1SD)	24.6 \pm 3.0	7F 5M	1.68 \pm 0.07	71.2 \pm 12.0	99.2 \pm 1.8	4.7 \pm 1.9	11 R 1 AMDX

(SD=standard deviation; M=male; F=female; R=right; ADMX= Ambidextrous, y= years, m= meters, kg= kilograms, * did not perform obstacle height 60 cm)

4.2 Total number of trials

Table 4 outlines the total and average number of trials collected (static trial, non-valid, and valid trials), the number of valid trials, the number of labelled trials in Motive software (version 2.1.1), the number of trials processed in Visual3D, and the number of trials processed in MATLAB.

Table 4. Total and average number of trials.

	Trials collected	Valid trials	Labelled trials	Trials used for inverse dynamics calculations	Trials used for energy bursts calculations
Total	1269	800	684	581	548
Median (per participant)	97.5	65	57	47	44

In summary, 1269 trials were collected for the 12 participants, with a median of 97.5. Of the 1269 trials, 800 were considered valid, with 85.5 % of the valid trials being labelled, 72.63% of the valid trials being used for inverse dynamic calculations, and 68.5% of the valid trials being used for energy bursts calculations (Appendix G).

Appendix G provides a breakdown of the total number of trials, the total number of trials used to generate the energy bursts, and the total number of trials per obstacle condition.

4.3 Crossing leg adaptations to obstructed walking

4.3.1 Crossing leg average duration

The crossing leg gait cycle average duration was calculated and plotted as a function of obstacle height (Figure 13).

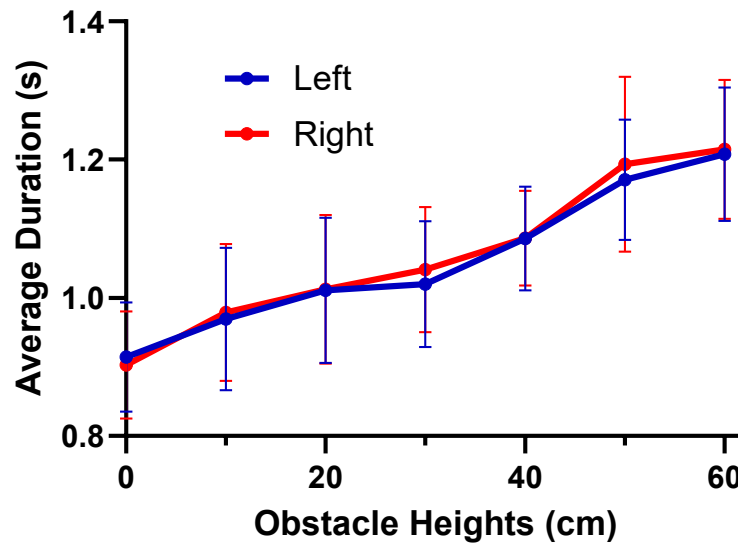


Figure 13. Average duration of the crossing leg gait cycle as a function of unilateral obstacle height. Obstacle heights were ranging from 10 to 60 centimeters (cm).

There was a significant main effect of obstacle height ($F(6,141)=98.99$, $p<0.0001$). There was, however, no main effect of leg ($F(1,141)=0.766$, $p=0.38$), nor was there an interaction between the two ($F(6,141)=0.29$, $p<0.93$). Post hoc comparisons using the Tukey HSD on obstacle height indicated that significant differences were found between height 0 cm and all the other heights ($p<0.001$), between height 10 and heights 30, 40, 50 and 60 cm ($p<0.01$), between height 20 and heights 40, 50 and 60 ($p<0.001$), between height 30 and heights 40, 50 and 60 cm ($p<0.01$), and between height 40 and height 50 cm ($p<0.001$), and between height 40 and height 60 cm ($p<0.001$).

4.3.2 Crossing leg lower limb joint angles during obstructed walking

Figure 14 displays, for descriptive purposes, the ensemble average of the joint angles of the able-bodied group across the hip (sagittal and frontal), knee (sagittal) and ankle (sagittal) during the walking conditions of the crossing leg. No statistical analyses

were conducted on these data. For sections and figures to follow, LCL and RCL (Figure 14, for example) are abbreviations for left and right crossing leg, respectively.

There seemed to be similar patterns were seen for the obstacle conditions in terms of joint angles. Up until 40% of the Gait Cycle (GC), there did not seem to be a lot of changes in the sagittal plane, as it looked like hip flexion increased during late stance and swing phase for the obstacle conditions. In the frontal plane, again similarities were seen in hip adduction angles until midstance (until around 30% of the GC), with an increase in hip abduction angles as obstacle height increased during late stance and swing phase. The knee seemed to flex more as obstacle height increased after 30% of the GC. The ankle seemed to be more dorsiflexed during late stance, less plantar flexed during the 40 to 60% period of the GC and more dorsiflexed during the swing phase for the obstacle conditions.

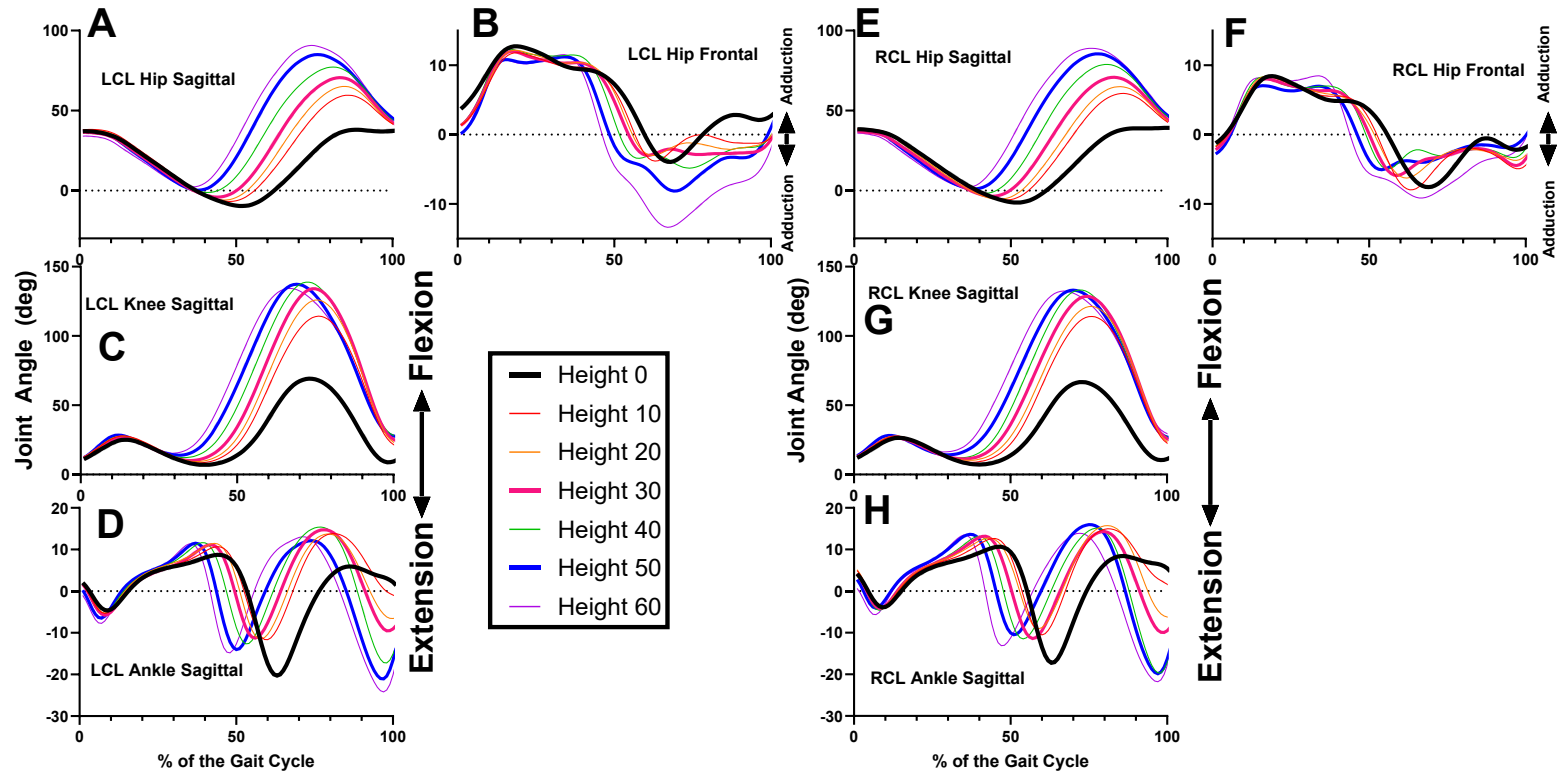


Figure 14. The ensemble average of the joint angles of the crossing legs during unobstructed and unilateral obstacles walking conditions. Positive Y angles: hip flexion, hip adduction, knee flexion and ankle dorsiflexion. LCL: left crossing leg, RCL: right crossing leg.

4.3.3 Crossing leg lower limb joint moments during obstructed walking

Figure 15 displays, for descriptive purposes, the ensemble average of the net joint moments of the able-bodied group across the hip (sagittal and frontal), knee (sagittal) and ankle (sagittal) during walking conditions on the crossing leg.

While patterns appeared consistent across all three joints during the initial half of the stance phase in obstacle conditions, subsequent adaptations to obstacle heights occurred. Hip flexion moment appeared to decrease for obstacle conditions from mid stance until mid swing. In the frontal plane, hip abduction moment seemed to decrease as obstacle height increased. Moreover, despite the usual abductor to adductor moment transition seen at around 55% of the GC for obstacle heights less than 40 cm, this transition for heights 50 and 60 cm was delayed as a new abductor moment seemed to emerge, to then transition into the usual adductor moment at around 60-65% of the GC for these two obstacles. Knee extensor moment appeared to increase as obstacle height increased during the 5 to 20% period of the GC. At around the 55 to 70% period of the GC, the knee exhibited a knee flexor moment seen only during obstacle conditions (knee extensor moment during unobstructed). Lastly for the knee, it looked like knee flexor moment decreased at the end of the swing as obstacle height increased. The ankle plantar flexor moment during push-off phase seemed to decrease as obstacle height increased.

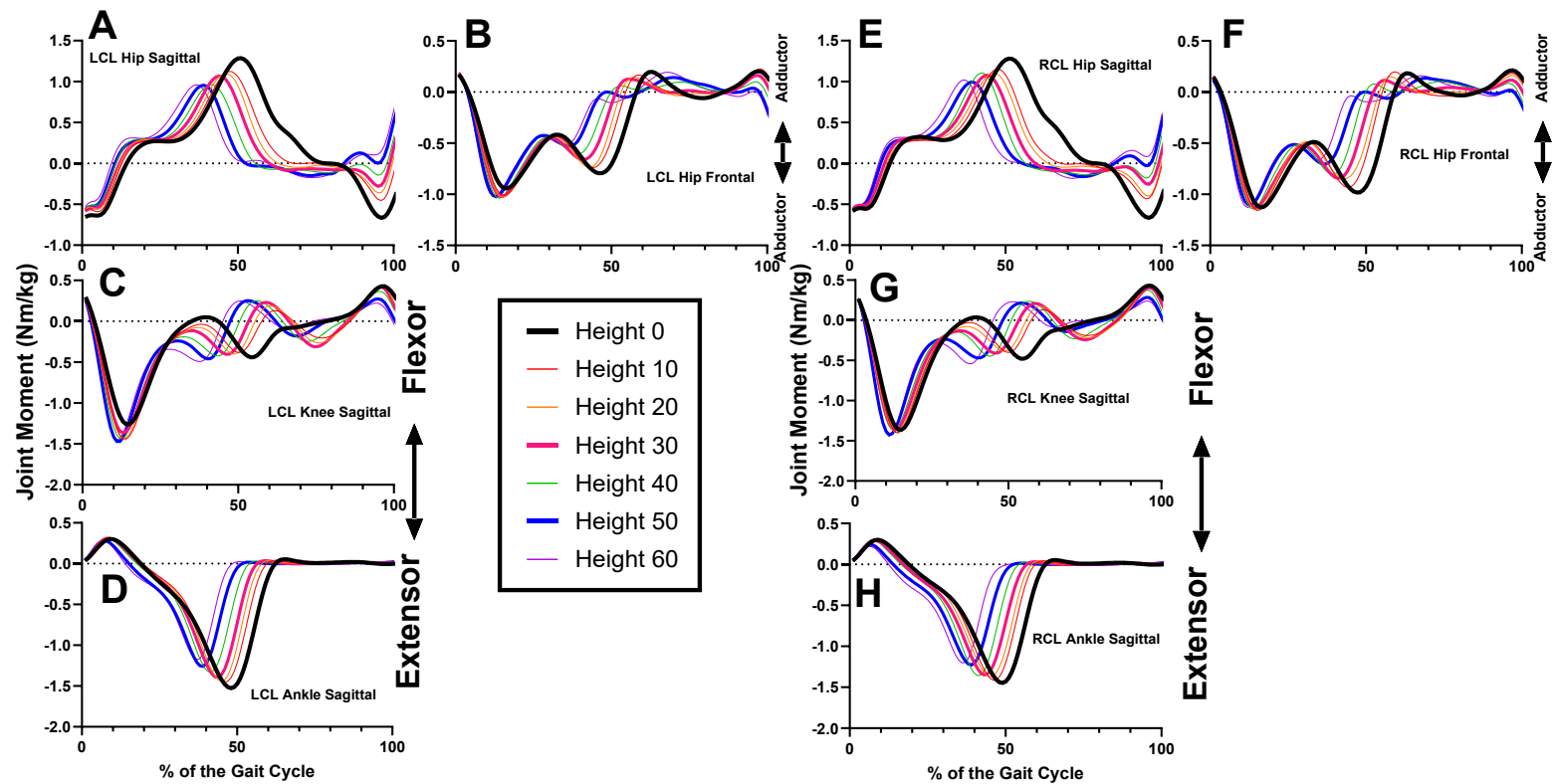


Figure 15. The ensemble average of the net joint moments of the crossing legs during unobstructed and unilateral obstacles walking conditions. Positive Y moments: hip flexion, hip adduction, knee flexion and ankle dorsiflexion. LCL: left crossing leg, RCL: right crossing leg.

4.3.4 Crossing leg lower limb joint powers during obstructed walking

Figure 16 displays, for descriptive purposes, the ensemble average of the net joint powers of the able-bodied group across the hip (sagittal and frontal), knee (sagittal) and ankle (sagittal) during our walking conditions on the crossing leg. This section focuses on the net joint power time history curves, whereas more information is provided in the next section regarding muscle power bursts.

The hip seemed to generate less power in the sagittal plane for the obstacle conditions during the 0 to 15% period of the GC. The hip looked like it generated less power during the swing phase. In the frontal plane, it appeared as if there was a new generation phase that was seen during the 50 to 65% period of the GC for heights 50 and 60 cm, compared to the usual absorption phase for heights less than 40 cm. At the knee, power absorption seemed to increase as obstacle height increased during the 5 to 15% period of the GC, while absorption seemed to decrease for the obstacle conditions during the initial part of the swing. Moreover, between the 55 to 70% period of the GC, a power generation phase emerged for the obstacle conditions, which was absent during unobstructed walking. At the ankle, there seemed to be more absorption during the stance phase, but less generation during the push off phase for the obstacle conditions.

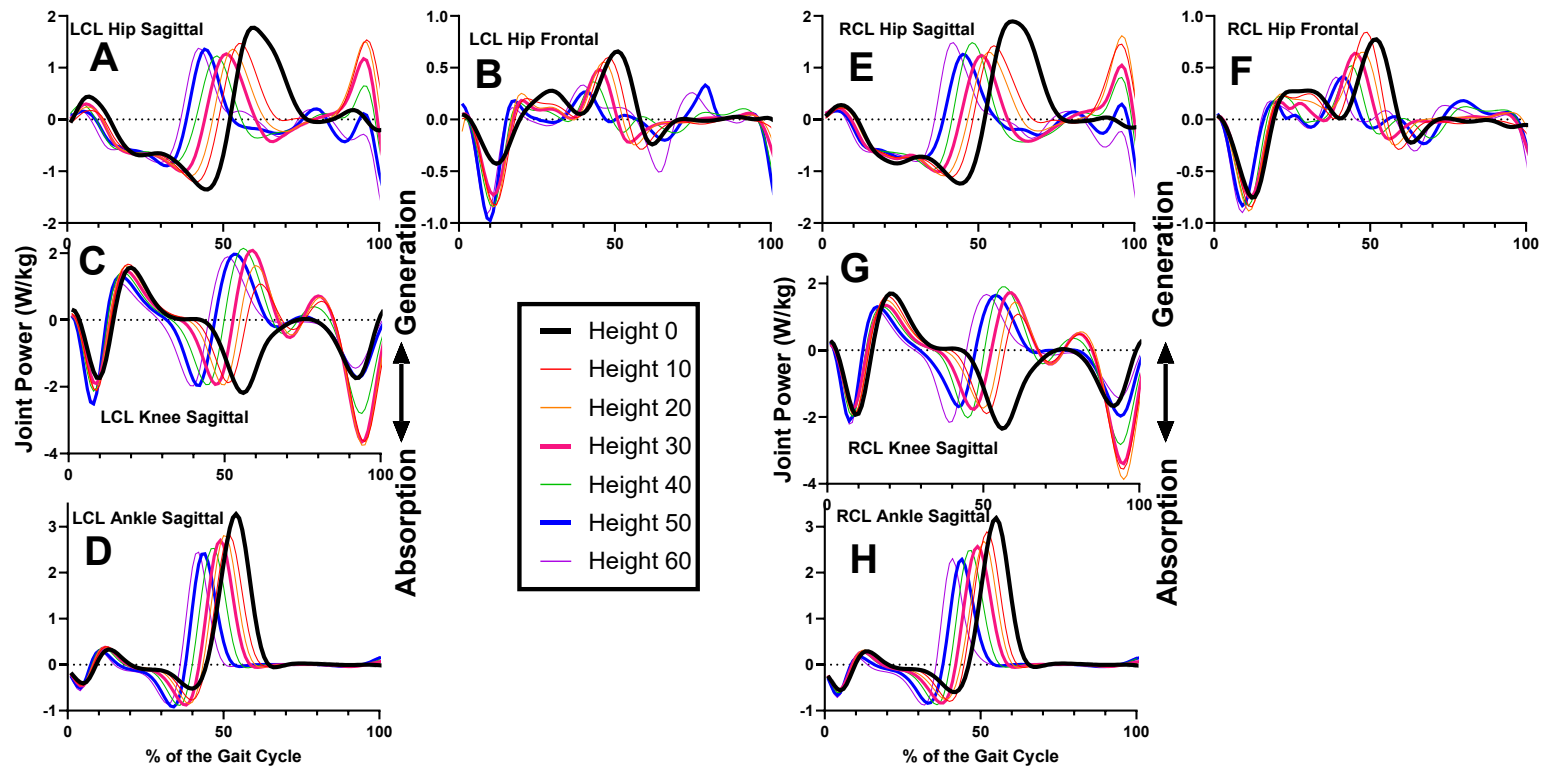


Figure 16. The ensemble average of the net joint powers of the crossing legs during unobstructed and unilateral obstacles walking conditions. Positive Y: energy generation. LCL: left crossing leg, RCL: right crossing leg.

4.3.5 Crossing leg anticipatory locomotor adjustments

Figure 17 displays, for descriptive purposes, the ensemble average of the selective muscle power bursts as a function of obstacle height for the crossing leg.

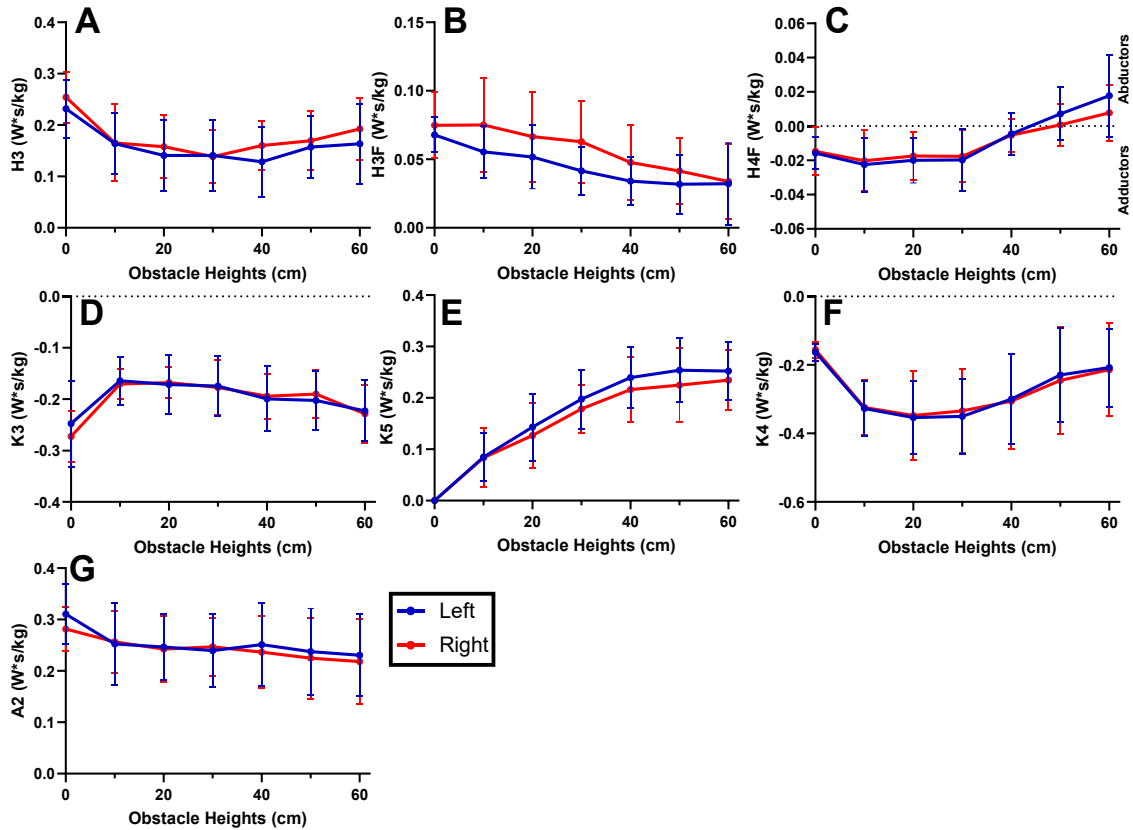


Figure 17. Mean selected muscle power bursts of the crossing leg as a function of unilateral obstacle height (cm) (Mean \pm 1SD). Positive power for the left (blue) and right (red) leg indicates energy generation. H3: hip flexor energy generation, H3F: hip abductor energy generation, H4F: transition of hip adductor energy absorption to hip abductor energy generation, K3: knee extensors energy absorption, K5: knee flexors energy generation, K4: knee flexors energy absorption, A2: ankle plantar flexors energy generation.

Shapiro Wilks' test revealed that the hip flexors energy generation (H3), the hip abductors energy generation (H3F), the hip adductors energy absorption (H4F), the knee extensors energy absorption (K3), the knee flexors energy generation (K5), the knee flexors energy absorption (K4) and the ankle plantar flexors energy generation (A2) were not normal. Levene's test on each outcome measure revealed no significant differences with obstacle height, meaning that the assumption of homogeneity of variances holds. The normality of the residuals for each outcome measure was assessed, and it revealed normality.

For the hip flexor energy generation (H3, Figure 17A), there was a significant main effect of obstacle height ($F(6,141)=19.55$, $p<0.001$), and a significant main effect of leg ($F(1,141)= 6.81$, $p<0.05$). However, there was no interaction between the two ($F(6,141)= 0.65$, $p=0.69$). Post hoc comparisons of the main effect of leg indicated that the right leg had higher average values than the left leg across all obstacle conditions. Moreover, post hoc comparisons of the main effect of obstacle height indicated that significant differences were found between height 0 cm and all the heights ($p<0.001$), between height 30 and height 60 cm ($p<0.05$), and between height 40 and height 60 cm ($p<0.05$).

For the hip abductors energy generation (H3F, Figure 17B), there was a significant main effect of obstacle height ($F(6,141)=18.21$, $p<0.001$) and main effect of leg ($F(1,141)=24.59$, $p<0.001$). However, there was no interaction between the two ($F(6,141)=1.06$, $p=0.39$). Post hoc comparisons of the main effect of leg indicated that the right leg had higher average values than the left leg across all obstacle conditions. Moreover, post hoc comparisons of the main effect of obstacle height indicated that

significant differences were found between height 0 and heights 30, 40, 50 and 60 cm ($p<0.01$), heights 10 and 20 with heights 40, 50 and 60 cm ($p<0.01$), and height 30 with heights 50 and 60 cm ($p<0.05$).

For the hip adductors energy absorption (H4F, Figure 17C), there was a significant main effect of obstacle height ($F(6,141)=22.83$, $p<0.001$). There was, however, no main effect of leg ($F(1,141)=0.42$, $p=0.52$) nor was there an interaction between the two ($F(6,141)=0.77$, $p=0.59$). Moreover, post hoc comparisons of the main effect of obstacle height indicated that significant differences were found between height 0 and heights 50 and 60 cm ($p<0.001$), between height 10 and heights 40, 50 and 60 cm ($p<0.001$), between height 20 and heights 40, 50 and 60 cm ($p<0.01$), between height 30 and heights 40, 50 and 60 cm ($p<0.01$), and between height 40 and 60 cm ($p<0.001$).

For the knee extensors energy absorption (K3, Figure 17D), there was a significant main effect of obstacle height ($F(6,141)=11.62$, $p<0.001$). There was, however, no main effect of leg ($F(1,141)=0.11$, $p=0.73$) nor was there an interaction between the two ($F(6,141)=0.36$, $p=0.90$). Moreover, post hoc comparisons of the main effect of obstacle height indicated that significant differences were found between height 0 cm and all the heights ($p<0.001$) apart from height 60 cm, and between heights 10, 20 and 30 with height 60 cm ($p<0.01$).

For the knee flexors energy generation (K5, Figure 17E), there was a significant main effect of obstacle height ($F(6,141)=136.94$, $p<0.0001$) and main effect of leg ($F(1,141)=6.48$, $p<0.05$). There was, however, no interaction between the two ($F(6,141)=0.47$, $p=0.83$). Post hoc comparisons of the main effect of leg indicated that the left leg had higher average values than the right leg across all obstacle conditions.

Moreover, post hoc comparisons of the main effect of obstacle height indicated that significant differences were found between height 0 cm and all the heights ($p < 0.001$), between height 10 cm and all the heights ($p < 0.001$), between height 20 cm and all the heights ($p < 0.001$), and between height 30 cm and all the heights ($p < 0.01$).

For the knee flexors energy absorption (K4, Figure 17F), there was a significant main effect of obstacle height ($F(6,141)=28.9$, $p < 0.001$). There was, however, no main effect of leg ($F(1,141)=0.0047$, $p=0.94$) nor was there an interaction between the two ($F(6,141)=0.15$, $p=0.98$). Moreover, post hoc comparisons of the main effect of obstacle height indicated that significant differences were found between height 0 cm and all the heights ($p < 0.01$) apart from height 60 cm, between height 10 and heights 50 and 60 cm ($p < 0.001$), between height 20 and heights 50 and 60 cm ($p < 0.001$), between height 30 and heights 50 and 60 cm ($p < 0.001$), and between height 40 and heights 50 and 60 cm ($p < 0.05$).

For the plantar flexors energy generation (A2, Figure 17G), there was significant main effect of obstacle height ($F(6,141)=8.56$, $p < 0.001$). There was, however, no main effect of leg ($F(1,141)=1.96$, $p=0.16$) nor was there an interaction between the two ($F(6,141)=0.57$, $p=0.75$). Moreover, post hoc comparisons of the main effect of obstacle height indicated that the only significant differences were found between height 0 cm and all the heights ($p < 0.01$).

4.4 Supporting leg adaptations to obstructed walking

4.4.1 Supporting leg average duration

Supporting leg gait cycle average duration was calculated and plotted as a function of obstacle height (Figure 18).

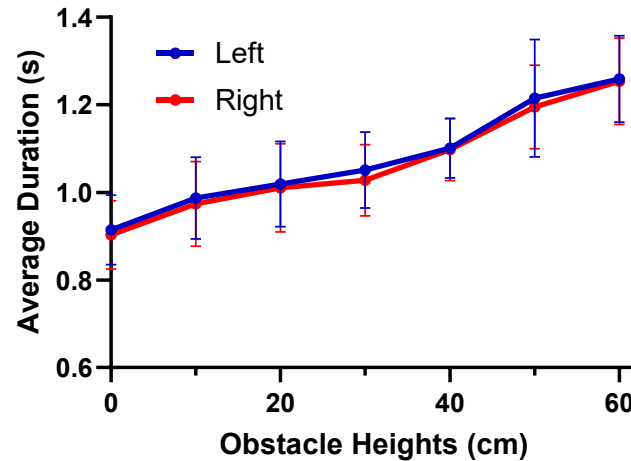


Figure 18. Average duration of the supporting leg gait cycle as a function of unilateral obstacle height. Obstacle heights were ranging from 10 to 60 centimeters (cm).

There was a significant main effect of obstacle height ($F(6,141)=124.19$, $p<0.0001$). There was, however, no main effect of leg ($F(1,141)=2.10$, $p=0.14$) nor was there an interaction between the two ($F(6,141)=0.11$, $p=0.99$).

Post hoc comparisons of the main effect of obstacle height indicated that significant differences were found between height 0 and all the other heights ($p<0.001$), between height 10 and heights 30, 40, 50 and 60 cm ($p<0.01$), between height 20 and heights 40, 50 and 60 cm ($p<0.001$), height 30 and heights 40, 50 and 60 cm ($p<0.01$), between heights 40 and heights 50 and 60 cm ($p<0.001$), and between height 50 and height 60 cm ($p<0.01$).

4.4.2 Supporting leg lower limb joint angles during obstructed walking

Figure 19 displays, for descriptive purposes, the ensemble average of the joint angles of the able-bodied group across the hip (sagittal and frontal), knee (sagittal) and ankle (sagittal) during obstructed walking conditions on the supporting leg. No statistical analyses were conducted on these data. For sections and figures to follow, LSL and RSL (Figure 19, for example) are abbreviations for left and right supporting leg, respectively.

There seemed to be similar patterns for obstacle conditions that were seen at the hip and knee joints in the sagittal plane. However, in the frontal plane for the hip, the hip adopted adduction angles during the stance phase for lower obstacle heights (left: 0 to 30 cm, right: 0 to 20 cm) compared to abduction angles for higher heights (left: 40 to 60 cm, right: 30 to 60 cm). At the ankle, a heel strike was seen for heights 0 to 30 cm, due to the angles transitioning from dorsiflexion to plantar flexion and then dorsiflexion again during the 0 to 20% period of the GC. However, for heights 40 to 60 cm, a seemingly forefoot strike. This could be associated with the plantar flexion angles seen from the 0 to 25-30% period of the GC, which then adopted a dorsiflexion angle. The ankle also seemed to be more plantar flexed during the swing phase as obstacle height increased.

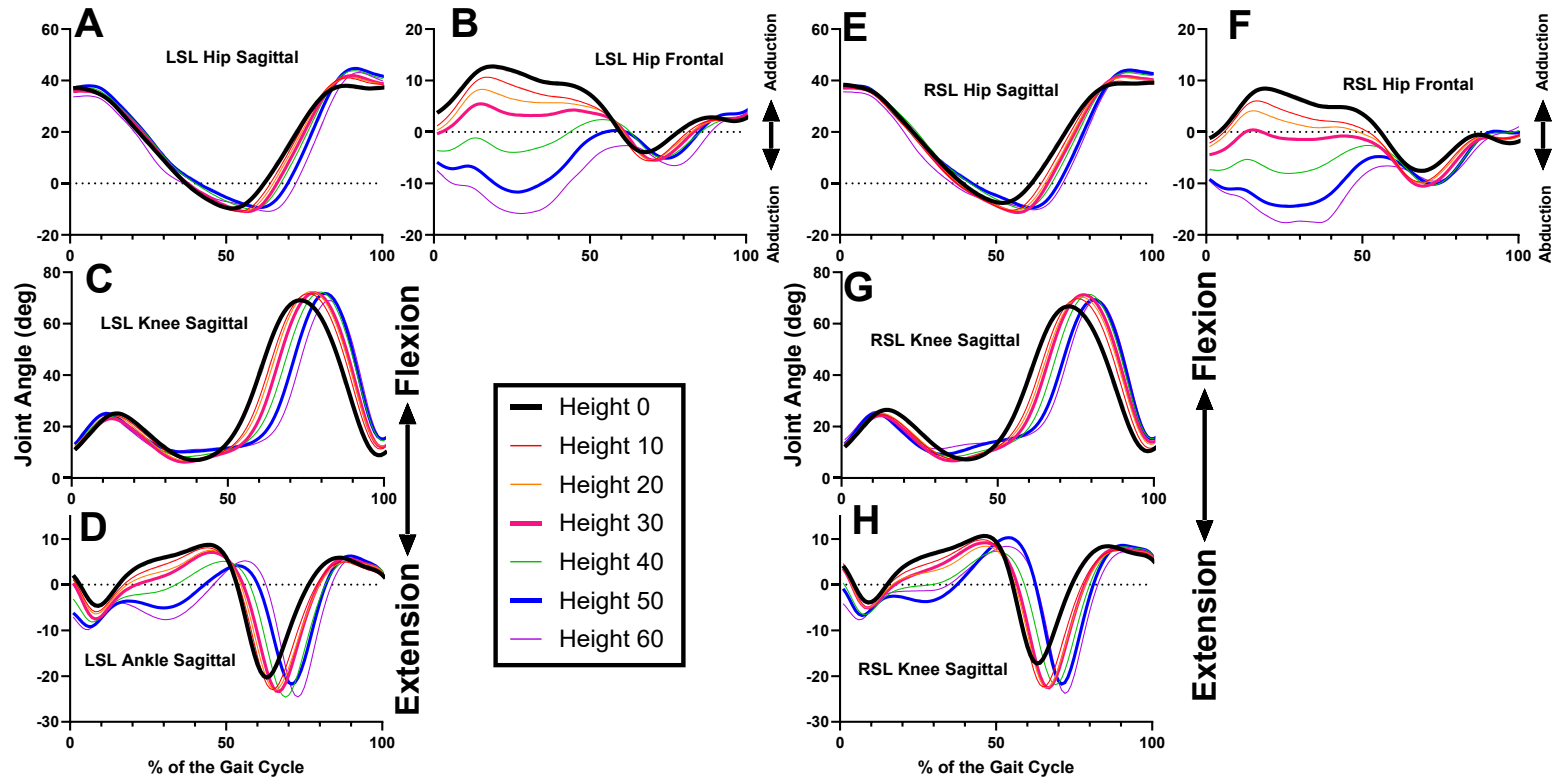


Figure 19. The ensemble average of the joint angles of the supporting legs during unobstructed and obstructed walking conditions. Positive Y angles: hip flexion, hip adduction, knee flexion and ankle dorsiflexion. LSL: left supporting leg, RSL: right supporting leg.

4.4.3 Supporting leg lower limb joint moments during obstructed walking

Figure 20 displays, for descriptive purposes, the ensemble average of the net joint moments of the able-bodied group across the hip (sagittal and frontal), knee (sagittal) and ankle (sagittal) during obstructed walking conditions on the supporting leg.

There seemed to be similar patterns for obstacle conditions were seen across the three joints. The hip extensor moment seemed to decrease as obstacle height increased during the 20 to 50% period of the GC. In the frontal plane, it seemed that the abductor moment during the stance phase seemed to decrease as obstacle height increased. At the knee, minimal changes were seen. At the ankle, the peak extensor moment seemed to be similar for obstacle conditions. However, different adaptations were reported across obstacle conditions. There was a dorsiflexor moment at weight acceptance that increased as obstacle height increased. From the 20 to 50% period of the GC, the ankle displayed an extensor moment across all conditions. This extensor moment was ascending for heights 0 to 30 cm. For heights 40 to 60 cm, however, it was still an extensor moment, but during the 25 to 40% period of the GC, the extensor moment seemed to remain constant and then increased.

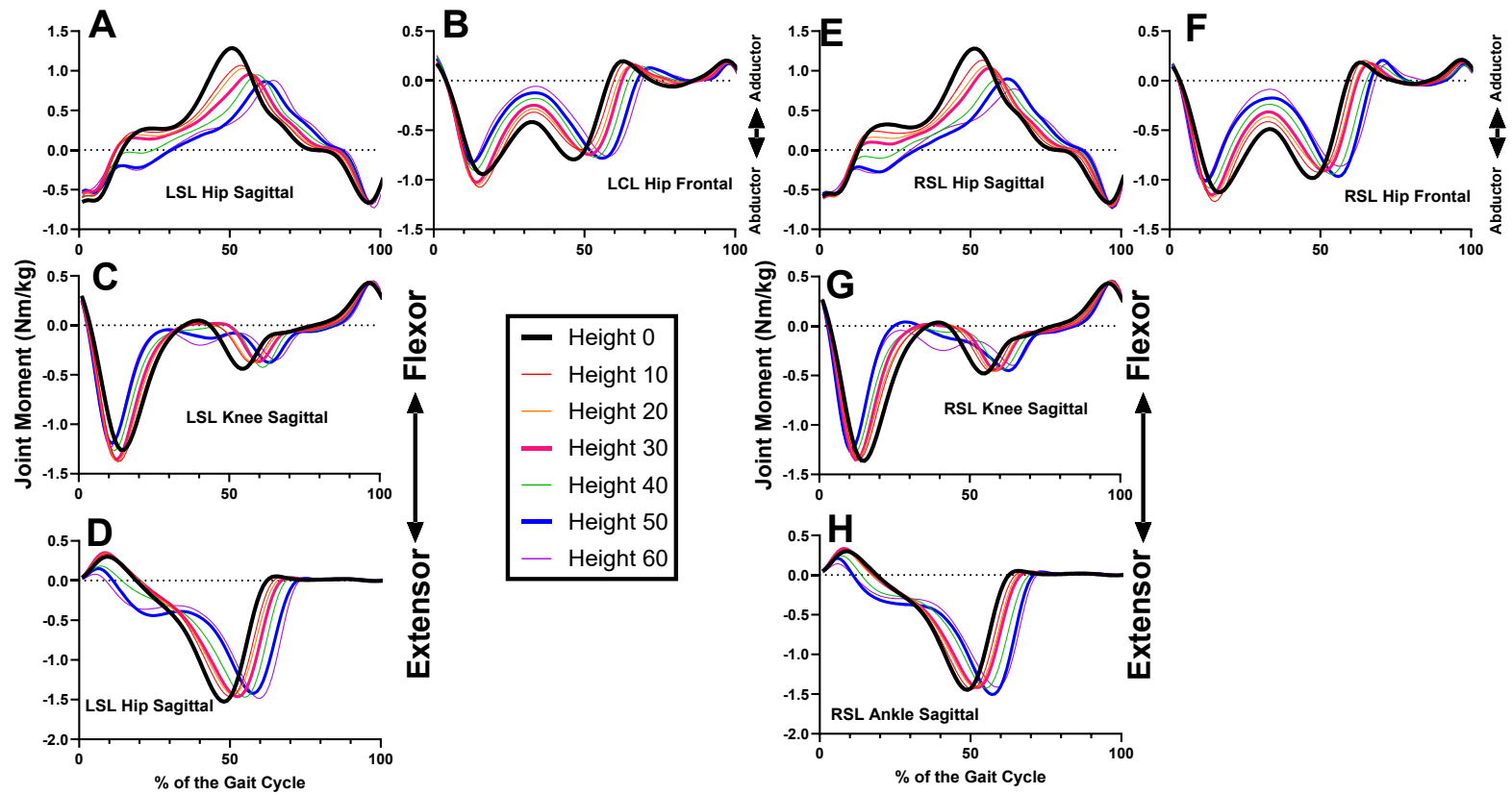


Figure 20. The ensemble average of the net joint moments of the supporting legs during unobstructed and obstructed walking conditions. Positive Y moments: hip flexion, hip adduction, knee flexion and ankle dorsiflexion. LSL: left supporting leg, RSL: right supporting leg.

4.4.4 Supporting leg lower limb joint powers during obstructed walking

Figure 21 displays, for descriptive purposes, the ensemble average of the net joint powers of the able-bodied group across the hip knee and ankle during obstructed walking conditions on the supporting leg. This section focuses on the net joint power time history curves, whereas more information is provided in the next section regarding muscle power bursts.

Similar patterns across obstacle conditions were observed at the hip, knee, and ankle joints. In the sagittal plane at the hip, increasing obstacle height was associated with greater and longer-lasting power generation during the initial stance phase, followed by a decrease in absorption during the latter stance phase. In the frontal plane, power absorption during the first 10–15% of the gait cycle (GC) decreased with increasing obstacle height, followed by an apparent increase in generation across conditions. Around 45–60% of the GC, power generation was observed for heights of 0–30 cm, whereas power absorption occurred at heights of 40–60 cm.

At the knee, no change was observed during the 0–15% period of the GC. However, from 15–40%, increased obstacle height was associated with reduced power generation, followed by decreased absorption during 45–70% of the GC.

At the ankle, power absorption increased with obstacle height during the first 10% of the GC. For heights of 0–30 cm, a power generation phase occurred between 10–20%, followed by absorption from 20–45%. In contrast, at heights of 40–60 cm, initial power generation was greater and extended from 20–35%, followed by an absorption phase continuing until push-off.

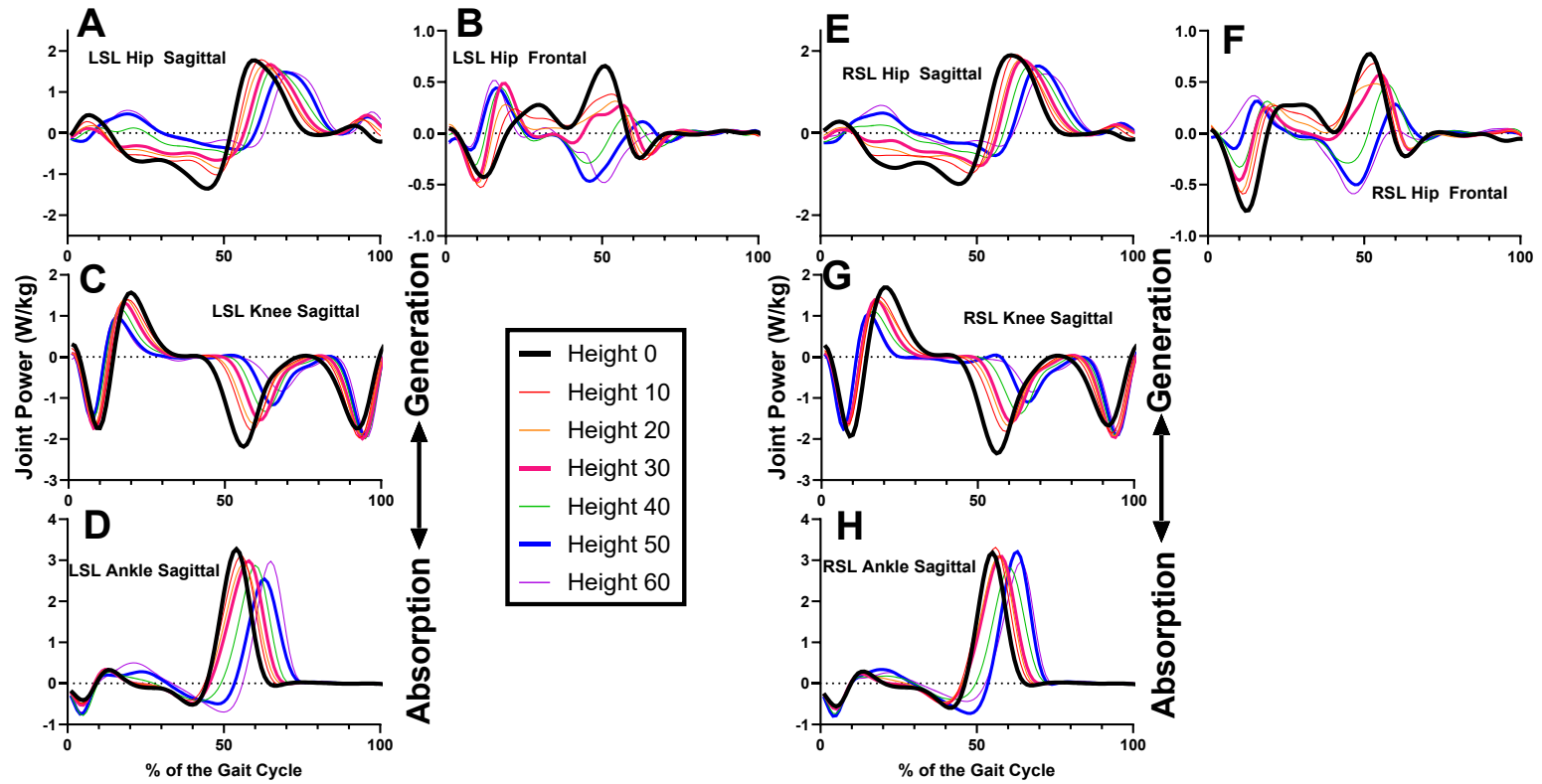


Figure 21. The ensemble average of the net joint powers of the supporting legs during unobstructed and obstructed walking conditions. Positive Y: energy generation. LSL: left supporting leg, RSL: right supporting leg.

4.4.5 Supporting leg anticipatory locomotor adjustments

4.4.5.1 Supporting leg ALAs at the hip, knee and ankle

Figure 22 displays, for descriptive purposes, the ensemble average of the selective muscle power bursts as a function of obstacle height for the supporting leg.

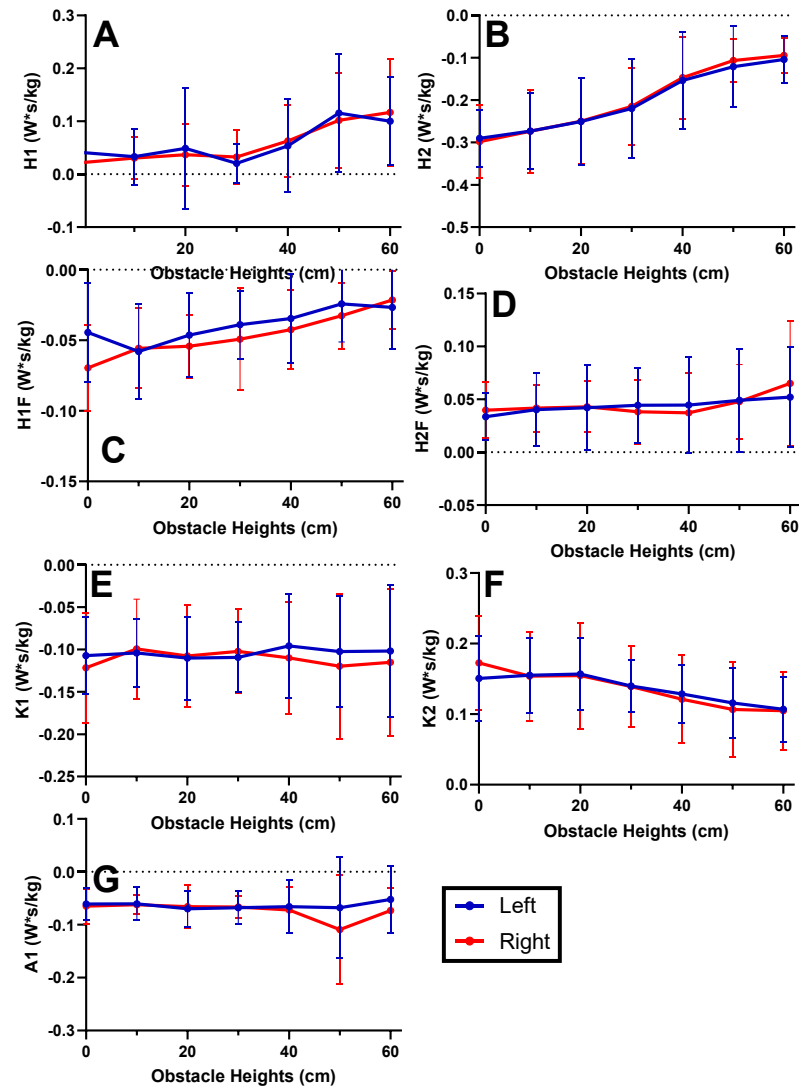


Figure 22. Mean selected muscle power bursts of the supporting legs as a function of unilateral obstacle height (cm) (Mean \pm 1SD). Positive power for the left (blue) and right (red) leg indicates energy generation. H1: hip extensors energy generation, H2: hip flexors energy absorption, H1F: hip abductors energy absorption, H2F: hip abductors energy generation, K1: knee extensors energy absorption, K2: knee extensors energy generation, A1: ankle plantar flexors energy absorption.

Shapiro Wilks' test revealed that the hip extensors energy generation (H1), the hip flexors energy absorption (H2), the hip abductors energy absorption (H1F), the hip abductors energy generation (H2F), the knee extensors energy absorption (K1), the knee extensor energy generation (K2), and the ankle plantar flexors energy absorption (A1), were not normal. Levene's test on each outcome measure revealed no significant differences with obstacle height, meaning that the assumption of homogeneity of variances holds. The normality of the residuals for each outcome measure was assessed, and it revealed normality.

For the hip extensors energy generation (H1, figure 22A), there was a significant main effect of obstacle height ($F(6,141)=14.23$, $p<0.001$). There was, however, no main effect of leg, ($F(1,141)=0.0297$, $p=0.86$) nor was there an interaction between the two ($F(1,141)=0.466$, $p=0.83$). Moreover, post hoc comparisons of the main effect of obstacle height indicated that significant differences were found between the heights 0 and heights 50 and 60 cm ($p<0.001$), height 10 and heights 50 and 60 cm ($p<0.001$), height 20 and heights 50 and 60 cm ($p<0.001$), height 30 and heights 50 and 60 cm ($p<0.001$), and height 40 and heights 50 and 60 cm ($p<0.001$).

For the hip abductors energy absorption (H1F, figure 22C), there was a significant main effect of obstacle height ($F(6,141)=6.40$, $p<0.001$). There was, however, no main effect of leg ($F(1,141)=3.80$, $p=0.053$) nor was there an interaction between the two ($F(1,141)=0.93$, $p=0.47$). Moreover, post hoc comparisons of the main effect of obstacle height indicated that significant differences were found between height 0 and heights 50 and 60 cm ($p<0.01$), height 10 and heights 50 and 60 cm ($p<0.01$), height 20 and heights 50 and 60 cm ($p<0.05$).

For the hip flexors energy absorption (H2, figure 22B), there was a significant main effect of obstacle height ($F(6,141)=64.64$, $p<0.001$). There was, however, no main effect of leg ($F(1,141)=0.30$, $p=0.58$) nor was there an interaction between the two ($F(1,141)=0.13$, $p=0.99$). Moreover, post hoc comparisons of the main effect of obstacle height indicated that significant differences were found between height 0 and all the other heights ($p<0.05$) apart from height 10, height 10 and all the other heights ($p<0.01$), height 20 and heights 40, 50 and 60 cm ($p<0.001$), height 30 and heights 40, 50 and 60 cm ($p<0.001$), and height 40 and heights 50 and 60 cm ($p<0.01$).

For the hip abductors energy generation (H2F, figure 22D), there was a significant main effect of obstacle height ($F(6,141)=2.64$, $p<0.05$). There was, however, no main effect of leg ($F(1,141)=0.05$, $p=0.81$) nor was there an interaction between the two ($F(1,141)=0.35$, $p=0.91$). Moreover, post hoc comparisons of the main effect of obstacle height indicated that significant differences were found between height 0 and height 60 cm ($p<0.05$).

For the knee extensors energy absorption (K1, figure 22E), there was no main effect of obstacle height ($F(6,141)=0.25$, $p=0.95$), main effect of leg ($F(1,141)=0.86$, $p=0.35$) nor interaction between the two ($F(6,141)=0.34$, $p=0.91$).

For the knee extensors energy generation (K2, figure 22F), there was a significant main effect of obstacle height ($F(6,141)=10.32$, $p<0.001$). There was, however, no main effect of leg ($F(1,141)=0.0008$, $p=0.97$) nor was there an interaction between the two ($F(6,141)=0.53$, $p=0.77$). Moreover, post hoc comparisons of the main effect of obstacle height indicated that significant differences were found between height 0 and heights 40,

50 and 60 cm ($p < 0.01$), height 10 and heights 50 and 60 cm ($p < 0.001$), height 20 and heights 40, 50 and 60 cm ($p < 0.05$), and between height 30 and height 60 cm ($p < 0.05$).

For the plantar flexors energy absorption (A1, figure 22G), there was no main effect of obstacle height ($F(6,141)=1.04$, $p=0.40$), main effect of leg ($F(1,141)=2.20$, $p=0.14$) nor interaction between the two ($F(6,141)=0.84$, $p=0.54$).

4.4.5.2 Supporting leg ALA at the ankle

During unobstructed walking, the net ankle joint power time history curve consists of A1 (plantar flexor energy absorption) and A2 (plantar flexor energy generation) (Figure 2). With the addition of an obstacle, adaptations at the supporting leg ankle occurred, resulting in the emergence of a new energy generation (A1G) along with an energy absorption by the plantar flexors (A1A) (Figure 22B), followed by the usual A2 at push-off.

For the plantar flexors energy generation (A1G, figure 23C), there was a significant main effect of obstacle height ($F(6,141)=6.74$, $p < 0.001$). There was, however, no main effect of leg ($F(1,141)=0.0024$, $p=0.96$) nor was there an interaction between the two ($F(6,141)=0.69$, $p=0.65$). Moreover, post hoc comparisons of the main effect of obstacle height indicated that significant differences were found between height 0 and heights 50 and 60 cm ($p < 0.05$), height 10 and heights 50 and 60 cm ($p < 0.05$), height 20 and height 60 ($p < 0.01$), height 30 and heights 50 and 60 cm ($p < 0.05$), height 40 and height 60 cm ($p < 0.05$).

For the plantar flexors energy absorption (A1A, figure 23D), there was a significant main effect of obstacle height ($F(6,141)=6.87$, $p < 0.001$). There was, however,

no main effect of leg ($F(1,141)=0.47$, $p=0.49$) nor was there an interaction between the two ($F(6,141)=0.61$, $p=0.71$). Moreover, post hoc comparisons of the main effect of obstacle height indicated that significant differences were found between height 0 and heights 50 and 60 cm ($p<0.01$), height 10 and heights 50 and 60 cm ($p<0.01$), height 20 and height 60 cm ($p<0.01$), height 30 and height 60 cm ($p<0.001$), height 40 and height 60 cm ($p<0.05$).

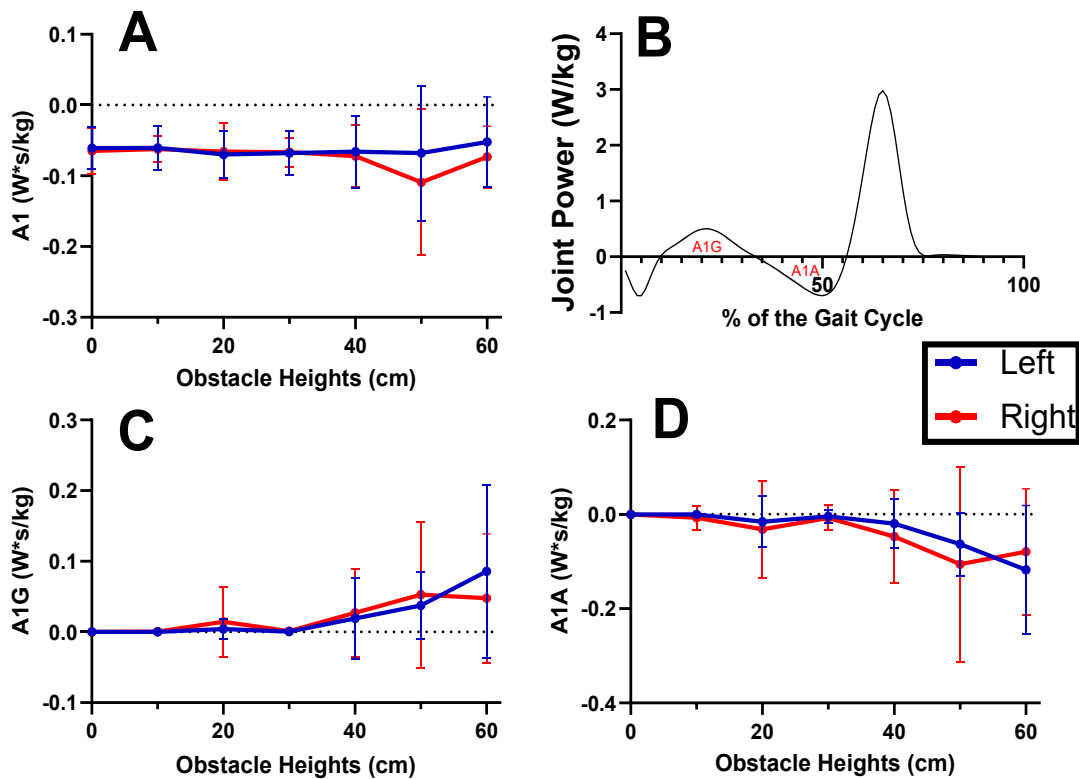


Figure 23. Mean selected ankle muscle power bursts of the supporting legs as a function of unilateral obstacle height (cm) (Mean \pm 1SD). Plots on top left, bottom left and bottom right represent left and right selective muscle power burst as a function of obstacle height. Positive power for the left and right leg indicates energy generation. Figure 23B represents the net ankle joint power curve throughout the gait cycle of the left supporting leg of the able-bodied group, which showcases the new behaviour at the ankle. Positive power corresponds to energy generation. A1G: Plantar flexors energy generation, A1A: Plantar flexors energy absorption.

Chapter 5: Discussion

The first aim of this study was to investigate how able-bodied participants adapted to unilateral obstacles of a wide range of heights. To do so, participants were recruited and performed obstructed walking across seven different heights (including unobstructed). Synchronized motion capture and force plate systems were used to acquire the kinematic and kinetic data. While variables such as joint angles and moments provide insights on gait, a more insightful and better understanding of its control was done by analyzing net joint power across the three joints of the lower body. Muscle power bursts of the crossing and supporting legs were calculated and analyzed to understand the behaviour of each limb further and whether they operated differently. When going over unilateral obstacles, the pre-swing and initial swing phase adaptations for the crossing leg were: the emergence of the knee flexors energy generation (K5) that increased as obstacle height increased, a reduction in the knee extensors energy absorption (K3), the hip adductors energy absorption (H4F), the hip flexors energy generation (H3), the hip abductors energy generation (H3F), and the ankle plantar flexors energy generation (A2). In the terminal swing phase, there was an increase in the knee flexors energy absorption (K4). The initial contact and loading response phase adaptations for the supporting leg were: an increase in the hip extensors energy generation (H1), the hip abductors energy generation (H2F), the emergence of the ankle plantar flexors energy generation (A1G), the plantar flexors energy absorption (A1A), a reduction in the hip abductors energy absorption (H1F), the knee extensors energy generation (K2), the hip flexors energy absorption (H2), no change in the knee extensors energy absorption (K1), and ankle plantar flexors energy absorption (A1).

The secondary aim was to determine if there is lateralization of the ALAs of able-bodied participants during unilateral obstructed walking. Significant differences between right and left ALAs of the able-bodied participants were found for the knee flexor energy generation (K5), the hip flexor energy generation (H3) and the hip abductors energy generation (H3F). No differences were found for the remaining outcome measures.

5.1 Able-bodied participants' adaptations to obstructed walking

To ensure safe crossing over the obstacle and minimize tripping, individuals adopt strategies that involve elevating the toe high enough (higher foot elevation) and providing upward support by the supporting leg (upward bias of the swing limb) (Patla and Rietdyk, 1993). The former involves altering the muscle energy flow of the crossing leg, while the latter involves increasing the vertical GRF on the stance limb which would cause a hip hiking on the crossing leg (Patla and Rietdyk, 1993).

5.1.1 Mechanisms of elevating the foot higher

The findings of the study and their association with the first hypothesis of the specific aim on able-bodied participants can be found in Table 5.

Table 5. Summary of the crossing leg energy burst changes observed during the unobstructed and obstructed walking conditions.

Outcome measure	Hypothesis	Result	Hypothesis supported?
Knee flexor energy generation (K5)	Increase	Increase	Yes
Knee extensor energy absorption (K3)	Decrease	Decrease	Yes
Hip flexor energy generation (H3)	Decrease	Decrease	Yes

Hip abductor energy generation (H3F)	Decrease	Decrease	Yes
--------------------------------------	----------	----------	-----

Able-bodied participants adapted to unilateral obstacles by seemingly increasing flexion angles at the hip, knee and ankle. These adaptations allowed for adequate toe elevation to cross the obstacle. These findings seem to be consistent with previous studies, which have reported an increased flexion at all three lower-body joints to clear obstacles (McFadyen and Carnahan, 1997; McFadyen and Winter, 1991; Patla and Rietdyk, 1993). Notably, as in these earlier studies, there seemed to be minimal change in joint angles at the hip, knee, and ankle leading up to the obstacle and prior to the swing phase. This supports the interpretation that limb elevation adaptations occur primarily during the latter part of the stance phase, just before the obstacle interaction (McFadyen et al., 1993). Additionally, Ladouceur (2025) discussed the kinematic behaviour across the three joints in their study, where the hip joint flexion increased linearly as obstacle height increased, while the knee and ankle joints increased with an exponential association function.

5.1.1.1 Adaptations occurring at the end of the stance phase and early swing phase

The findings of this study aligned with previous literature regarding the emergence of the knee flexor (K5) strategy during obstructed walking on the crossing leg (MacLellan, 2017; McFadyen et al., 1993; McFadyen and Prince, 2002; McFadyen and Winter, 1991; Niang and McFadyen, 2004; Patla et al., 1991). This strategy, driven by energy generation from the knee flexors (MacLellan, 2017; McFadyen et al., 1993; McFadyen and Winter, 1991), was essential for lifting the crossing leg foot to an adequate height and preventing tripping. The emergence of the knee flexors energy

generation (K5) was concomitant to a decrease in knee extensors energy absorption (K3) and hip flexors energy generation (H3) (McFadyen and Winter, 1991). The reorganized knee flexor strategy enhanced flexion at both the knee and hip joints, with the hamstrings playing a key role in this process (McFadyen and Winter, 1991). The hamstrings, a bi-articulate muscle responsible for extending the hip and flexing the knee (Stewart et al., 2008), significantly contributed to hip flexion during the swing phase due to intersegmental dynamics among the hip, knee, and ankle (Patla and Prentice, 1995). Bi-articular muscles tend to decrease their activation when acting as agonists on one joint and antagonists on another, as seen with the hamstrings during squats (Yamashita, 1988). This is important for understanding the role of the hamstrings during obstructed walking, as inactivation of these muscles would reduce hip flexion. Although the hip moment decreased, the increased hip flexion resulted from passive moments generated by the surrounding segments, contributing to both hip and knee flexion simultaneously (McFadyen and Carnahan, 1997; Patla and Prentice, 1995). Additionally, the increase in K5 muscle power burst as a function of unilateral obstacle height was consistent with the exponential increase in K5 energy burst seen by Ladouceur (Ladouceur, 2025), while the hip flexors energy generation (H3) and the knee extensors energy absorption (K3) decreased as obstacle height increased (McFadyen et al., 1993; Winter et al., 1990) (Figure 16).

Not only does the hip contribute significantly to total body work in the sagittal plane, but it also plays a key role in the frontal plane (Eng and Winter, 1995). During the swing phase, the hip abductors energy generation (H3F) and the hip adductors energy absorption (H4F) are responsible for providing thigh control. The hip abductors energy

generation (H3F), responsible for raising the pelvis during unobstructed walking and shifting the CoM towards the stance leg (Eng and Winter, 1995), significantly decreased as obstacle height increased (Figure 17B). This adaptation was reported in bilateral obstacles, and this decrease was attributed to a reduction in the vertical impulse during the initial double support phase (Patla and Rietdyk, 1993). This phase reflects knee flexion during the weight acceptance of the supporting leg, which results in assisting in hip hiking on the crossing leg to provide adequate toe placement elevation (Patla and Rietdyk, 1993). This decrease in hip abductors energy generation (H3F) can be somewhat corroborated by a study investigating hip frontal plane behaviour during uphill walking. This study showed that hip abductors energy generation (H3F) decreased during uphill walking (Yang et al., 2018).

Another explanation would be the modulation of the energy absorption by the hip adductors (H4F) for lower heights that transition into a generation phase by the hip abductors for higher obstacles (Figure 17C). As suggested in the literature review, during unobstructed walking, the energy absorption by the hip adductors (H4F) at the early swing phase might be used to control the movement of the thigh during the swing phase. The result of this study showed that the hip adductors energy absorption (H4F) decreased as obstacle height increased. Interestingly, this energy absorption by the hip adductors was converted into energy generation by the abductors at obstacle heights of 50 and 60 cm. This finding suggested a shift from the net hip adductors moment to the net hip abductors moment, resulting in hip circumduction like movement for higher obstacle heights. The transition of the hip adductor energy absorption to hip abductor energy

generation (H4F) is a novel variable that has not been discussed in the literature, for this reason, further research regarding this should be conducted.

The energy generation by the plantar flexors (A2) plays an important role during unobstructed walking, helping to accelerate the leg during push-off, as it reduces energy dissipation in the contralateral leg during ground contact (Zhao et al., 2021). A lack of ankle plantar flexors energy generation (A2) would require the hip flexors to increase their work to propel the leg forward (Judge et al., 1996). However, during obstructed walking, there is a decrease in the ankle plantar flexors energy generation (A2) in comparison to the unobstructed condition. This finding contrasted with the literature, which reported no differences in the ankle plantar flexors energy generation (A2) for obstacles set at 10% of leg length. (McFadyen et al., 1993; McFadyen and Winter, 1991). A possible reason for this decrease could be due to the increase in tibialis anterior electromyographic activity (McFadyen and Winter, 1991; Patla et al., 1991; Patla and Rietdyk, 1993). This increase in tibialis anterior activity is one of the proposed strategies to provide sufficient flexion of the foot. This would counteract the plantar flexion and decrease the plantar flexor angular velocity at toe-off (Patla and Rietdyk, 1993). This is necessary to ensure adequate clearance at the ankle by providing greater dorsiflexion to cross over the obstacle (Patla and Rietdyk, 1993), seemingly occurring around push-off as obstacle height increases (Figures 29D, H).

In summary, for the crossing leg adaptations, the higher elevation of the foot strategy was characterized by a flexor strategy with decreased plantar flexor energy generation (A2), increased knee and hip flexion with the emergence of knee flexors energy generation (K5), a possible decrease in leg rotation velocity at the hip through a

reduction in the hip flexor energy generation (H3) and a possible increase in thigh abduction (hip circumduction) through the reduction in hip adductor energy absorption (H4F), that transitioned into hip abductor energy generation for higher obstacles.

5.1.1.2 Adaptations occurring at the end of the swing phase

It is important to note that some changes in the muscle energy flow also occur at the end of the swing phase after having cleared the obstacle. In the present study, the knee flexors energy absorption (K4) increased across most obstacle conditions, with the exception of height 60 cm. This increase was significantly different from the energy absorption observed during unobstructed walking, specifically during the end swing phase, when the knee flexors control the shank's forward acceleration in preparation for foot contact. (McFadyen and Carnahan, 1997). This increase in the knee flexors energy absorption (K4) for obstacle conditions aligned with a previous study (McFadyen and Carnahan, 1997). However, despite the increase in power absorption, there was no noticeable change in flexor moment. A possible explanation could be attributed to the increased velocities at the knee, which would allow greater energy absorption by the knee flexors without a change in moment, as a greater amount of energy was absorbed for the same period (McFadyen and Carnahan, 1997). Additionally, the increased energy absorption and decreased hip extensor moment during end swing were probably caused by passive flexor moments from the thigh's angular and linear movement (McFadyen and Carnahan, 1997; Patla and Prentice, 1995).

5.1.2 Mechanisms of upward bias of the swing limb

The findings of the study and its association with the second hypothesis of specific aim one of able-bodied participants can be found in Table 6.

Table 6. Summary of the supporting leg energy burst change observed during the unobstructed and obstructed walking conditions.

Outcome measure	Hypothesis	Result	Hypothesis supported?
Hip abductor energy generation (H1F)	Decrease	Decrease	Yes

Ensuring adequate toe clearance of the crossing leg involves the two strategies of upward bias of the stance limb and increase in flexion of the crossing leg (higher foot elevation) (Patla et al., 1991; Patla and Rietdyk, 1993). These two strategies go hand in hand to provide sufficient clearance. For lower obstacle heights, simply increasing flexion of the crossing leg would be sufficient to provide this clearance (Ladouceur et al., 2005). However, this strategy by itself was not enough for higher obstacles, as hip hiking (due to an increase in greater trochanter elevation) played a significant role as its contribution to clearance increased from 5 to 38%, while the contribution of lower limb flexion decreased from 95 to 62% (Ladouceur, 2025). This suggests that hip hiking was achieved due to increased vertical impulse on the supporting leg, which lifts the CoM high enough to cross over the obstacle (McFadyen and Prince, 2002).

Not many changes were seen in joint angles of the supporting leg at the hip and the knee in the sagittal plane. However, notable changes were seen during the stance phase in the frontal plane at the hip and sagittal plane at the ankle. For obstacles less than 40 cm, a strategy involving hip adduction was observed, along with heel strike concomitant with the transition from dorsiflexion to plantar flexion during the stance phase. In contrast, for heights greater than 40 cm, a hip abduction strategy and a forefoot strike due to plantar flexion throughout the stance phase were observed. This suggests

kinematic adaptations occurring that are influenced by moments and powers acting on those joints.

In the sagittal plane, the hip extensors are active by generating power (H1) to accept the weight of the body, control the forward momentum of the trunk, and extend the hip (Neumann, 2016), while also providing enough power to raise the CoM. As obstacle height increased, there was greater demand for power generation by the hips (Figure 21). This power became especially apparent for obstacles at heights of 50 and 60 cm. This finding is corroborated by the previous results showing that greater trochanter elevation on the crossing leg contributed to 38% of the limb's elevation for higher heights, compared to just 5% for lower heights (Ladouceur, 2025). This substantial increase in the hip extensors energy generation (H1) was a mechanism that allowed the pelvis to elevate during early to mid stance, hence creating an upward bias of the swing limb to an adequate toe clearance height.

Following this power generation at the hip, the hip flexors absorb energy (H2) to decelerate hip extension (Neumann, 2016). An increase in the hip flexors energy absorption (H2) means that more energy is absorbed by the hips, which can potentially lead to dropping the pelvis. This would counteract the process of elevating the pelvis to provide adequate height for foot clearance. For this reason, as obstacle height increased, the hip flexors energy absorption (H2) further decreased to assist in keeping the pelvis elevated. Additionally, knee extensors energy generation (K2) decreased as obstacle height increased. A possible explanation to the decrease in the knee extensor energy generation (K2) and the hip flexors energy absorption (H2) could be concomitant with a decrease in activation of the rectus femoris, a bi-articulate muscle responsible for hip

flexion and knee extension. This suggestion needs to be investigated using electromyography. A different interpretation can be put forward based on a study conducted to investigate muscular coordination during gait through dynamic simulations (Zajac et al., 2003), where it was reported that during the early stance phase, the uniarticular quadriceps and hip extensors muscle groups (vasti and gluteus maximus, respectively) are responsible for providing support to the body and facilitating forward progression (Neptune et al., 2004). In addition to decelerating knee flexion through a pliometric contraction (Perry, 2010), the vasti muscle group also functions to accelerate the forward progression velocity of the trunk. In the present study, the K2 muscle power burst, which corresponds to energy generation by the vasti muscles (the rectus femoris is less active during this phase of the gait cycle (Perry, 2010)), decreases as a function of obstacle height (Figure 22F). A plausible explanation for this observation is that the vasti muscle group reduced its energy generation primarily to decelerate the forward progression of the trunk. Furthermore, the hip flexors energy absorption (H2), which additionally plays a role in controlling sagittal plane trunk movement, decreased under obstacle conditions. This reduction in the hip flexors energy absorption (H2) was necessary to ensure that the trunk remains upright during obstructed walking rather than being leaned over. In summary, both the knee extensor energy generation (K2) and the hip flexors energy absorption (H2) decreased under obstacle conditions to initially decelerate trunk acceleration through reduced energy generation by the vasti muscles and to maintain trunk uprightness due to diminished energy generation by the hip flexors during obstructed walking.

The hip abductors are active during stance phase to control the pelvis, by absorbing energy during early stance (H1F) to control the slight lowering of the contralateral limb (Neumann, 2016), followed by energy generation (H2F) during mid to late stance that aim to raise the pelvis (Eng and Winter, 1995). While a decrease in joint moment and power typically suggests muscle weakness or inefficiency (Sloot and van der Krogt, 2018), the reduction in the hip abductors energy absorption (H1F), combined with the increase in the hip extensors energy generation (H1) during early stance, was a strategy to elevate the pelvis. This was further maintained by a gradual decrease in the hip flexors energy absorption (H2) and an increase in the hip abductors energy generation (H2F), with the latter being significantly higher only between heights 0 and 60 cm, though it showed a non-significant increase overall. Like the hip extensors energy generation (H1), the energy absorption by the hip abductors (H1F) decreased to prevent the pelvis from lowering. The energy generation by the hip abductors (H2F) kept increasing slowly as obstacle height increased to further keep the pelvis high and eventually becoming significant at height 60 cm. Although the increase in the hip abductors energy generation (H2F) was significant only at height 60 cm, this increase, along with the decrease in the hip abductors energy absorption (H1F), aligns with the adaptations that McFadyen et al. (2002) reported regarding the trailing leg during bilateral obstructed walking.

At the knee, there was no significant change in the energy absorption by the knee extensors (K1) during early stance, but generation by the knee extensors (K2) significantly decreased for heights 40, 50 and 60 cm. This finding implies that there might be a reduction on the knee to elevate the CoM for clearing the obstacle, which is in

line with the McFadyen and Prince (2002) study in bilateral obstacles, but contrasts the unobstructed walking literature in which the knee is thought to contribute significantly in its control (Eng and Winter, 1995).

At the ankle, energy absorption by the plantar flexors (A1) did not change across obstacle conditions (Figure 22G). However, a new phase of energy generation by the plantar flexors (A1G) emerged during early stance (Figure 23C). As the objective of obstructed walking is to raise the CoM, positive work must be performed (Alexander and Schwameder, 2023). The hip contributed significantly to raising the CoM by a significant increase in the hip extensors energy generation (H1) during early stance for higher obstacles. This, combined with the new ankle plantar flexors energy generation (A1G), further increased the CoM to provide sufficient clearance for the higher obstacles. The ankle plantar flexors energy generation (A1G) can be concomitant to increased activation of the gastrocnemius and soleus to counteract the increased external ankle dorsiflexor moment (Alexander and Schwameder, 2023); however, EMG has not been conducted in the present study to confirm this increased activation in the plantar flexors. Additionally, a foot strike pattern at higher obstacle heights was seen in the present study (Figure 19D,H). This adaptation of the ankle energy flow is similar to the foot strike shown during uphill walking. Adopting a foot strike pattern resulted in a lower absolute CoM displacement, meaning that the difference between maximum and minimum CoM in foot strike was lower than heel strike (Alexander and Schwameder, 2023).

In summary, for the supporting leg adaptations, a sequential action occurs during the early stance phase to facilitate an upward bias of the crossing leg from the supporting leg during unilateral obstructed walking. This process initially involves an increase in the

hip extensors energy generation (H1), which supports the body and controls the thigh's forward motion. Notably, it also elevates the CoM and provides additional vertical height. This was succeeded by the emergence of an A1G muscle power burst, which contributed positive work from the ankle to further raise the CoM. Concurrently, the hip abductors energy absorption (H1F) diminishes during this phase to prevent a downward pelvis tilt and alterations in its inclination. Following this, there is a reduction in the knee extensors energy absorption (K2) to manage the forward acceleration of the trunk, as well as a decrease in the hip flexors energy absorption (H2) to maintain an upright posture of the trunk.

5.1.3 Unilateral obstructed walking as a bilateral behaviour

Ensuring safe crossing over the obstacle is achieved by elevating the foot as well as upward bias of the pelvis (Patla et al., 1991; Patla and Rietdyk, 1993). This starts with the reorganization of the muscle energy flow in the crossing leg by decreasing the hip flexor energy generation (H3) and knee extensor energy absorption (K3) in favour of the emergence of the knee flexors energy generation (K5). This would increase flexion of the crossing leg, providing adequate foot clearance. This emergence of the knee flexors energy generation (K5), which continued to increase as obstacle height increased, seemed enough to achieve foot clearance for lower heights. On the supporting leg, there is a small increase in hip extensors energy generation (H1) and hip abductors energy generation (H2F), which aid in providing additional pelvis height. However, as the obstacle reached a height of 40 cm, solely relying on elevating the foot was not enough. For this reason, the new plantar flexors energy generation at the ankle (A1G) provided the increase in supporting leg pelvis and body CoM height needed for the crossing leg to safely cross

over the obstacle, corroborated by the nonsignificant increase in hip extensors energy generation (H1) and the hip abductors energy generation (H2F). For height 50 cm, there was an increased demand for positive work to cross over the obstacle. The ankle of the supporting leg contributed more work by increasing the ankle plantar flexors energy generation (A1G), corroborated by a significant increase in the hip extensors energy generation (H1) that further increased the CoM as the approach was closer to the obstacle. Moreover, for the crossing leg, the hip flexors energy generation (H3) did not increase significantly to potentially increase toe clearance. A new frontal plane adaptation emerged, corresponding to a transition from absorption by the hip adductors to generation by the hip abductors (H4F) to provide hip circumduction like movement. This additional positive work provided the frontal plane lift of the crossing leg to clear the obstacle. Finally, at height 60 cm, the hip extensors energy generation (H1), the ankle plantar flexors energy generation (A1G), and the hip abductors energy generation (H2F) all contributed significantly to providing the positive work of upward bias of the crossing leg from the supporting leg. Additionally, the transition to hip abductors energy generation (H4F), increase in the hip flexors energy generation (H3) and the knee extensors energy absorption (K3), and continuous increase in the knee flexors energy generation (K5) contributed to higher foot elevation.

It is suggested that bilateral obstacles would require greater modifications of the energy generation and absorption pattern, greater foot trajectory, body weight support and upper body postural control adjustments (Barbeau et al., 1999; Ladouceur et al., 2005). Based on the information provided by the current study, some similarities can be drawn between the behaviour occurring when going over bilateral and unilateral obstacles. It

can be suggested that in bilateral obstacles, the trailing limb (the second limb that goes over the obstacle) would behave as a supporting leg (as seen in unilateral obstacles) based on the ALAs of decreased hip abductor energy absorption (H1F) and increase in hip abductor energy generation (H2F) that occur during initial contact and loading response (McFadyen and Prince, 2002). In addition, the trailing and leading (first limb that goes over the obstacle) limb behave as a crossing leg based on the ALAs of the emergence of the knee flexor energy generation (K5) coupled with decreased knee extensor energy absorption (K3) and hip flexor energy generation (H3) during pre-swing and initial swing. Nothing additional can be said regarding the leading limb as it is not clear if it behaves as a supporting leg due to it not being investigated while the trailing leg is going over the obstacle (McFadyen and Prince, 2002).

5.1.4 ALAs complementarity in able-bodied participants

The findings of the study and its association with the hypothesis of specific aim two of able-bodied participants can be found in Table 7.

Table 7. Summary of energy bursts complementarity between during unobstructed and obstructed walking conditions.

Outcome measure	Hypothesis	Result	Hypothesis supported?
Knee flexor energy generation (K5)	No difference between legs	Difference between the legs	No
Knee extensor energy absorption (K3)	No difference between legs	No difference between the legs	Yes
Hip flexor energy generation (H3)	No difference between legs	Difference between the legs	No
Hip abductor energy generation (H3F)	No difference between legs	Difference between the legs	No

Hip abductor energy generation (H1F)	No difference between legs	No difference between the legs	Yes
--------------------------------------	----------------------------	--------------------------------	-----

In our sample of right-footed participants, lateralization of the ALAs in able-bodied participants was shown on the crossing leg, with a lower left hip flexor generation of energy burst (H3), a higher left knee flexor generation of energy burst (K5), and a lower left hip abductor generation of energy burst (H3F) compared to the right leg. To our knowledge, the differences of the knee flexors energy generation (K5) and the hip flexors energy generation (H3) when walking over unilateral obstacles have not been previously reported in the literature. However, this difference in energy flow during obstacle crossing can be related to the asymmetry in joint angles of the leading limb while crossing a bilateral obstacle. In a study looking at the effect of cold temperature, it was shown that the left leg had greater flexion angles for obstacles of 20 and 30% of leg length (Yao et al., 2022). Additionally, it has been suggested that in bilateral obstacles, the knee flexor energy generation (K5) is responsible for elevating the limb while the hip flexor energy generation (H3) is responsible for progressing the limb through the swing phase (MacLellan and McFadyen, 2013; Niang and McFadyen, 2004). For this reason, it can be initially suggested that the left leg relies more on elevating the limb by pulling the knee due to the increased knee flexor energy generation (K5). Additionally, it can also be suggested that the greater increase in the knee flexors energy generation (K5) observed on the left leg might indicate more activation by the hamstrings, which generates a flexor moment at the knee joint and an extensor moment at the hip joint. The hip extension moment might explain the decrease in net energy generation by the hip flexor on the left

leg. This finding of activation patterns is speculative as EMG was not captured in the present study.

Additionally, the crossing leg left hip abductor muscle generation of energy (H3F) at the end of the stance phase was smaller than the right leg (Figure 17B). This reduced energy generation by the hip abductors is happening during the transition of the CoM toward the right leg. Interestingly, the right leg also exhibited a higher hip flexors energy generation (H3) compared to the left leg, suggesting that there is better hip flexion and abduction on the right leg compared to the left. The muscles that are responsible for hip flexion and abduction are the tensor fasciae latae (TFL) and sartorius (Neumann, 2016). During walking, the hip abductors (gluteus medius, gluteus minimus, and TFL) are significantly active during the stance phase, sartorius is active during the early to mid swing (Neumann, 2016) (60 to 80% of the GC), while the gluteus medius is active during end swing in preparation for heel contact (Neumann, 2016). Though the hip abductors are primarily responsible for providing pelvic support (Ganderton et al., 2017), these findings of increased hip flexors energy generation (H3) and the hip abductors energy generation (H3F) on the right could suggest that the TFL and sartorius increased their activations during obstructed walking to provide additional elevation on the right side for foot clearance. However, this is speculative as EMG was not captured in the present study to investigate muscle activation patterns.

In summary, it is suggested that when behaving as a crossing leg, the left leg predominantly emphasizes the enhancement of knee flexor energy generation (K5) rather than shifting its CoM toward the right leg. This observation is further corroborated by

reduced hip flexor energy generation (H3) and hip abductor energy generation (H3F). This finding suggests that the left leg relies on a pulling motion at the knee.

5.2 Limitations

While this study provides important insights into the adaptations observed in able-bodied during unilateral obstructed walking, it does have certain limitations.

Although complementarity was examined during this study, footedness was not a control variable. Given that most participants were right-footed (based on scores from the WFQ-R), comparing them to a group of left-footed participants would have offered valuable insights into the contribution of limb dominance to walking control during unobstructed and obstructed walking. It is suggested that the dominant limb is responsible for mobility and propulsion, whereas the non-dominant leg plays a role in control (Sadeghi et al., 2000). This could be a relevant observation during unilateral obstructed walking since each leg operates and contributes differently to achieve higher foot elevation. It would be valuable to investigate how dominance would contribute to the main task of higher foot elevation and safely going over the obstacle.

This study analyzed the participants' behaviour based on the absolute values of the obstacle heights rather than also analyzing and normalizing the adaptations as a function of relative obstacle height based on their leg length. This approach could have eliminated some of the discrepancies that may arise from height differences (Sakurai et al., 2025) as some of the constraints regarding adaptations to obstructed walking have been suggested to be related to the obstacle heights (Lu et al., 2006; Patla and Rietdyk, 1993; Sparrow et al., 1996).

Safety margin and toe clearance variables were not tested, as these would have offered additional insight into how able-bodied individuals would adapt in these conditions. They would supplement the literature by providing information regarding the different strategies that may be adopted across various populations, as elderly individuals going over bilateral obstacles tend to adopt riskier and lower foot trajectories compared to young adults (McFadyen and Prince, 2002).

The time series data (joint angles, net joint moment and net joint power) were normalized to the duration of the gait cycle. However, it is evident that a different time normalization is needed. It is suggested to try using piecewise linear time normalization based on phases and subphases of the gait cycle (Helwig et al., 2011). Once a proper time normalization is done, it is suggested that a statistical parametric mapping (SPM) analysis be conducted. This analysis would have offered a deeper understanding of the adaptations related to kinematic and kinetic data during obstructed walking rather than relying solely on mechanical adaptations that occurred. However, having multiple levels within the factors must also be initiated to better understand the adaptations occurring between each obstacle height. An example of this would be to investigate the differences between each obstacle height in terms of changes in joint angles, rather than merely examining the differences between obstacle heights 0 and 50 cm.

Not performing electromyography was also a limitation of this study, as it would have revealed additional information regarding the muscular activation patterns during the tested conditions (MacLellan, 2017).

5.3 Future directions

Future studies could investigate age differences during unilateral obstructed walking, since the obstructed walking literature suggests that adaptations due to weaknesses may arise during this task (McFadyen and Prince, 2002; Muir et al., 2019; Patla et al., 1996). McFadyen and Prince (2002) revealed that the elderly population adopted riskier foot trajectories, which they attributed to differences in frontal plane control at the hip and decreased stride length. Investigating adaptations during unilateral obstructed walking based on age differences may be less risky for the elderly, as bilateral obstacles are more complex and demanding to go over (Ladouceur et al., 2005).

Kinematic data for the present study were collected; however, spatiotemporal and kinematic variables, such as changes in pelvic angles, hip position, toe clearance, and safety margin, could provide valuable additional insight into mechanical adaptations analyzed in this study. Investigating hip position during obstructed walking would enhance the literature, as this variable has been reported in bilateral obstructed walking to be associated with a safety adaptation of positioning the hip further back to prevent tripping, while also providing additional information regarding the upward bias strategy that can be reflected in vertical hip position (Patla and Rietdyk, 1993).

The present study also explored adaptations in individuals post-anterior cruciate ligament reconstruction (see Appendix H for more details).

Chapter 6: Conclusion

The study explored several novel aspects of control of walking in able-bodied individuals. It is the first study to conduct kinematic and kinetic analysis on the supporting leg of able-bodied participants during unilateral obstructed walking for obstacle heights as high as 60 cm.

The findings of this study show that for the crossing leg ALAs, the able-bodied participants would achieve higher foot elevation through a reorganization of the lower limb kinetics, with the emergence of the knee flexor energy generation (K5) due to a decrease in knee extensor energy absorption (K3) and hip flexor energy generation (H3). Moreover, circumduction-like movement occurred due to transition to hip abductors energy generation during the swing phase (H4F).

Additionally, the supporting leg ALAs consist of an increase in hip extensors energy generation (H1), coupled with an emergence of ankle plantar flexor energy generation (A1G) during early stance. This is followed by a decrease in knee extensor energy generation (K2) to decelerate forward trunk acceleration and a decrease in hip flexor energy absorption (H2) to maintain an upright posture.

The complementarity of the lower limbs during unilateral obstructed walking was also assessed, revealing that the left leg displayed higher knee flexors energy generation (K5), lower hip flexors energy generation (H3) and hip abductors energy generation (H3F), which suggests that the left leg relies more on a pulling motion at the knee to go over the obstacle by increasing the activation of the knee flexors.

References

- Aldaihan, M. M. (2023). Cross-cultural adaptation of the Arabic version of the Waterloo Footedness Questionnaire-Revised to assess footedness in Arabic-speaking adults. *Cureus, 15*(8), e44421. <https://doi.org/10.7759/cureus.44421>
- Alexander, N., and Schwameder, H. (2023). A forefoot strike pattern during 18° uphill walking leads to greater ankle joint and plantar flexor loading. *Gait and Posture, 103*, 44–49. <https://doi.org/10.1016/j.gaitpost.2023.04.011>
- Allard, P., Lachance, R., Aissaoui, R., and Duhaime, M. (1996b). Simultaneous bilateral 3-D able-bodied gait. *Human Movement Science, 15*(3), 327–346. [https://doi.org/10.1016/0167-9457\(96\)00004-8](https://doi.org/10.1016/0167-9457(96)00004-8)
- Ancillao, A., Aertbeliën, E., and De Schutter, J. (2022). Effect of the soft tissue artifact on marker measurements and on the calculation of the helical axis of the knee during a squat movement: A study on the CAMS-Knee dataset. *Medical Engineering and Physics, 110*, None. <https://doi.org/10.1016/j.medengphy.2022.103915>
- Aoi, S., and Funato, T. (2016). Neuromusculoskeletal models based on the muscle synergy hypothesis for the investigation of adaptive motor control in locomotion via sensory-motor coordination. *Neuroscience Research, 104*, 88–95. <https://doi.org/10.1016/j.neures.2015.11.005>
- Arsenault, A. B., Winter, D. A., and Marteniuk, R. G. (1986). Bilateralism of EMG profiles in human locomotion. *American Journal of Physical Medicine, 65*(1), 1–16.
- Aurand, A. M., Dufour, J. S., and Marras, W. S. (2017). Accuracy map of an optical motion capture system with 42 or 21 cameras in a large measurement volume. *Journal of Biomechanics, 58*, 237–240. <https://doi.org/10.1016/j.jbiomech.2017.05.006>
- Baker, P. A., and Hewison, S. R. (1990). Gait recovery pattern of unilateral lower limb amputees during rehabilitation. *Prosthetics and Orthotics International, 14*(2), 80–84. <https://doi.org/10.3109/03093649009080327>
- Barbeau, H., Ladouceur, M., Norman, K. E., Pépin, A., and Leroux, A. (1999). Walking after spinal cord injury: Evaluation, treatment, and functional recovery. *Archives of Physical Medicine and Rehabilitation, 80*(2), Article 2. [https://doi.org/10.1016/S0003-9993\(99\)90126-0](https://doi.org/10.1016/S0003-9993(99)90126-0)
- Beckham, G., Suchomel, T., and Mizuguchi, S. (2014). Force plate use in performance monitoring and sport science testing. *New Studies in Athletics, 29*, 25–37.

- Bell, A. L., Brand, R. A., and Pedersen, D. R. (1989). Prediction of hip joint centre location from external landmarks. *Human Movement Science*, 8(1), 3–16. [https://doi.org/10.1016/0167-9457\(89\)90020-1](https://doi.org/10.1016/0167-9457(89)90020-1)
- Boucher, J. P. (1993). Anatomical, mechanical, and functional factors in patello-femoral pain syndrome. *Chiropractic Sports Medicine*, 7(1), S. 1-5.
- Bovi, G., Rabuffetti, M., Mazzoleni, P., and Ferrarin, M. (2011). A multiple-task gait analysis approach: Kinematic, kinetic and EMG reference data for healthy young and adult subjects. *Gait and Posture*, 33(1), 6–13. <https://doi.org/10.1016/j.gaitpost.2010.08.009>
- Bresler, B., and Frankel, J. P. (2022). The forces and moments in the leg during level walking. *Transactions of the American Society of Mechanical Engineers*, 72(1), 27–36. <https://doi.org/10.1115/1.4016578>
- Calancie, B., Needham-Shropshire, B., Jacobs, P., Willer, K., Zych, G., and Green, B. A. (1994). Involuntary stepping after chronic spinal cord injury. Evidence for a central rhythm generator for locomotion in man. *Brain: A Journal of Neurology*, 117 (Pt 5), 1143–1159. <https://doi.org/10.1093/brain/117.5.1143>
- Cappozzo, A., Cappello, A., Croce, U. D., and Pensalfini, F. (1997). Surface-marker cluster design criteria for 3-D bone movement reconstruction. *IEEE Transactions on Biomedical Engineering*, 44(12), 1165–1174. <https://doi.org/10.1109/10.649988>
- Carse, B., Meadows, B., Bowers, R., and Rowe, P. (2013). Affordable clinical gait analysis: An assessment of the marker tracking accuracy of a new low-cost optical 3D motion analysis system. *Physiotherapy*, 99(4), 347–351. <https://doi.org/10.1016/j.physio.2013.03.001>
- Chodera, J. D. (1974). Analysis of gait from footprints. *Physiotherapy*, 60(6), 179–181.
- Chodera, J. D., and Levell, R. W. (1973). Footprint patterns during walking. In R. M. Kenedi (Ed.), *Perspectives in Biomedical Engineering: Proceedings of a Symposium organised in association with the Biological Engineering Society and held in the University of Strathclyde, Glasgow, June 1972* (pp. 81–90). Palgrave Macmillan UK. https://doi.org/10.1007/978-1-349-01604-4_14
- Chou, L. S., Song, S. M., and Draganich, L. F. (1995). Predicting the kinematics and kinetics of gait based on the optimum trajectory of the swing limb. *Journal of Biomechanics*, 28(4), 377–385. [https://doi.org/10.1016/0021-9290\(94\)00083-g](https://doi.org/10.1016/0021-9290(94)00083-g)
- Collins, T. D., Ghousayni, S. N., Ewins, D. J., and Kent, J. A. (2009). A six degrees-of-freedom marker set for gait analysis: Repeatability and comparison with a modified Helen Hayes set. *Gait and Posture*, 30(2), 173–180. <https://doi.org/10.1016/j.gaitpost.2009.04.004>

- D'Août, K., Healy, A., Eddison, N., and Chockalingam, N. (2022). Introduction to gait analysis (pp. 1–16). https://doi.org/10.1049/PBHE031E_ch1
- Dempster, W. T. (1955). Space requirements of the seated operator: geometrical, kinematic, and mechanical aspects of the body, with special reference to the limbs. Wright air development center, air research and development command, united states air force <http://deepblue.lib.umich.edu/handle/2027.42/4540>
- DeVita, P., Hong, D., and Hamill, J. (1991). Effects of asymmetric load carrying on the biomechanics of walking. *Journal of Biomechanics*, 24(12), 1119–1129. [https://doi.org/10.1016/0021-9290\(91\)90004-7](https://doi.org/10.1016/0021-9290(91)90004-7)
- DeVita, P., Hortobagyi, T., and Barrier, J. (1998). Gait biomechanics are not normal after anterior cruciate ligament reconstruction and accelerated rehabilitation. *Medicine and Science in Sports and Exercise*, 30(10), 1481–1488. <https://doi.org/10.1097/00005768-199810000-00003>
- Dickey, J. P., and Winter, D. A. (1992). Adaptations in gait resulting from unilateral ischaemic block of the leg. *Clinical Biomechanics (Bristol, Avon)*, 7(4), 215–225. [https://doi.org/10.1016/S0268-0033\(92\)90004-N](https://doi.org/10.1016/S0268-0033(92)90004-N)
- Drew, T. (1988). Motor cortical cell discharge during voluntary gait modification. *Brain Res*, 457(1), Article 1.
- Drew, T. (1993). Motor cortical activity during voluntary gait modifications in the cat. I. Cells related to the forelimbs. *Journal of Neurophysiology*, 70(1), 179–199..
- Dyson, K. S., Miron, J.P., and Drew, T. (2014). Differential modulation of descending signals from the reticulospinal system during reaching and locomotion. *Journal of Neurophysiology*, 112(10), 2505–2528. <https://doi.org/10.1152/jn.00188.2014>
- Eng, J. J., and Winter, D. A. (1995b). Kinetic analysis of the lower limbs during walking: What information can be gained from a three-dimensional model? *Journal of Biomechanics*, 28(6), 753–758. [https://doi.org/10.1016/0021-9290\(94\)00124-m](https://doi.org/10.1016/0021-9290(94)00124-m)
- Engsberg, J. R., Lee, A. G., Patterson, J. L., and Harder, J. A. (1991). External loading comparisons between able-bodied and below-knee-amputee children during walking. *Archives of Physical Medicine and Rehabilitation*, 72(9), 657–661.
- Faul, F., Erdfelder, E., Lang, A.-G., and Buchner, A. (2007). GPower 3: A flexible statistical power analysis program for the social, behavioral, and biomedical sciences. *Behavior Research Methods*, 39(2), 175–191. <https://doi.org/10.3758/Bf03193146>
- Forssberg, H. (1982). Spinal locomotor functions and descending control. *Brain Stem Control of Spinal Mechanisms*, 253–271.

- Forsberg, H., Grillner, S., and Halbertsma, J. (1980). The locomotion of the low spinal cat. I. Coordination within a hindlimb. *Acta Physiologica Scandinavica*, 108(3), 269–281. <https://doi.org/10.1111/j.1748-1716.1980.tb06533.x>
- Ganderton, C., Pizzari, T., Harle, T., Cook, J., and Semciw, A. (2017). A comparison of gluteus medius, gluteus minimus and tensor fascia latae muscle activation during gait in post-menopausal women with and without greater trochanteric pain syndrome. *Journal of Electromyography and Kinesiology*, 33, 39–47. <https://doi.org/10.1016/j.jelekin.2017.01.004>
- Grillner, S. (2006). Biological pattern generation: The cellular and computational logic of networks in motion. *Neuron*, 52(5), 751–766. <https://doi.org/10.1016/j.neuron.2006.11.008>
- Haefeli, J., Vögeli, S., Michel, J., and Dietz, V. (2011). Preparation and performance of obstacle steps: Interaction between brain and spinal neuronal activity. *The European Journal of Neuroscience*, 33(2), 338–348. <https://doi.org/10.1111/j.1460-9568.2010.07494.x>
- Hahn, M. E., Lee, H.-J., and Chou, L.-S. (2005). Increased muscular challenge in older adults during obstructed gait. *Gait and Posture*, 22(4), 356–361. <https://doi.org/10.1016/j.gaitpost.2004.11.012>
- Hamill, J., Bates, B. T., and Knutzen, K. M. (1984). Ground reaction force symmetry during walking and running. *Research Quarterly for Exercise and Sport*, 55(3), 289–293. <https://doi.org/10.1080/02701367.1984.10609367>
- Hanavan, E. P. (1964). A mathematical model of the human body. *AMRL-TR. Aerospace Medical Research Laboratories (U.S.)*, 1–149.
- Hannah, R. E., Morrison, J. B., and Chapman, A. E. (1984). Kinematic symmetry of the lower limbs. *Archives of Physical Medicine and Rehabilitation*, 65(4), 155–158.
- Helwig, N. E., Hong, S., Hsiao-Weckler, E. T., and Polk, J. D. (2011). Methods to temporally align gait cycle data. *Journal of Biomechanics*, 44(3), Article 3. <https://doi.org/10.1016/j.jbiomech.2010.09.015> [doi]
- Herzog, W., Nigg, B. M., and Read, L. J. (1988). Quantifying the effects of spinal manipulations on gait using patients with low back pain. *Journal of Manipulative and Physiological Therapeutics*, 11(3), 151–157.
- Herzog, W., Nigg, B. M., Read, L. J., and Olsson, E. (1989). Asymmetries in ground reaction force patterns in normal human gait. *Medicine and Science in Sports and Exercise*, 21(1), 110.

- Hesse, S., Reiter, F., Jahnke, M., Dawson, M., Sarkodie-Gyan, T., and Mauritz, K. H. (1997). Asymmetry of gait initiation in hemiparetic stroke subjects. *Archives of Physical Medicine and Rehabilitation*, 78(7), 719–724. [https://doi.org/10.1016/s0003-9993\(97\)90079-4](https://doi.org/10.1016/s0003-9993(97)90079-4)
- Hinrichs, R. N. (1992). Case studies of asymmetrical arm action in running. *Journal of Applied Biomechanics*, 8(2), 111–128. <https://doi.org/10.1123/ijbs.8.2.111>
- Hirokawa, S. (1989). Normal gait characteristics under temporal and distance constraints. *Journal of Biomedical Engineering*, 11(6), 449–456. [https://doi.org/10.1016/0141-5425\(89\)90038-1](https://doi.org/10.1016/0141-5425(89)90038-1)
- Ivanenko, Y. P., Poppele, R. E., and Lacquaniti, F. (2006). Motor control programs and walking. *The Neuroscientist: A Review Journal Bringing Neurobiology, Neurology and Psychiatry*, 12(4), 339–348. <https://doi.org/10.1177/1073858406287987>
- Judge, J. O., Davis, R. B., and Ounpuu, S. (1996). Step length reductions in advanced age: The role of ankle and hip kinetics. *The Journals of Gerontology. Series A, Biological Sciences and Medical Sciences*, 51(6), M303-312. <https://doi.org/10.1093/gerona/51a.6.m303>
- Kharb, A., Saini, V., Jain, Y. K., & Dhiman, S. (2011). A review of gait cycle and its parameters. *International Journal of Computational Engineering & Management*, 13(01), 78-83.
- Kiehn, O. (2006). Locomotor circuits in the mammalian spinal cord. *Annual Review of Neuroscience*, 29, 279–306. <https://doi.org/10.1146/annurev.neuro.29.051605.112910>
- Krouchev, N., and Drew, T. (2013). Motor cortical regulation of sparse synergies provides a framework for the flexible control of precision walking. *Frontiers in Computational Neuroscience*, 7, 83. <https://doi.org/10.3389/fncom.2013.00083>
- Kuster, M., Sakurai, S., and Wood, G. A. (1995). Kinematic and kinetic comparison of downhill and level walking. *Clinical Biomechanics (Bristol, Avon)*, 10(2), 79–84. [https://doi.org/10.1016/0268-0033\(95\)92043-1](https://doi.org/10.1016/0268-0033(95)92043-1)
- Ladouceur, M., Guéguen, N., Gustafson, E., and Floyd, B. (2005). Effect of obstacle placement on the strategy used to cross over an obstacle during walking. *Gait and Posture*, 21. [https://doi.org/10.1016/S0966-6362\(05\)80222-X](https://doi.org/10.1016/S0966-6362(05)80222-X)
- Ladouceur, M., Barbeau, H. (2025). Going over unilateral obstacles during walking results from a non-linear modulation of the knee flexor strategy and a linear increase in contribution from hip hiking. Submitted for publication
- Latash, M. L. (2016). Biomechanics as a window into the neural control of movement. *Journal of Human Kinetics*, 52, 7–20. <https://doi.org/10.1515/hukin-2015-0190>

- Lavaill, M., Martelli, S., Kerr, G. K., and Pivonka, P. (2022). Statistical quantification of the effects of marker misplacement and soft-tissue artifact on shoulder kinematics and kinetics. *Life*, *12*(6), 819. <https://doi.org/10.3390/life12060819>
- Lu, T.-W., Chen, H.-L., and Chen, S.-C. (2006). Comparisons of the lower limb kinematics between young and older adults when crossing obstacles of different heights. *Gait and Posture*, *23*(4), 471–479. <https://doi.org/10.1016/j.gaitpost.2005.06.005>
- MacKinnon, C. D., and Winter, D. A. (1993). Control of whole body balance in the frontal plane during human walking. *Journal of biomechanics*, *26*, 633-644.
- MacLellan, M. J. (2017). Modular organization of muscle activity patterns in the leading and trailing limbs during obstacle clearance in healthy adults. *Experimental Brain Research*, *235*(7), 2011–2026. <https://doi.org/10.1007/s00221-017-4946-z>
- MacLellan, M. J., and McFadyen, B. J. (2013). Proximal lower limb muscle energetics and the adaptation of segment elevation angle phasing for obstacle avoidance. *Gait and Posture*, *37*(2), 274–279. <https://doi.org/10.1016/j.gaitpost.2012.07.019>
- Malus, J., Skypala, J., Silvernail, J. F., Uchytíl, J., Hamill, J., Barot, T., and Jandacka, D. (2021). Marker placement reliability and objectivity for biomechanical cohort study: Healthy aging in industrial environment (HAIE—program 4). *Sensors (Basel, Switzerland)*, *21*(5), 1830. <https://doi.org/10.3390/s21051830>
- McFadyen, B. J., and Carnahan, H. (1997). Anticipatory locomotor adjustments for accommodating versus avoiding level changes in humans. *Experimental Brain Research*, *114*(3), 500–506. <https://doi.org/10.1007/pl00005659>
- McFadyen, B. J., Fiset, F., and Charette, C. (2018). Substituting anticipatory locomotor adjustments online is time constrained. *Experimental Brain Research*, *236*(7), 1985–1996. <https://doi.org/10.1007/s00221-018-5277-4>
- McFadyen, B. J., Magnan, G. A., and Boucher, J. P. (1993). Anticipatory locomotor adjustments for avoiding visible, fixed obstacles of varying proximity. *Human Movement Science*, *12*(3), 259–272. [https://doi.org/10.1016/0167-9457\(93\)90019-L](https://doi.org/10.1016/0167-9457(93)90019-L)
- McFadyen, B. J., and Prince, F. (2002). Avoidance and accommodation of surface height changes by healthy, community-dwelling, young, and elderly men. *The Journals of Gerontology Series A: Biological Sciences and Medical Sciences*, *57*(4), B166–B174. <https://doi.org/10.1093/gerona/57.4.B166>
- McFadyen, B. J., and Winter, D. A. (1991). Anticipatory locomotor adjustments during obstructed human walking. *Neuroscience Research Communication*, *9*, 37–44.

- McFadyen, B. J., Winter, D. A., and Allard, F. (1994). Simulated control of unilateral, anticipatory locomotor adjustments during obstructed gait. *Biological Cybernetics*, 72(2), 151–160. <https://doi.org/10.1007/BF00205979>
- Milner, M., Basmajian, J. V., and Quanbury, A. O. (1971). Multifactorial analysis of walking by electromyography and computer. *American Journal of Physical Medicine*, 50(5), 235–258.
- Minassian, K., Hofstoetter, U. S., Dzeladini, F., Guertin, P. A., and Ijspeert, A. (2017). The human central pattern generator for locomotion: does it exist and contribute to walking? *The Neuroscientist*, 23(6), 649–663. <https://doi.org/10.1177/1073858417699790>
- Muir, B. C., Haddad, J. M., van Emmerik, R. E. A., and Rietdyk, S. (2019). Changes in the control of obstacle crossing in middle age become evident as gait task difficulty increases. *Gait and Posture*, 70, 254–259. <https://doi.org/10.1016/j.gaitpost.2019.01.035>
- Nashner, L. M. (1980). Balance adjustments of humans perturbed while walking. *Journal of Neurophysiology*, 44(4), 650–664. <https://doi.org/10.1152/jn.1980.44.4.650>
- Nashner, L. M. (1982). Adaptation of human movement to altered environments. *Trends in Neurosciences*, 5, 358–361. [https://doi.org/10.1016/0166-2236\(82\)90204-1](https://doi.org/10.1016/0166-2236(82)90204-1)
- Neptune, R. R., Zajac, F. E., and Kautz, S. A. (2004). Muscle force redistributes segmental power for body progression during walking. *Gait and Posture*, 19(2), 194–205. [https://doi.org/10.1016/S0966-6362\(03\)00062-6](https://doi.org/10.1016/S0966-6362(03)00062-6)
- Neumann, D. A. (2016). *Kinesiology of the musculoskeletal system*. Elsevier Health Sciences.
- Niang, A. E. S., and McFadyen, B. J. (2004). Adaptations in bilateral mechanical power patterns during obstacle avoidance reveal distinct control strategies for limb elevation versus limb progression. *Motor Control*, 8(2), 160–173. <https://doi.org/10.1123/mcj.8.2.160>
- Olree, K. S., and Vaughan, C. L. (1995). Fundamental patterns of bilateral muscle activity in human locomotion. *Biological Cybernetics*, 73(5), 409–414. <https://doi.org/10.1007/BF00201475>
- Ounpuu, S., Gage, J. R., and Davis, R. B. (1991). Three-dimensional lower extremity joint kinetics in normal pediatric gait. *Journal of Pediatric Orthopaedics*, 11(3), 341.
- Ounpuu, S., and Winter, D. A. (1989). Bilateral electromyographical analysis of the lower limbs during walking in normal adults. *Electroencephalography and Clinical Neurophysiology*, 72(5), 429–438. [https://doi.org/10.1016/0013-4694\(89\)90048-5](https://doi.org/10.1016/0013-4694(89)90048-5)

- Patla, A. E. (1985). Some characteristics of EMG patterns during locomotion: Implications for the locomotor control process. *Journal of Motor Behavior*, 17(4), 443–461. <https://doi.org/10.1080/00222895.1985.10735360>
- Patla, A. E., and Prentice, S. D. (1995). The role of active forces and intersegmental dynamics in the control of limb trajectory over obstacles during locomotion in humans. *Experimental Brain Research*, 106(3), 499–504. <https://doi.org/10.1007/BF00231074>
- Patla, A. E., Prentice, S. D., Robinson, C., and Neufeld, J. (1991). Visual control of locomotion: Strategies for changing direction and for going over obstacles. *Journal of Experimental Psychology: Human Perception and Performance*, 17(3), 603–634. <https://doi.org/10.1037/0096-1523.17.3.603>
- Patla, A. E., and Rietdyk, S. (1993). Visual control of limb trajectory over obstacles during locomotion: Effect of obstacle height and width. *Gait and Posture*, 1, 45–60.
- Patla, A., Prentice, S., and Gobbi, L. (1996). Visual control of obstacle avoidance during locomotion: Strategies in young children, young and older adults. *Advances in Psychology*, 114, 257–277. [https://doi.org/10.1016/S0166-4115\(96\)80012-4](https://doi.org/10.1016/S0166-4115(96)80012-4)
- Patla, A., and Rietdyk, S. (1993). Visual control of limb trajectory over obstacles during locomotion: Effect of obstacle height and width. *Gait and Posture*, 1(1), 45–60. [https://doi.org/10.1016/0966-6362\(93\)90042-Y](https://doi.org/10.1016/0966-6362(93)90042-Y)
- Perry, J. (2010). *Gait analysis: Normal and pathological function*, second edition (2nd ed). SLACK, Incorporated.
- Peters, M. (1988). Footedness: Asymmetries in foot preference and skill and neuropsychological assessment of foot movement. *Psychological Bulletin*, 103(2), 179–192. <https://doi.org/10.1037/0033-2909.103.2.179>
- Robertson, D. G. E. (2014). *Research methods in biomechanics* (Second edition.). Human Kinetics. <https://doi.org/10.5040/9781492595809>
- Robertson, D. G., and Winter, D. A. (1980). Mechanical energy generation, absorption and transfer amongst segments during walking. *Journal of Biomechanics*, 13(10), Article 10.
- Sadeghi, H., Allard, P., and Duhaime, M. (1997). Functional gait asymmetry in able-bodied subjects. *Human Movement Science*, 16(2), 243–258. [https://doi.org/10.1016/S0167-9457\(96\)00054-1](https://doi.org/10.1016/S0167-9457(96)00054-1)
- Sadeghi, H., Allard, P., Prince, F., and Labelle, H. (2000). Symmetry and limb dominance in able-bodied gait: A review. *Gait and Posture*, 12(1), 34–45. [https://doi.org/10.1016/S0966-6362\(00\)00070-9](https://doi.org/10.1016/S0966-6362(00)00070-9)

- Sakurai, R., Miura, Y., and Kodama, K. (2025). Effect of obstacle depth and height on step-over behavior: Focus on age-related changes. *Human Movement Science*, 99, 103323. <https://doi.org/10.1016/j.humov.2025.103323>
- Schache, A. G., Baker, R., and Vaughan, C. L. (2007). Differences in lower limb transverse plane joint moments during gait when expressed in two alternative reference frames. *Journal of Biomechanics*, 40(1), 9–19. <https://doi.org/10.1016/j.jbiomech.2005.12.003>
- Scholz, J. P., and Schöner, G. (1999). The uncontrolled manifold concept: Identifying control variables for a functional task. *Experimental Brain Research*, 126(3), 289–306. <https://doi.org/10.1007/s002210050738>
- Shevtsova, N. A., and Rybak, I. A. (2016). Organization of flexor-extensor interactions in the mammalian spinal cord: Insights from computational modelling. *The Journal of Physiology*, 594(21), 6117–6131. <https://doi.org/10.1113/JP272437>
- Sloot, L. H., and van der Krogt, M. M. (2018). Interpreting joint moments and powers in gait. In *Handbook of Human Motion* (pp. 625–643). Springer International Publishing. https://doi.org/10.1007/978-3-319-14418-4_32
- Sparrow, W. A., Shinkfield, A. J., Chow, S., and Begg, R. K. (1996). Characteristics of gait in stepping over obstacles. *Human Movement Science*, 15(4), 605–622. [https://doi.org/10.1016/0167-9457\(96\)00022-X](https://doi.org/10.1016/0167-9457(96)00022-X)
- Stewart, C., Postans, N., Schwartz, M. H., Rozumalski, A., and Roberts, A. P. (2008). An investigation of the action of the hamstring muscles during standing in crouch using functional electrical stimulation (FES). *Gait and Posture*, 28(3), 372–377. <https://doi.org/10.1016/j.gaitpost.2008.05.007>
- Thewlis, D., Bishop, C., Daniell, N., and Paul, G. (2013). Next-generation low-cost motion capture systems can provide comparable spatial accuracy to high-end systems. *Journal of Applied Biomechanics*, 29(1), 112–117. <https://doi.org/10.1123/jab.29.1.112>
- Wall, J. C., and Turnbull, G. I. (1986). Gait asymmetries in residual hemiplegia. *Archives of Physical Medicine and Rehabilitation*, 67(8), 550–553.
- Weerdesteyn, V., Nienhuis, B., Hampsink, B., and Duysens, J. (2004). Gait adjustments in response to an obstacle are faster than voluntary reactions. *Human Movement Science*, 23(3–4), 351–363. <https://doi.org/10.1016/j.humov.2004.08.011>
- Winter, D. A. (1983a). Biomechanical motor patterns in normal walking. *Journal of Motor Behavior*, 15(4), 302–330. <https://doi.org/10.1080/00222895.1983.10735302>

- Winter, D. A. (1983b). Energy generation and absorption at the ankle and knee during fast, natural, and slow cadences. *Clinical Orthopaedics and Related Research*, 175, 147–154.
- Winter, D. A. (1987). *The biomechanics and motor control of human gait*. University of Waterloo Press.
- Winter, D. A. (1991). *Biomechanics and motor control of human gait: Normal, elderly and pathological - 2nd edition (Vol. Ed2)*. <https://trid.trb.org/View/770965>
- Winter, D. A., McFadyen, B. J., and Dickey, J. P. (1991). Adaptability of the CNS in human walking. In A. E. Patla (Ed.), *Advances in Psychology* (Vol. 78, pp. 127–144). North-Holland. [https://doi.org/10.1016/S0166-4115\(08\)60740-2](https://doi.org/10.1016/S0166-4115(08)60740-2)
- Winter, D. A., Patla, A. E., and Frank, J. S. (1990). Assessment of balance control in humans. *Medical Progress Through Technology*, 16(1–2), 31–51.
- Wu, G., Siegler, S., Allard, P., Kirtley, C., Leardini, A., Rosenbaum, D., Whittle, M., D’Lima, D. D., Cristofolini, L., Witte, H., Schmid, O., and Stokes, I. (2002). ISB recommendation on definitions of joint coordinate system of various joints for the reporting of human joint motion—Part I: Ankle, hip, and spine. *Journal of Biomechanics*, 35(4), Article 4. [https://doi.org/10.1016/S0021-9290\(01\)00222-6](https://doi.org/10.1016/S0021-9290(01)00222-6)
- Wu, G., van der Helm, F. C., Veeger, H. E., Makhsous, M., Van Roy, P., Anglin, C., Nagels, J., Karduna, A. R., McQuade, K., Wang, X., Werner, F. W., and Buchholz, B. (2005). ISB recommendation on definitions of joint coordinate systems of various joints for the reporting of human joint motion—Part II: shoulder, elbow, wrist and hand. *Journal of Biomechanics*, 38(5), Article 5.
- Yakovenko, S., and Drew, T. (2015). Similar motor cortical control mechanisms for precise limb control during reaching and locomotion. *The Journal of Neuroscience*, 35(43), 14476–14490. <https://doi.org/10.1523/JNEUROSCI.1908-15.2015>
- Yamashita, N. (1988). EMG activities in mono- and bi-articular thigh muscles in combined hip and knee extension. *European Journal of Applied Physiology and Occupational Physiology*, 58(3), 274–277. <https://doi.org/10.1007/BF00417262>
- Yang, J. F., and Winter, D. A. (1985). Surface EMG profiles during different walking cadences in humans. *Electroencephalography and Clinical Neurophysiology*, 60(6), 485–491. [https://doi.org/10.1016/0013-4694\(85\)91108-3](https://doi.org/10.1016/0013-4694(85)91108-3)
- Yang, N., Waddington, G., Adams, R., and Han, J. (2018). Translation, cultural adaption, and test-retest reliability of chinese versions of the edinburgh handedness inventory and waterloo footedness questionnaire. *Laterality*, 23(3), 255–273. <https://doi.org/10.1080/1357650X.2017.1357728>

- Yang, Z., Qu, F., Cui, C., and Rietdyk, S. (2018). The Contribution of Frontal Hip Power to Slope Walking. <https://www.semanticscholar.org/paper/The-Contribution-of-Frontal-Hip-Power-to-Slope-Yang-Qu/df6f5bd9863b8858f0289cd8a01ec7e7dfc9e228>
- Yao, S., Su, Y., Jiang, Y.H., Lei, T.H., Wang, I.L., and Hsieh, S.L. (2022). Increased asymmetry of lower limbs and leading joint angles during crossing obstacles in healthy male with cold exposure. *Applied Bionics and Biomechanics*, 2022, 6421611. <https://doi.org/10.1155/2022/6421611>
- Zajac, F. E., Neptune, R. R., and Kautz, S. A. (2002). Biomechanics and muscle coordination of human walking. Part I: Introduction to concepts, power transfer, dynamics and simulations. *Gait and Posture*, 16(3), Article 3.
- Zajac, F. E., Neptune, R. R., and Kautz, S. A. (2003). Biomechanics and muscle coordination of human walking: Part II: Lessons from dynamical simulations and clinical implications. *Gait and Posture*, 17(1), 1–17. [https://doi.org/10.1016/S0966-6362\(02\)00069-3](https://doi.org/10.1016/S0966-6362(02)00069-3)
- Zhao, G., Grimmer, M., and Seyfarth, A. (2021). The mechanisms and mechanical energy of human gait initiation from the lower-limb joint level perspective. *Scientific Reports*, 11, 22473. <https://doi.org/10.1038/s41598-021-01694-5>
- Żuk, M., and Pezowicz, C. (2015). Kinematic analysis of a six-degrees-of-freedom model based on ISB recommendation: A repeatability analysis and comparison with conventional gait model. *Applied Bionics and Biomechanics*, 2015, 503713. <https://doi.org/10.1155/2015/503713>

Appendix A: Informed consent form

Project title: Effects of Anterior Cruciate Ligament Reconstruction on Unilateral Obstructed Walking.

Biodynamics
Ergonomics
Neuroscience



Lead researcher:

Michel Ladouceur, PhD
School of Health and
Human Performance
Division of Kinesiology
Dalhousie University
Michel.Ladouceur@dal.ca

[a](#)

Research Team:

Garó Gary Ohanessian, MSc (Kinesiology)
School of Health and Human Performance
Division of Kinesiology
Dalhousie University
Gr733911@dal.ca

Afarin Kebritchi, MSc (Kinesiology)
School of Health and Human Performance
Division of Kinesiology
Dalhousie University
ft740170@dal.ca

Introduction

We invite you to take part in a study being conducted by Michel Ladouceur, a researcher at Dalhousie University. Choosing to take part in this research is entirely your choice. There will be no impact on you if you decide not to participate. The information below tells you about what is involved in the research, what you will be asked to do and about any benefit, risk, inconvenience, or discomfort that you might experience.

You should discuss any questions you have about this study with Michel Ladouceur. Please ask as many questions as you like. If you have questions later, please contact Michel Ladouceur.

Purpose and Outline of the Research Study

Over the years, the number of Anterior Cruciate Ligament (ACL) reconstruction has increased. This is worrying because an injury or a tear of this ligament results in knee instability. In past years, ACL tears have been deemed

to be “career ending” for athletes. In recent years, studies have been done to try to lower the risks of an injury and to reduce the limitations post ACL reconstruction.

In our everyday life, we encounter obstacles while walking. The purpose of this study is to look at the pattern of joint energy in the leg that is still on the ground (supporting leg) when you encounter an obstacle on one side of your body. The findings of this study will help us understand the biomechanics of the supporting leg while crossing over the obstacle. We are aiming to fill the gap because little to no study has been done on this population of interest using this specific task. We use motion capture and force plate data to calculate joint moment and joint energy.

Who Can Take Part in the Research Study

To be included in this study, you need to be between the ages of 18 to 35 years old.

You will not be able to participate if you have any walking difficulties or difficulties crossing over an obstacle. You will not be able to participate if you suffered any leg muscle or leg bone injuries in the past 6 months.

You will be part of the ACLR group if:

- you underwent a unilateral ACL reconstruction, your ACL injury occurred more than 1 year ago, it was a non-contact ACL injury,
- you have returned to your activities of daily living, and did not have suffer a second ACL injury.

If you have suffered an ACL injury but do not meet the previous conditions, you will not be able to participate.

You will be part of the healthy group if you do not have any ACL injuries.

What You Will Be Asked to Do

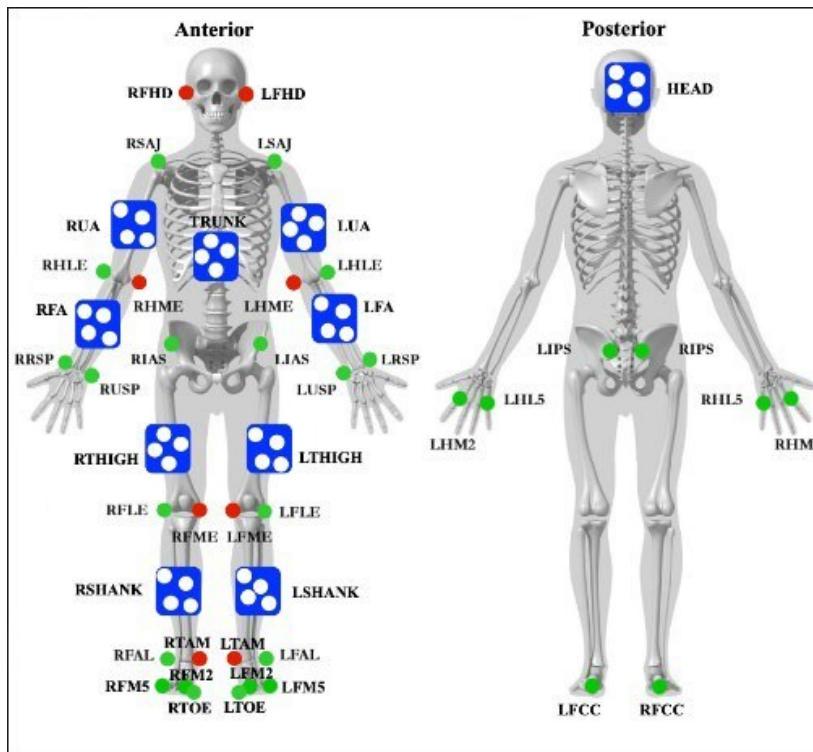
If you decide to participate in this research, you will be asked to visit the BENLab (Biomechanics, Ergonomics, Neuroscience) at Dalplex, room 217 of Dalhousie University, located at 6260 South St, Halifax, Nova Scotia, B3H 4R2. The visit will take approximately **three hours**. The visit will consist in different parts:

1. You will be asked to first sign this consent form before starting the study.
2. You will be asked to complete questionnaires related to the functional status of your knee, your activities, and your foot preference.
3. You will be asked to change into tight fitting clothes. This is done to reduce marker displacement.
4. We will then take your height and weight.
5. We will ask for permission to touch and feel for bony landmarks. This is done to place markers on your body. This will allow us to record your body movements. The member of the research team placing the markers on your body will be the same sex as you. The cameras recording your body movements only record the marker positions and will not be recording your face.
6. You will be asked to walk at your usual speed across the walkway. You will repeat this 10 times. You will get some rest (20 -30 seconds) between the repetitions.
7. After walking with no obstacles on the walkway, you will be asked to walk, and walk over obstacles of different heights placed on one side of your body. These obstacles (Width: 20 cm, Depth: 5 cm, Height: Variable) will have six different heights between 10 and 60 cm. You will be asked to repeat each height six times. You will also be asked to walk over the obstacle with your right and left leg. In total, you will do 72 obstructed walking trials (6 repetitions for 6 different heights and with 2 different legs). You will get some rest (20 -30 seconds) between the repetitions.
8. The markers will be removed.
9. After the markers are removed, you will be seated on a device that measures the strength of your knee muscle strength (Cybex Dynamometer).
10. Velcro straps will be put around your ankle, thigh, and torso to stabilize yourself and provide better results.
11. The device will be adjusted to your body size to align your knee with the axis of the device.
12. You will then be asked to relax, and a member of the research will measure the amount of rotation that can be recorded by the device. This will allow us to set safety stops on the device.
13. You will then be asked to lift your lower leg horizontally and allow it to drop by relaxing your muscles as much as possible. This allows us to measure the force that is generated with only the weight of your leg.
14. You will then be asked to warm up by doing knee movement

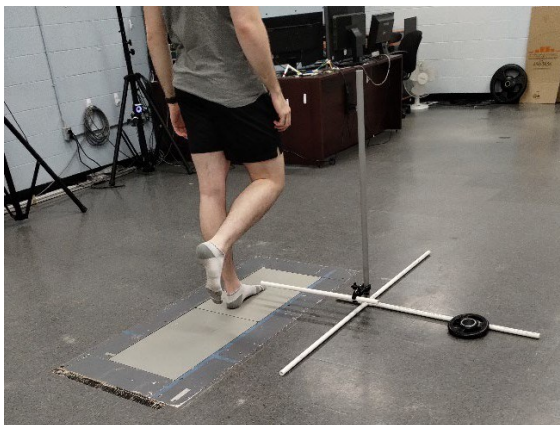
(extension and flexion) to warm up your muscles. You will repeat the movement approximately 10 times. This will be done with minimal resistance.

15. You will then be asked to push and pull three times (3 repetitions) as hard as you can against the device both while extending and flexing your knee. The device will allow you to move only at a predetermined speed and you will need to try to make it move faster than it allows. The predetermined speeds are from slow to rapid speeds (60, 120, 180, and 240 degrees per second). The predetermined speed order is not fixed.
16. You will repeat the strength measure for all 4 speeds.
17. After doing one leg, we will modify the settings of the machine and will repeat the warmup and measurement steps with your other leg.
18. Once the measurement of your knee muscles is finished, the straps will be removed, and you will be able to cool down/stretch on your own.
19. If you are no longer interested in having your results included in the study after your visit to the laboratory. You will have one month to let the lead researcher know so that all your data collected can be destroyed.

Below is a picture of how the markers will be placed, green and red will be placed on specific bony landmarks while blue rigid bodies will be placed on different segments for tracking purposes.



Below is a picture of the obstacle (on the left) and a picture of the muscle strength measurement device (on the right).



Possible Benefits, Risks and Discomforts

Benefits: There will be no direct benefits for your participation. Because there has been little to no research on obstructed walking and ACL reconstruction, the findings for this study can be used to characterize the changes in the gait of participants that underwent ACL reconstruction.

Risks:

Fatigue: The visit will take approximately three hours. You may become fatigued by the protocol, but ample rest time will be provided, as needed, throughout the protocol. The maximum voluntary contractions may result in some muscle soreness. However, this will be no different than that experienced during typical exercise and should resolve within 1-2 days. You will also have a short rest period between each movement task. If you feel the movement tasks are too difficult, and/or suffer prolonged muscle soreness or any discomfort, you may stop the data collection, decline to perform any more trials, or withdraw from the study, at any time.

Risk of contact with the obstacle: The study has a minimal risk of contacting the obstacle, from wrongly anticipating the obstacle's height that may lead to touching the obstacle while elevating the leg that leads to the fall of the obstacle. We will be using different heights for our study which will likely change the anticipation of the approach to clear the obstacle.

Discomfort placing/removing markers on body landmarks: This study required markers to be placed over anatomical positions, this may lead to irritations on the participant's skin. In addition to that, removing the markers may also cause discomfort for participants with thick and more body hair. To address this, we will use skin sensitive tape that is less likely to irritate skin as compared to regular tape. Hypoallergenic adhesives will be used to attach markers on your body. Any redness from the adhesives should resolved within 1-2 days.

Discomfort during palpation: Since the placement of the retroreflective markers needs to be accurate on the anatomical structure, palpation is required to search on participant's prime locations, which may cause moderate discomfort for individuals in the process. Therefore, we will be as gentle as possible during palpation.

Risk to privacy: **The risk of access to identifying information is minimal because there is a chance that the data is compromised by unauthorized individuals. Though, we will do our best to ensure all hard copies (including, consent with participant's name, and inertial characteristics (segment length, width)) will be safety locked in the file cabinet of the BENLab at Dalplex of Dalhousie**

University and electronic coded information data (raw data of the force plate or position data) will be on BEN Lab's password secured computer.

Compensation / Reimbursement

You will be reimbursed 25\$ for your expenses (transportation and parking) and time. You will be reimbursed even if you do not complete the study.

How your information will be protected:

Privacy: Your participation in this research will be known only to the lead researcher (Michel Ladouceur) and the other members of the research team.

Confidentiality: The information that you provide to us will be kept confidential. Only the lead researcher (Michel Ladouceur) will have access to this information. The people who work with us have an obligation to keep all research information confidential. All your identifying information (such as your name and contact information) will be securely stored separately from your research information. We will use a participant coded name (not your actual name) in our written and computer records so that the research information we have about you contains de-identified name. During the study, all electronic records will be kept secure in an encrypted file on the researcher's password-protected computer. All paper records will be kept secure in a locked filing cabinet located in the researcher's lab. We will describe and share our findings in thesis and presentations. We will only report group results and not individual results. This means that you will not be identified in any way in our reports.

Data retention: With your permission, the information you provide in this research project may be kept for other uses in the future. These raw data include the force plate, position data, the analyzed data in Visual3D, and inertial characteristics form. Once the study is over, your data will be irreversibly anonymized by demolishing the master key sheet that obtain each of participant's coded file name, which link back to participant's name. To protect your identity, I will remove personal information that could identify you to ensure that no one will be able to identify you. Despite these measures I cannot guarantee your anonymity.

If You Decide to Stop Participating

You are free to leave the study at any time. There will be no impact on your academic standing for withdrawal. If you decide to stop participating during the study, you can decide whether you want any of the information that you have provided up to that point to be removed or if you will allow us to use that information. After participating in the study, please contact us within 1 month to withdraw your data. After that time, it will be very difficult to withdraw your information.

How to Obtain Results

We will provide you with a short description of group results when the study is finished. If you are interested in your individual results, they can be provided to you during a scheduled meeting with the lead researcher. You can obtain these results by including your email at the end of the signature page on the visit.

Questions

We are happy to talk with you about any questions or concerns you may have about your participation in this research study. Please contact Michel Ladouceur (at michel.ladouceur@dal.ca) at any time with questions, comments, or concerns about the research study.

If you have any ethical concerns about your participation in this research, you may also contact Research Ethics, Dalhousie University at (902) 494-3423, or email: ethics@dal.ca (and reference REB file # 2024-7253).”

In the next part, you will be asked if you agree (consent) to join this study. If the answer is “Yes”, you will need to sign the form.

Signature Page

Project Title: Effects of ACL reconstruction on Unilateral Obstructed Walking

Lead Researcher: Michel Ladouceur, PhD

I have read the explanation about this study. I have been given the opportunity to discuss it and my questions have been answered to my satisfaction. I understand that I have been asked to take part in a trial that will occur at a location acceptable to me. I agree to take part in this study. I agree that the duration of the trial is three hours. I realize that my participation is voluntary and that I am free to withdraw from the study at any time, until one month after the trial is completed.

Name	Signature	Date
I agree to have my data included in the BENLab walking database		Yes No

Name	Signature	Date

Please provide an email address below if you would like to be sent a summary of the study results.

Email address: _____

Please provide an email address below if you would like to be contacted to schedule a meeting where your individual study results will be presented once they have been analyzed.

Email address: _____

Appendix B: Participant's characteristics form

ACLR Study

Coded File Name:	
Lysholm Knee Questionnaire:	
Tegner Activity Scale (Current):	
Healthy Group	
Preferred (Operational) Side:	
ACL reconstruction Group	
ACL reconstruction Side:	
Preferred (Operational) Side:	
Age:	
Sex:	
Height (m):	
Mass (kg):	
BMI:	

Appendix C: Lysholm Knee Questionnaire

Code File Name:		Date:	
------------------------	--	--------------	--

Check the corresponding descriptor for each section

Section 1 – Limp	
	I have no limp when I walk. (5)
	I have a slight or periodical limp when I walk. (3)
	I have a severe and constant limp when I walk. (0)
Section 2 – Using cane or crutches	
	I do not use a cane or crutches. (5)
	I use a cane or crutches with some weight-bearing (2)
	Putting weight on my hurt leg is impossible. (0)
Section 3 – Locking Sensation in the knee	
	I have no locking and no catching sensation in my knee. (15)
	I have a catching sensation but no locking sensation in my knee. (10)
	My knee locks occasionally. (6)
	My knee locks frequently. (2)
	My knee feels locked at this moment. (0)
Section 4 – Giving way sensation from the knee	
	My knee never gives way. (25)
	My knee rarely gives way, only during athletics or vigorous activity. (20)
	My knee frequently gives way during athletics or other vigorous activities. In turn I am unable to participate in these activities. (15)
	My knee frequently gives way during daily activities. (10)
	My knee often gives way during daily activities. (5)
	My knee gives way every step I take. (0)

Section 5 – Pain	
	I have no pain in my knee. (25)
	I have intermittent or slight pain in my knee during vigorous activities. (20)
	I have marked pain in my knee during vigorous activities. (15)
	I have marked pain in my knee during or after walking more than 1 mile. (10)
	I have marked pain in my knee during or after walking less than 1 mile. (5)
	I have constant pain in my knee. (0)
Section 6 -Swelling	
	I have no swelling in my knee. (10)
	I have swelling in my knee only after vigorous activities. (6)
	I have swelling in my knee after ordinary activities. (2)
	I have swelling constantly in my knee. (0)
Section 7 – Climbing Stairs	
	I have no problems climbing stairs. (10)
	I have slight problems climbing stairs. (6)
	I can climb stairs only one at a time. (2)
	Climbing stairs is impossible for me. (0)
Section 8 – Squatting	
	I have no problems squatting. (5)
	I have slight problems squatting. (4)
	I cannot squat beyond a 90° bend in my knee. (1)
	Squatting is impossible because of my knee. (0)

Score (/100):

Briggs, K. K., Lysholm, J., Tegner, Y., Rodkey, W. G., Kocher, M. S., and Steadman, J. R. (2009). The reliability, validity, and responsiveness of the Lysholm score and Tegner activity scale for anterior cruciate ligament injuries of the knee: 25 years later. *The American journal of sports medicine*, 37(5), 890–897

Appendix D: Tegner Activity Scale

Code File Name:		Date:	
------------------------	--	--------------	--

	Level
Activity Level Before Injury	
Activity Level Following Surgery (if applicable)	
Current Activity Level	

Description of the Tegner Activity Scale levels

Level	Activity
10	Competitive sports: soccer, football, rugby (national and international elite)
9	Competitive sports: soccer, football, rugby (lower divisions), ice hockey, wrestling, gymnastics, basketball
8	Competitive sports: racquetball or bandy, squash or badminton, athletics (jumping, etc.), downhill skiing
7	Competitive sports: tennis, athletics (running), motocars speedway, handball Recreational sports: soccer, football, rugby, bandy, ice hockey, basketball, squash, racquetball, athletics (running)
6	Recreational sports: tennis and badminton, handball, racquetball, downhill skiing, jogging at least five times per week
5	Work: heavy labor (e.g., building, forestry) Competitive sports: cycling, cross-country skiing. Recreational sports: jogging on uneven ground at least twice weekly
4	Work: moderately heavy labor (e.g., truck driving, heavy domestic work)
3	Work: light labor (e.g., nursing) Competitive and recreational sports: swimming, walking in forest possible
2	Work: light labor Walking on uneven ground possible but impossible to back pack or hike
1	Work: sedentary work (secretarial, etc)
0	Sick leave or disability pension because of knee problems

Briggs, K. K., Lysholm, J., Tegner, Y., Rodkey, W. G., Kocher, M. S., and Steadman, J. R. (2009). The reliability, validity, and responsiveness of the Lysholm score and Tegner activity scale for anterior cruciate ligament injuries of the knee: 25 years later. *The American journal of sports medicine*, 37(5), 890–897

Appendix E: Waterloo Footedness Questionnaire-Revised (WFQ-R)

Code File Name:		Date:	
------------------------	--	--------------	--

Questions (check the side that applies)

Activity	Left	Right
If you were asked to shoot a ball on target, which leg would you use to shoot the ball?		
If you had to pick up marbles while standing and put marbles in a box, which foot would you use to pick them up?		
If you were asked to stand on one leg, on which leg would you stand?		
Which foot would you use to smooth sand while standing?		
If you had to step up onto a chair, which foot would you place on the chair first?		
Which foot would you use to stomp an insect while you were standing?		
If you were to balance on one foot on a railway track, which foot would you use?		
If you had to hop on one foot, which foot would you use?		
Which foot would you use to help push a shovel into the ground while digging?		
During relaxed standing, people initially put most of their weight on one foot, leaving the other slightly bent. Which foot do you put most of your weight on first?		
	YES	NO
In the past, have you had any special training which stimulates the use of a certain leg in a certain situation or activity? (Sports and/or work related?)		
Is there a reason why your leg preference has changed, such as an injury?		

EliasLJ, Bryden MP, Bulman-Fleming MB. Footedness is a better predictor than is handedness of emotional lateralization. *Neuropsychologia*. 1998; 36

Appendix F: Supplementary material for the methodology section

Motion capture system

The validity and accuracy of the Optitrack system were measured and compared to the Vicon system. Studies have used different types of cameras, some older (Flex V100R2) and some newer (Prime). When comparing the 12 Optitrack Flex: V100R2 cameras to 12 Vicon MXF20 cameras at a sampling rate of 100 Hz, researchers were able to conclude that the errors were less than 1%, confirming the high validity of the usage of these cameras (Thewlis et al., 2013). Another study using 8 Optitrack Flex: V100R2 (sampling frequency at 100 Hz) cameras was compared to two different Vicon cameras, the Vicon Mx (sampling frequency at 100 Hz) and the Vicon 612 (sampling frequency at 120 Hz). It was concluded that when compared to the Vicon Mx, the Optitrack system had similar results; however, results were different when compared to the Vicon 612 (Carse et al., 2013). Other studies have focused on newer cameras, such as the Optitrack Prime 41 cameras, which collect at a sampling frequency of 180 Hz. These cameras were compared to ThorLabs LTS300 linear motion stage using 42 or 21 Optitrack cameras, respectively, to determine if more cameras result in better accuracy. They were able to conclude that for the 42 cameras setup when compared to the LTS 300, the error was less than 200 μm (0.2mm) in the 97% volume being captured compared to the 91% of the captured volume with the 21 cameras setup (Aurand et al., 2017).

Despite reliability, errors that may arise could be attributed to the researcher, as the accuracy of marker placement is crucial to ensure proper data collection (Lavaill et

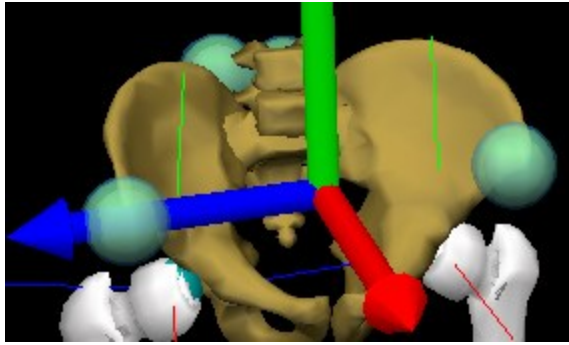
al., 2022; Malus et al., 2021). Errors could also arise due to skin movement artifacts (Ancillao et al., 2022).

Four markers were placed on the rigid bodies, as the number of recommended markers should be no less than four to better represent the segments being defined (Cappozzo et al., 1997). Rigid body tracking requires at least three markers. One axis is defined along the line connecting two markers, while the plane established by the three markers is taken perpendicular to the second axis. The third axis is obtained by taking the cross-product of the first two axes. Sometimes, a marker might be missing during data collection; hence, it is recommended that no less than four markers be used.

Lower body model

Pelvis segment model

The pelvis segment was defined as a CODA model (embedded in Visual3D) using the Anterior Superior Iliac Spine (ASIS) and Posterior Superior Iliac Spine (PSIS) markers. The origin of the pelvic coordinate system was determined as being halfway between the right and left ASIS. The z-x plane was formed by the line connecting the right and left ASIS as well as by the midpoint of right and left PSIS. From the origin and towards the right ASIS is the Z axis, the Y axis is the axis perpendicular to the plane formed from the two ASIS and the midpoint between both PSIS. The cross product of the Z and Y axis is the X axis, corresponding to the anteroposterior axis, pointing forward.



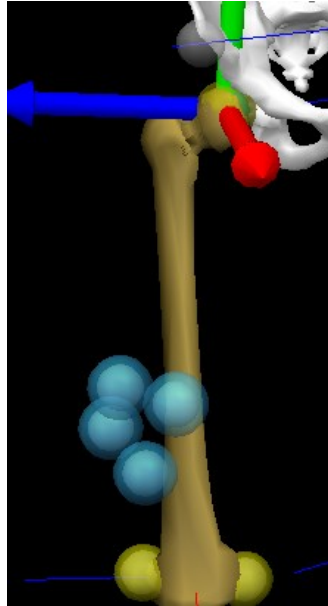
Thigh segment model

Proximally, the thigh was defined by the hip joint center as well as the radius corresponding to half of the distance between both ASIS. Distally, the thigh was defined by the medial and lateral epicondyles of the femur. Thigh cluster markers were used to track the segment's motion. Two new landmarks corresponding to the right and left hip joint centers (RHJC and LHJC) were generated based on the following regression equations (Bell et al., 1989).

$$\text{RHJC} = (0.36 * \text{ASIS Distance}, -0.19 * \text{ASIS Distance}, -0.3 * \text{ASIS Distance})$$

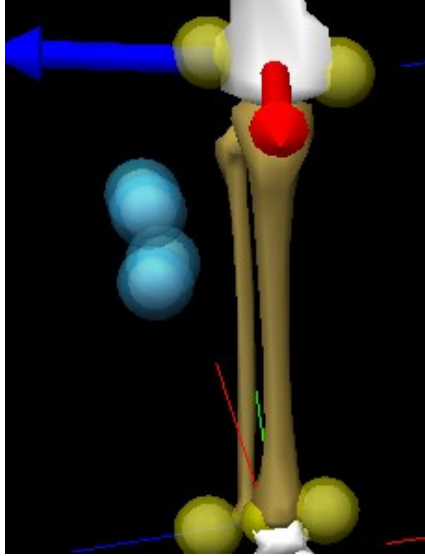
$$\text{LHJC} = (-0.36 * \text{ASIS Distance}, -0.19 * \text{ASIS Distance}, -0.3 * \text{ASIS Distance})$$

The hip joint center was the origin of the hip joint coordinate system. The knee joint center was determined to be at the distal portion of the thigh, midway between the epicondyles of the femur (Hanavan, 1964). The Y axis was defined from the knee joint center towards the hip joint center. A vector V was created using the medial to lateral epicondyles of the femur. The cross product of V with the Y axis was defined as the X axis, pointing anteriorly. The cross product of Y and X was defined as the Z axis, directed laterally. The thigh segment had axes in the same direction as the hip joint coordinate system and originated at the center of the segment's center of mass (COM).



Shank segment model

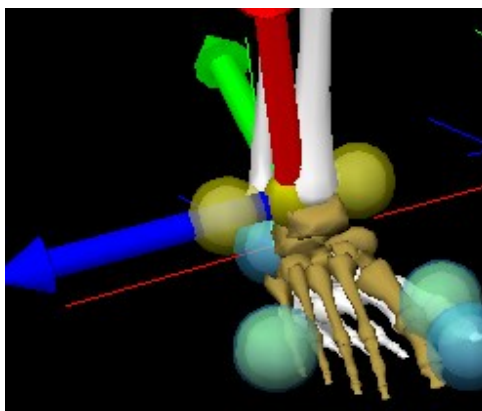
Proximally, the shank was defined by using the medial and lateral epicondyles of the femur. Distally, it was defined by using the medial and lateral malleoli. Shank cluster markers were used as tracking markers. The ankle joint center was situated at the distal portion of the shank, midway between the malleoli of the ankle. The coordinate system of the knee joint was defined as follows: the Y axis was defined from the ankle joint center to the knee joint center (origin). A vector V was created using the two femoral condyles. The cross product of V with the Y axis defined the X axis, pointing anteriorly. The cross product of Y and X defined the Z axis, directed laterally. The shank segment had its axes in the same direction as the knee joint coordinate system and had its origin at the location of the segment's center of mass.



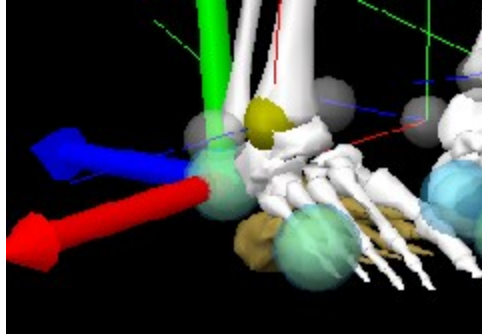
Foot segment model

The foot segment had a model for the kinematic calculations and one for the kinetic calculations.

For kinetic purposes, the proximal end of the foot was defined using the medial and lateral malleoli markers. The distal end was defined using the fifth metatarsal and toe markers. Markers of the calcaneus, first metatarsals, fifth metatarsal, and toe markers were selected to track the segment. The ankle joint coordinate system originated from the ankle joint center, with its coordinates being as follows: the Y axis was defined from the midpoint of the first and fifth metatarsal heads towards the ankle joint center. A vector V was created using the medial to lateral malleoli. The cross product of the Y axis with V defines the X axis. The cross-product of Y and X defined the Z axis.



Since the Y axis would not be vertical, joint angles would not be accurately calculated. Hence, a virtual ankle joint coordinate system was created solely for kinematics use. The calcaneus was the origin of the kinematic foot segment with a radius of 0.1 m for the proximal portion of the segment. The toe marker was used along a defined radius of 0.1 m on the distal side. Moreover, an additional lateral marker was used to define the segment, which in this case is the marker placed on the fifth metatarsal. The aforementioned markers, as well as the marker placed at the first metatarsal, were used as tracking markers for the kinematic foot segment. Its coordinate system was defined as follows: the anteroposterior axis X was defined from the origin (calcaneus) towards the toe target. A vector V was created using the medial and lateral malleoli. The cross product of the X axis and vector V defined the Y axis. The cross product of the X and Y axis was defined as the Z axis. The foot segment would have its axes in the same direction as the ankle joint coordinate system. The kinematic foot segment had its origin at the location of its center of mass.



Segment's inertial properties (mass, location of their CoM, mass moment of inertia)

The inertial properties of each segment were determined. The mass of the segments in Visual3D is based on the regression equations provided by Dempster (1955), $m_s = p_s M$, with m_s being the segment's mass and p_s being the percentage of the total mass M . For the lower extremity, the p_s of the thigh is 0.10, the shank is 0.0465, and the foot is 0.0145. The center of mass location was calculated as the point at which the segment's mass can be considered to be concentrated (Robertson, 2014).

The COM was positioned along the vector passing through the distal and proximal ends of the segment at a ratio distance c , from the proximal end of the segment in the local coordinate system (LCS) (Robertson, 2014).

The equations used for calculating c are as follows:

$$x = \frac{R_{distal}}{R_{proximal}}$$

$$c = \frac{1 + 2x + 3x^2}{4(1 + x + x^2)} \text{ for } R_{distal} < R_{proximal}$$

$$c = 1 - \frac{1 + 2x + 3x^2}{4(1 + x + x^2)} \text{ for } R_{proximal} < R_{distal}$$

Joint angular velocity and acceleration

In Visual3D, joint angular velocity can be expressed in Euler angles using the following:

Angular velocity in body coordinates $\omega = \begin{bmatrix} \omega_x \\ \omega_y \\ \omega_z \end{bmatrix}$, which can be expressed in terms of

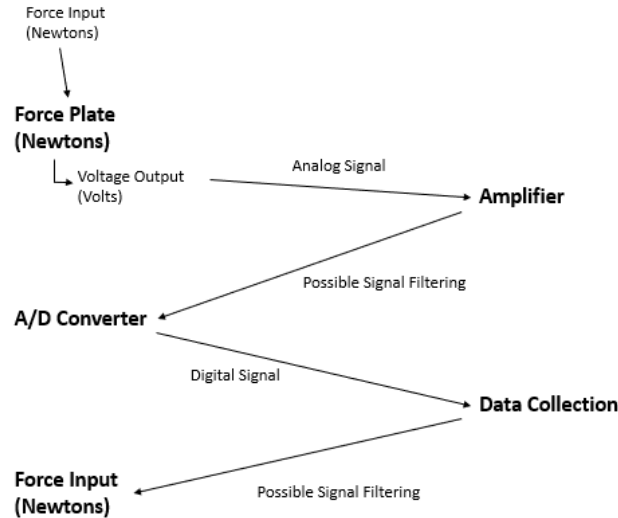
derivatives of the Euler angles $\dot{\theta} = \begin{bmatrix} \dot{\theta}_x \\ \dot{\theta}_y \\ \dot{\theta}_z \end{bmatrix}$, as:

$$\begin{bmatrix} \omega_x \\ \omega_y \\ \omega_z \end{bmatrix} = \begin{bmatrix} \dot{\theta}_x \\ 0 \\ 0 \end{bmatrix} + \begin{bmatrix} 0 \\ c_x \dot{\theta}_y \\ s_x \dot{\theta}_y \end{bmatrix} + \begin{bmatrix} s_y \dot{\theta}_z \\ -s_x c_y \dot{\theta}_z \\ c_x c_y \dot{\theta}_z \end{bmatrix} = \begin{bmatrix} \dot{\theta}_x + s_y \dot{\theta}_z \\ c_x \dot{\theta}_y - s_x c_y \dot{\theta}_z \\ s_x \dot{\theta}_y + c_x c_y \dot{\theta}_z \end{bmatrix} \text{ where } s_i = \sin(\theta_i), c_i = \cos(\theta_i) \text{ for } i=x,y,z.$$

Force plate system

In summary, the force plate sensors (strain gauges) transduce the forces acting on the surface of the force plate and transform it into an initial analog signal. These strain gauges are placed on pillars to measure these acting forces along all three axes. An amplifier is then used to increase the voltage of the signal, as it needs to be higher than the one the sensors detected. The amplified signal is then converted from an analog signal to a digital signal using an Analog to Digital converter (A/D). It is important to note that the analog signal went through a 2-pole 1000 Hz low-pass anti-aliasing filtering process after amplification and before being converted to a digital signal. The digital signal also

goes through a filtering process to be processed by the computer software and prepared for data analysis (Beckham et al., 2014).



Internal joint moment calculation

The following is an example of the process the ground reaction forces (GRF) exerted on the human body. The calculation of the ankle joint force was as follows:

$$\Sigma F_{\text{foot}} = m_{\text{foot}}\alpha_{\text{foot}} \quad F_{\text{ankle}} + m_{\text{foot}}g + F_{\text{GRF}} = m_{\text{foot}}\alpha_{\text{foot}} \quad F_{\text{ankle}} = m_{\text{foot}}\alpha_{\text{foot}} - m_{\text{foot}}g - F_{\text{GRF}}$$

where m_{foot} is mass of the foot, α_{foot} is acceleration of the foot, g is gravity acceleration, F_{ankle} is ankle joint force, which can be derived from the resultant force on the foot minus the weight and GRF. The proximal couple moment was be calculated in Visual3D as:

$$M^i_{\text{foot}} = I_{\text{foot}}\alpha_{\text{foot}} + \omega_{\text{foot}} \times (I_{\text{foot}}\omega_{\text{foot}})$$

where I =moment of inertia, α =angular acceleration, ω =angular velocity.

$$\Sigma M_{\text{foot}} = M^i_{\text{foot}}$$

$$M_{\text{ankle}} + M_{\text{GRF}} - \mathbf{r}_{\text{ankle to foot}} \times \mathbf{F}_{\text{ankle}} + (\mathbf{r}_{\text{ankle to grf}} - \mathbf{r}_{\text{ankle to foot}}) \times \mathbf{F}_{\text{GRF}} = M^i_{\text{foot}}$$

where $\mathbf{r}_{\text{ankle to foot}}$ refers to the vector from the ankle to the foot's CoM, $\mathbf{r}_{\text{ankle to grf}}$ refers to the vector from the ankle to the CoP.

$$\begin{aligned} M_{\text{ankle}} &= M^i_{\text{foot}} - M_{\text{GRF}} + (\mathbf{r}_{\text{ankle to foot}} \times \mathbf{F}_{\text{ankle}}) - [(\mathbf{r}_{\text{ankle to grf}} - \mathbf{r}_{\text{ankle to foot}}) \times \mathbf{F}_{\text{GRF}}] \\ &= M^i_{\text{foot}} - M_{\text{GRF}} + [\mathbf{r}_{\text{ankle to foot}} \times [\mathbf{m}_{\text{foot}} (\boldsymbol{\alpha}_{\text{foot}} - \mathbf{g}) - \mathbf{F}_{\text{GRF}}]] - [(\mathbf{r}_{\text{ankle to grf}} - \mathbf{r}_{\text{ankle to foot}}) \times \mathbf{F}_{\text{GRF}}] \\ &= M^i_{\text{foot}} - M_{\text{GRF}} - [\mathbf{r}_{\text{ankle to grf}} \times \mathbf{F}_{\text{GRF}}] + \mathbf{r}_{\text{ankle to foot}} \times [\mathbf{m}_{\text{foot}} (\boldsymbol{\alpha}_{\text{foot}} - \mathbf{g})] \end{aligned}$$

Appendix G: Breakdown of the number of trials

Below can be found the tables number of trials processed per participant.

Participant	Total trials	Valid Trials	Labelled Trials	Trials used for inverse dynamics calculations	Trials used for energy bursts calculations
1	100	75	70	57	54
2	94	75	62	58	56
3	91	65	55	45	40
4	85	65	53	46	43
5	115	65	50	46	44
6	100	65	62	52	50
7	137	65	57	42	40
8	90	55	45	36	34
9	95	65	50	39	37
10	82	65	61	51	49
11	100	75	62	61	57
12	180	65	57	48	44
Total	1269	800	684	581	548
Median (±SD)	97.5 ±27.6	65 ±5.8	57 ±6.8	47 ±7.6	44 ±7.5

Below are the number of trials per obstacle and leg conditions processed to generate the energy bursts.

	Left SL		Right SL	
	Total	Median	Total	Median
Height 0 cm	45	3.8		
Height 10 cm	44	3.8	45	4
Height 20 cm	44	3.8	45	3.9
Height 30 cm	42	3.7	44	3.7
Height 40 cm	44	3.9	38	3.2
Height 50 cm	45	3.9	34	3
Height 60 cm	40	3.8	38	3.6

Appendix H: ALAs during walking over unilateral obstacles following anterior cruciate ligament reconstruction

Section 1: Introduction

Section 1.1 Statement of the problem

The presence of pathology, with the associated altered mechanics, may present an opportunity to investigate the behavioural changes that occur to ensure the appropriate control during gait. A common injury, the anterior cruciate ligament (ACL) rupture, is a serious knee injury garnering significant attention due to its severity, long-term consequences, and ongoing efforts to prevent its occurrence (Gilchrist et al., 2008; Pollard et al., 2017). A typical ACL tear occurs when the hip is internally rotated and adducted, the knee is in a valgus position, the tibia is externally rotated and anteriorly translated, and the ankle is in eversion (Boden et al., 2000). An ACL tear often leads to knee instability due to the ligament's role in providing rotational and translational stability (Bohn et al., 2016; Zantop et al., 2005). Individuals with ACL injuries typically undergo conservative treatment or surgical intervention to restore knee stability, with Anterior Cruciate Ligament Reconstruction (ACLR) being the most common surgical approach. Despite prolonged rehabilitation, ACLR patients are still at significant risk of re-injury, contralateral leg injury, and early onset osteoarthritis (Andriacchi and Dyrby, 2005; Baumeister et al., 2008; Brophy et al., 2012; Neto et al., 2019; Paterno et al., 2012; Salmon et al., 2005).

Walking has been studied extensively in individuals post-ACLR, with research focusing on net joint moments (Davis-Wilson et al., 2020; Lisee et al., 2022) and few studies examining net joint power (DeVita et al., 1997, 1998; Roewer et al., 2011). As

presented above, analyzing net joint muscle power could provide a more critical understanding of walking control. During walking, participants post-ACLR adopt a stiffened knee strategy, which combines decreased knee flexion angles with decreased knee extensor moments (Roewer et al., 2011). Increased hip extensor activity is also observed (DeVita et al., 1998). These findings (increased hip extensor activity and adoption of stiffened knee strategy) are corroborated by EMG data, which show decreased quadriceps activity, increased hamstrings activity, and increased gastrocnemius activity (Andriacchi and Birac, 1993; Rudolph et al., 2001). Despite meeting the criteria for return to sport (RTS), deficits between the limbs of participants post-ACLR (Davis-Wilson et al., 2020; Roewer et al., 2011) and differences compared to able-bodied individuals remain (DeVita et al., 1998). This provides an impetus for treating ACL injuries as a neurophysiological dysfunction rather than solely a peripheral musculoskeletal injury (Kapreli et al., 2009).

Despite the lower forces occurring during walking in comparison to sport-related movements, like cutting and decelerating, compensations that arise while performing walking tasks in individuals post-ACLR place the knee under compressive and shear forces that can further damage the knee joint, disrupt its function and increase the risk of post-traumatic osteoarthritis (Pfeiffer et al., 2019; Pietrosimone et al., 2017). The complex nature of ACL injuries extends beyond structural damage, emphasizing the need to assess neurophysiologic aspects of recovery. The rationale for assessing these ALAs in participants post-ACLR stems from the altered gait mechanics and compensations exhibited by this population, especially after RTS. This assessment would provide insight into how the muscles behave in response to the addition of unilateral obstacles.

Section 1.2 Purpose and significance of the study

This study provides a case study of two participants post-ACLR. It is one of the first studies investigating kinematic and kinetic adaptations during obstacle negotiation of heights as high as 60 centimetres (cm). By analyzing these adaptations, the study offers valuable insights into how participants post-ACLR adapt in comparison to able-bodied participants. Obstructed walking offers a challenge that requires a modification of the normal walking pattern. Using a unilateral obstacle provides an experimental situation where the control of the foot trajectory and the associated control of the balance of the HAT can be decoupled.

Despite successful rehabilitation, ACLR patients remain at a significantly increased risk of re-injury, contralateral leg injury, and early onset of osteoarthritis. Even after meeting RTS criteria, research has shown persistent gait asymmetries between the reconstructed and non-injured limbs, as well as compared to able-bodied controls. These ongoing deficits highlight the biomechanical challenges that continue long after surgery, suggesting that complete functional recovery may be difficult. The findings from this study may help refine rehabilitation strategies, improve RTS protocols, and reduce the risk of re-injury and long-term knee degeneration in ACLR patients.

Section 1.3 Specific aims of the study

This study aimed to perform a comprehensive analysis of ALAs during obstructed walking in participants post-ACLR.

The specific aim was to identify if the ALAs of participants post-ACLR for unilateral obstacles of increasing heights during walking are different between their

injured and non-injured legs as well as different from the ALAs of able-bodied participants.

Section 1.3.1 Hypotheses

The following hypotheses were tested to answer the specific aim of identifying whether the ALAs of participants post-ACLR for unilateral obstacles of increasing heights during walking are different between their injured and non-injured legs and different from the ALAs of able-bodied participants.

- a) There were no differences between the injured and non-injured leg ALAs of participants post-ACLR, while there were differences compared to the able-bodied participants walking over unilateral obstacles of increasing heights. The ALAs are defined as:
 - a. The crossing leg knee flexor muscles generation of energy at the initiation of swing (K5).
 - b. The crossing leg knee extensor muscles absorption of energy at the initiation of swing (K3).
 - c. The crossing leg hip flexor muscles generation of energy at the initiation of swing (H3).
 - d. The crossing leg hip abductor muscles generation of energy at the end of the stance phase (H3F).
 - e. The supporting leg hip abductor muscles absorption of energy at the start of the stance phase (H1F).

Section 2: ACLR literature review

Section 2.1 Anterior cruciate ligament rehabilitation and walking

ACL injuries can have considerable financial and physical impacts. The healthcare costs associated with treating these injuries have been reported to range from \$1 to \$2 billion annually, with approximately 200,000 ACL injuries occurring each year in the United States, and up to 90% of patients choosing to undergo ACLR procedures (Paterno, 2015). Athletes who suffer from these injuries face physical and mental challenges, as they need to undergo rehabilitation for a period of 9 to 12 months, despite some being cleared after an accelerated recovery (DeVita et al., 1998). Returning to pre-injury levels is often not achieved even with rehabilitation (Davis-Wilson et al., 2020; DeVita et al., 1998; Roewer et al., 2011). Studies of these injuries have been conducted to understand the mechanism, risk factors, and sex differences and to prevent and reduce this injury rate. Despite restoring limb strength, many individuals undergoing ACLR experience altered mechanics and postural control impairments (Baumeister et al., 2008). This suggests that ACL injury may be more than a peripheral musculoskeletal issue, extending to neurophysiological dysfunction (Kapreli et al., 2009).

Section 2.1.1 Introduction to the anterior cruciate ligament

The anterior cruciate ligament (ACL) is an intraarticular yet extra-synovial band of connective tissue (Bicer et al., 2010). The ACL originates on the posterior side of the femur, specifically on the posterior medial aspect of the lateral femoral condyle (Bicer et al., 2010). The ACL inserts on the tibia, specifically the anterior intercondylar fossa, anterolateral to the medial tibial spine (Bicer et al., 2010). Cadaveric reports and studies suggest that the ACL is formed by two bundles, the anteromedial (AM) and posterolateral

(PL) bundles (Amis et al., 2005; Bicer et al., 2010). Knee position results in a change of orientation of these bundles. With the knee extended, the PL bundle tightens while the AM bundle is lax, resulting in knee stability provided by the PL bundle. During knee flexion, the two bundles would cross as the AM bundle would move laterally and tighten, while the PL moves anteriorly and becomes lax, resulting in knee stability achieved by the AM bundle (Bicer et al., 2010; Mall et al., 2013).

The ligament bundle serves to provide stability to the knee in its various motions (Bohn et al., 2016; Zantop et al., 2005). The knee exhibits 6 DOF during dynamic activities due to its bicondylar-modified hinge joint structure (Komdeur et al., 2002). These 6 DOF are characterized by three rotations – flexion and extension, internal and external rotation, varus and valgus angulation- and three translations – anterior and posterior glide, medial and lateral shift, compression and distraction (Komdeur et al., 2002). Due to the ACL's oblique direction from origin to insertion, its primary role is to prevent anterior translation of the tibia (ATT) about the femur, contributing a total restraining force of 87% at 30° knee flexion and 85% at 90° knee flexion (Butler et al., 1980). In addition to being the primary preventor of ATT, the ACL also provides knee stability by preventing internal tibial rotation, a minor role in restraining frontal plane loading on the knee joint and preventing knee hyperextension (Fleming et al., 2001).

Section 2.1.2 ACL and movement control

The ACL is innervated by the posterior branches of the tibial nerve (Bicer et al., 2010). Mechanoreceptors have been found within the fibres of the ACL, including Ruffini receptors that act as stretch receptors, Vater-Pacini receptors that detect compression forces, and Golgi-like tendon receptors (Haus and Halata, 1990; Kennedy et

al., 1982). The ACL is also thought to contribute to proprioception through these mechanoreceptors located at both its proximal and distal attachments (Parus et al., 2015). These mechanoreceptors transmit proprioceptive feedback by converting strain into action potentials, which are then relayed to the central nervous system (Uchio, 2016). These receptors provide proprioceptive feedback in case of any postural changes. In the event of any subtle change, the afferent nerve fibres within the ACL are activated, which affects the muscular activity surrounding the knee (Konishi et al., 2002). This is known as the “ACL reflex,” which keeps the muscles prepared in case of any alteration and becomes more evident with ACL injury, as mechanoreceptors are damaged, leading to quadriceps weakness (Konishi et al., 2002). These mechanoreceptors can track and monitor the joint position angle of rotation and motion (Schutte et al., 1987), control the neuromuscular system in the activity of the muscles surrounding the knee joint, and have a proprioceptive function (Solomonow et al., 1987).

Beyond its primary role in restraining ATT and providing rotational stability to the knee (Butler et al., 1980; Fleming et al., 2001; Uchio, 2016), the proprioceptive function of the ACL may remain impaired even after ACLR. Following ACL injury, individuals often experience reduced neuromuscular and sensorimotor function, accompanied by diminished muscle strength and activation. This leads to impaired body balance and coordination (Kielè et al., 2020). Damage to the mechanoreceptors in the ACL during injury impairs proprioception and kinesthesia (the sense of joint movement), further compromising body stability (Swanik et al., 2007). This loss of proprioceptive feedback may persist even after reconstruction, continuing to affect muscle control and postural control and generating altered movement patterns via disrupted feedback pathways

(Baumeister et al., 2008; Parus et al., 2015). Additionally, the neuroplasticity observed in participants post-ACLR (Gokeler et al., 2019) suggests that the brain compensates for these deficits, which may impact muscle function and the ability to execute coordinated movements. Research has shown that individuals post-ACLR exhibit reduced maximal voluntary quadriceps contractions (Courtney et al., 2011), which can further hinder athletic performance and increase re-injury risk (Neto et al., 2019). Consequently, not only does the injured leg experience postural control deficits, but these deficits may also extend to the non-injured leg, increasing the risk of further injury (Culvenor et al., 2016).

Beyond physical rehabilitation, cognitive factors such as reaction time, processing speed, and memory play a significant role in ACL recovery (Swanik et al., 2007). These neurocognitive aspects are essential for motor control, especially in dynamic, sport-related tasks. Research indicates that individuals post-ACLR perform worse than able-bodied controls in tasks involving visual and verbal memory, reaction time, and processing speed (Swanik et al., 2007). Cognitive dysfunction, particularly slower reaction times, can compromise an athlete's ability to adapt to changes in their environment quickly, thus increasing the risk of further injury (Dault et al., 2001). Furthermore, decreased coordination due to cognitive deficits can affect muscle activity, reduce dynamic restraint, and contribute to re-injury risks (Swanik et al., 2007).

The recovery process for ACLR patients is not only about restoring musculoskeletal function but also about addressing neurophysiological impairments. Neuroplastic changes, such as increased motor cortex activity and altered sensory processing (Gokeler et al., 2019), suggest that the brain compensates for mechanical deficiencies in the knee. This neurophysiological compensation is crucial in providing

adequate knee stability but also highlights the need for comprehensive rehabilitation that targets both brain function and biomechanical recovery (Kapreli et al., 2009). Effective rehabilitation programs must, therefore, integrate neuromuscular and cognitive training to address both the physical and cognitive deficits that persist after ACL injury (Swanik et al., 2007). By considering both the neurophysiological and biomechanical aspects of recovery, athletes may achieve more holistic rehabilitation outcomes and reduce the risk of re-injury (Gokeler et al., 2019; Kapreli et al., 2009).

Section 2.1.3 Walking in individuals post-ACLR

During knee flexion and extension, the tibia undergoes both rotational and translational movements relative to the femur, with the knee's center of rotation shifting as the flexion angle changes (Marieswaran et al., 2018). Specifically, between 0° and 30° of knee flexion, there is minimal anterior translation of the femoral condyles, but this increases between 30° and 135° (Marieswaran et al., 2018). These variations in knee mechanics significantly influence the forces exerted on the ACL during movement.

Research has shown that the ACL experiences its greatest force when the knee is flexed less than 30°, particularly during hyperextension (-5°), where a combination of anterior force and internal torque results in peak ACL force of 300 N (Markolf et al., 1995). This highlights the critical vulnerability of the ACL at specific flexion angles, which is essential for understanding ACL injury dynamics, especially in individuals post-ACLR.

Further studies using in vivo and simulated walking models have provided insights into the forces acting on the ACL. Peak ACL forces vary across different studies, ranging from 156 N to 411 N (Harrington, 1976; Morrison, 1970). To investigate further,

a 3D full-body model was constructed to mirror experimental data closely (Shelburne et al., 2004). This model showed that muscle forces, such as 1188 N from the quadriceps, 849 N from the gastrocnemius, and 495 N from the hamstrings, continuously load the ACL throughout the stance phase, with a peak force of 303 N during contralateral toe-off. These findings underscore the sustained nature of ACL loading during walking (Shelburne et al., 2004).

In addition to muscle forces, shear forces are crucial in ACL loading during gait (Shelburne et al., 2004). Anterior shear forces generated by the patellar tendon and gastrocnemius peak at 260 N during contralateral toe-off, while posterior shear forces arise from the hamstrings and ground reaction forces (Shelburne et al., 2004). As the knee experiences a forward thrust, the combined shear forces generate a posterior force that exceeds the anterior forces, particularly as the knee angle increases during the stance phase (Shelburne et al., 2004). This complex interaction of forces further emphasizes the mechanical challenges the ACL faces during normal walking.

Section 2.1.3.1 Kinematic alterations in walking post-ACL

As a complex motor function, gait depends on pathways from the cortex to the muscles (Pratt, 1994). Essential to daily activities, it requires considerable neural system synchronization with several muscle groups to sustain upright stability when moving (Sadeghi et al., 2000).

Individuals with ACL injuries often report periods of their knee giving away, linking the connection between ACL injury and knee instability (Rudolph et al., 1998). In hopes of restoring the functional role of the knee following an ACL injury, individuals

would undergo an ACLR. However, full restoration of pre-injury mechanics is often challenging, as altered biomechanics can persist post-surgery (Slater et al., 2017). These biomechanical changes depend on the person's characteristics, the type of surgery, the rehabilitation program, their activity level, and the timing of the surgery (DeVita et al., 1998; Simon et al., 2015).

Although pre-surgery knee kinematics were similar to those of the able-bodied group, knee angles remained altered three- and five-weeks post-surgery, with the knee showing increased flexion during walking (DeVita et al., 1997). Similarly, hip angles followed comparable trends post-surgery by exhibiting greater flexion (DeVita et al., 1997). Six months post-surgery, joint angles had largely returned to normal, with individuals adopting a more erect posture during walking and demonstrating kinematic patterns similar to those of the able-bodied group (DeVita et al., 1998).

Section 2.1.3.2 Kinetic alterations in walking post-ACLR

Post-ACLR kinetic improvements can be observed across different joints, particularly in the knee and hip. Significant changes were seen at the knee from three to five weeks post-ACLR, with the knee initially displaying an extensor moment throughout the stance phase (DeVita et al., 1997). This extensor moment displayed a trend towards a flexor moment without changing the value signs (from extensor to flexor) (DeVita et al., 1997, 1998). At six months, the knee's moment pattern was closer to that of able-bodied individuals but still showed differences in magnitude (DeVita et al., 1998).

The alterations at the knee were complemented by changes at the hip, which also showed improvements over time. At three weeks post-surgery, the peak extensor moment at the hip was lower, but the average moment was higher than in the able-bodied group

(DeVita et al., 1998). The hip moment pattern improved by five weeks, reaching levels comparable to able-bodied individuals. However, following rehabilitation, the altered hip moment was marked not by an increase in peak moment but by a sustained extensor moment that extended further into the stance phase (DeVita et al., 1998). This prolonged moment enabled the hip extensors to generate more angular impulse and work during the first half of stance, with the hip extensors contributing 83% of the work in individuals post-ACLR, compared to just 56% in the able-bodied group (DeVita et al., 1998). This compensatory adaptation helped activate the hip extensors to provide vertical support and forward movement during walking (Kowalk et al., 1997).

The work and power at the hip showed greater recovery, particularly after six months. Five weeks post-ACLR, trend similarities to the able-bodied group for power bursts at the hip joint were reported (DeVita et al., 1997). However, by six months, partial recovery occurred, with the work at the hip being 77% higher compared to the able-bodied group (DeVita et al., 1998). This suggests that while early recovery was limited, adaptations in the later stages contributed to significant improvements at the hip. At the ankle, negative work was restored at six months, with no statistically significant difference observed between individuals post-ACLR and the able-bodied group (DeVita et al., 1997).

In contrast, recovery of the work occurring at the knee was slower. A notable decrease in knee positive and negative work was observed at three and five weeks post-ACLR (DeVita et al., 1997). At six months, positive and negative work had not recovered fully, remaining at 44% and 53% of the levels seen in the able-bodied group, respectively

(DeVita et al., 1998). This incomplete recovery in the magnitude of the work occurring at the knee highlights the challenges in restoring full function to the knee following ACLR.

Increased knee abduction angles and moments are considered risk factors for ACL injuries (Hewett et al., 2005), and these same factors are also strongly linked to the development of knee osteoarthritis (OA) (Kaufman et al., 2001). Given the relevance of these mechanics, examining frontal plane biomechanics in individuals who have undergone ACLR is crucial. Research indicates that during walking, individuals post-ACLR experience a 21% increase in peak knee abduction moments compared to able-bodied controls (Butler et al., 2009). The abduction moments observed during walking in individuals post-ACLR ($-0.36 \text{ Nm/kg}\cdot\text{m}$) are similar to those found in people with knee OA ($-0.38 \text{ Nm/kg}\cdot\text{m}$) and significantly higher than those in able-bodied individuals ($-0.30 \text{ Nm/kg}\cdot\text{m}$) (Butler et al., 2007). These findings highlight the persistent biomechanical changes following ACLR and underscore the need for targeted interventions to address these altered movement patterns.

Section 2.1.3.3 Muscular and walking pattern compensations

These joint-specific kinetic adaptations were supported by changes in muscle activity, as evidenced by EMG findings. The decreased quadriceps activity and increased hamstrings and gastrocnemius activity (Andriacchi and Birac, 1993; Rudolph et al., 2001) align with the observed changes in knee and hip moments. The knee adaptations persisted for up to 10 months post-ACLR, with the peak extensor moment only partially restored around 22 months post-surgery (Timoney et al., 1993).

Individuals who undergo ACLR often display a common stiffened knee pattern, also termed underloading (Herrington et al., 2017). This pattern is characterized by

decreased knee flexion angles, vertical ground reaction forces, extensor moments, and power absorption (Roewer et al., 2011; Rudolph et al., 1998), and is also related to the development of knee osteoarthritis (Andriacchi and Dyrby, 2005). At heel strike, a plyometric contraction by the quadriceps muscles is exerted to control knee flexion, loading the ACL by shifting the tibia forward (Ciccotti et al., 1994). To counteract knee instability, individuals may adopt a stiffened knee pattern and increase the energy absorption of their plantar flexors to prevent anterior translation of the tibia. However, this approach increases the compressive and shear forces at the knee, which can lead to degenerative damage to the knee cartilage over time (Setton et al., 1999; Strickland et al., 1992).

While walking involves lower levels of force compared to sports with cutting and deceleration movements, the repetitive shear and compressive forces on the knee can still pose a risk for joint damage if not properly managed. Insufficient lower body strength and neuromuscular control, often compromised in individuals after ACLR, may contribute to the development of this stiffened knee pattern (Lisee et al., 2022). This, in turn, alters movement mechanics, further disrupting knee stability. As knee mechanics deteriorate, individuals may compensate by limiting their activity, which can hinder the normalization of gait and delay a return to optimal walking patterns (Lisee et al., 2022). Over time, these abnormal gait mechanics are linked to changes in cartilage composition and overall knee function, increasing the risk of posttraumatic OA (Pfeiffer et al., 2019; Pietrosimone et al., 2017).

Recent research indicates that gait retraining interventions can effectively improve abnormal biomechanics (Davis et al., 2020). For instance, a single session of real-time

gait biofeedback has been shown to positively affect joint loading and tissue metabolism in patients who have undergone ACLR (Davis et al., 2020). These findings emphasize the potential of targeted interventions to address gait dysfunction, support recovery, and reduce the risk of long-term joint damage (Davis et al., 2020).

Despite restoring knee stability with rehabilitation, individuals post-ACLR display altered gait mechanics, which can lead to degenerative changes to the cartilage of the knee (Daniel et al., 1994). A study assigned individuals post-ACLR to four different groups depending on their conditions: ACL deficient (ACLD) group, weak ACLR group (Quadriceps strength index (QSI) < 80%), strong ACLR group (QSI >90 %), and control group (Lewek et al., 2002). The weak ACLR group had similar gait patterns to the ACLD group, displaying a stiffened approach at weight acceptance. On the other hand, the strong ACLR group displayed similar patterns to the control group, suggesting that sufficient pliometric quadriceps control was needed to walk. Studies looking at the knee moment during early stance and weight acceptance showed decreased knee moments at six months post-rehabilitation (DeVita et al., 1998; Timoney et al., 1993). During running, these knee extensor moments were correlated to quadriceps strength. Moreover, they have also been shown to be correlated to the knee excursion within the early stance phase during walking (Snyder-Mackler et al., 1991).

Altered mechanics have been reported at six months (Arhos et al., 2021; Di Stasi et al., 2015), two years and five years post-ACLR despite meeting return to sport criteria (Arundale et al., 2018; Capin et al., 2018). It was shown that at six months and two years post-ACLR, outcome measures such as knee flexion angle, knee extensor moments and power were different between the injured and non-injured legs of the individuals post-

ACLR, even though the quadriceps strength index (QSI) was not (Roewer et al., 2011). This was unsurprising as some studies reported a decrease in knee extensor moments at one year post-ACLR (Hooper et al., 2002; Timoney et al., 1993). A particular study compared groups six and 12 months post-ACLR to a matched control group (Davis-Wilson et al., 2020). It was shown that bilateral differences at both time points were reported, comprising reduced dynamic vertical ground reaction forces during the stance phase (reduced forces at the early stance and increased during mid-stance) and decreased knee extensor moments during the stance phase (Davis-Wilson et al., 2020). Despite not measuring QSI, these findings align with other studies that reported altered gait mechanics in participants showing restored QSI in individuals with knee OA (Davis et al., 2019; DeVita et al., 2018). These suggest that neuromuscular adaptations occur, and there is a further need for proper gait retraining to restore walking mechanics.

Section 2.1.4 Why use obstructed walking with individuals post-ACLR

Balance is critical for safely performing activities of daily living (ADL), particularly for individuals with balance impairments, who are at an increased risk of falls. Falls are a major public health concern, especially for older adults and those with neurological or musculoskeletal disorders, as balance issues and decreased mobility can severely impact health, ADL function, and overall quality of life (Tinetti, 2003).

However, for individuals recovering from ACLR, this investigation does not focus on fall risk. ACLR is a significant injury that sidelines athletes for an extended rehabilitation period. Even after being cleared to return to sports, athletes face a 20% chance of re-injury and an 80% chance of developing knee osteoarthritis (OA) later in life (Barber-Westin and Noyes, 2020; Holm et al., 2012).

Walking balance deficits and compensations have been observed in this population following return to sports. Since walking involves lower forces than activities such as cutting, decelerating, and rotational movement, these compensations during walking may not adequately protect the knee from re-injury. The ACL provides both translational and rotational support to the knee, as well as proprioceptive feedback through its mechanoreceptors. Therefore, investigating balance during unobstructed and obstructed walking is crucial, as any deficits or compensatory patterns could increase the risk of re-injuring the ligament.

Section 3: Methodology

Section 3.1 Ethics

The study protocol received approval from Dalhousie's Research Ethics Board (REB: 2024-7253). All participants provided written informed consent prior to data collection.

Section 3.2 Study location

The study was conducted in the Biodynamics, Ergonomics, and Neuroscience Laboratory, located in room 217 of the Dalplex facility at Dalhousie University.

Section 3.3 Participants

Section 3.3.1 Recruitment

Posters displayed throughout the Dalhousie premises, social media blurbs and posts, as well as word of mouth, served as recruitment strategies for this study. A contact email for the primary researcher was included in the recruitment materials. Potential participants who contacted the primary researcher received a more detailed description of the study in an email response. This included information on the inclusion and exclusion criteria, allowing participants to assess their eligibility for the study. A letter of information and informed consent were also attached to the email; however, these were intended to provide further details about the research project and were not to be completed until the participant arrived in the lab.

Section 3.3.2 Inclusion and exclusion criteria

The inclusion criteria for the participants post-ACLR group were being between 18 and 35 years old and having undergone ACLR. Participants were excluded from the

group if the date between their ACL and data collection was less than one year, they displayed difficulties in walking and obstructed walking, sustained any musculoskeletal injury in the past six months, and had not returned to their daily activities and sports.

Section 3.4 Research design

This section was primarily similar to section 3.4, involving able-bodied participants. Data for participants post-ACLR was collected on their injured and non-injured leg, while the average of the able-bodied right and left leg was used for comparison.

Section 3.5 Measurement and calculations of the outcome measures

The sections that consist of kinematic measurements (3.5.1) and kinetic measurements (3.5.2) that were described for the able-bodied participants were also applied for the participants post-ACLR.

Section 3.6 Statistical analysis

The statistical analysis section was distinct, as the part involving participants post-ACLR was intended as a pilot study. The analysis consisted of plotting the ensemble average of the outcome measures for each leg of the participants post-ACLR as a function of obstacle height. These were then contrasted with the averaged outcome measures of able-bodied individuals, with a 95% confidence interval calculated for comparison.

Section 4: Results of the participants post-ACLR

This section reports the pilot data collection of the two participants' post-ACLR data. ALAs were contrasted to the group of able-bodied participants based on the calculated able-bodied 95% confidence interval and represent a small pilot study.

Section 4.1 Demographic characteristics

Data were collected from two participants post-ACLR. Table 8 displays the characteristics of each ACLR participant.

The Waterloo Footedness Questionnaire-Revised (WFQ-R) revealed that one participant had a right foot preference, while the other was ambidextrous. A score of 90 on the LKQ for participant one is deemed an acceptable score, while a score of 75 for participant two is deemed a fair score. The TAS score showed that participant one seemed more engaged in recreational sports pre-injury, which changed to sedentary to light work following the injury, and at present activity level, respectively. Participant two seemed to be engaged in competitive sports throughout the entire period.

Table 8. *Participants post-ACLR demographics*

Participant	Age	Gender	Height	Mass	LKQ	TAS			WFQ-R
1	22	F	1.64	83.2	90	6	1	3	Right
2	20	M	1.79	80	75	10	10	10	AMDX

(M=male; F=female; R=right; ADMX= Ambidextrous, y= years, m= meters, kg= kilograms).

Section 4.2 Crossing leg adaptations to obstructed walking

Section 4.2.1 Crossing leg average duration

The crossing leg gait cycle average duration was calculated and plotted as a function of obstacle height (Figure 24).

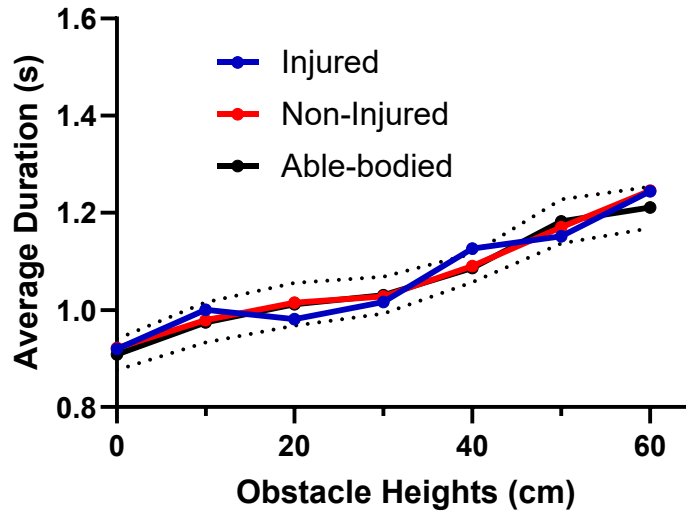


Figure 24. Average duration of the crossing leg gait cycle for the participants post-ACLR as a function of unilateral obstacle height (cm).

Statistical analysis was not performed; however, it was seen that the crossing leg average duration of the injured and non-injured legs of the participants post-ACLR were within the able-bodied 95% CI across all obstacle heights.

Section 4.2.2 Crossing leg lower limb joint angles during obstructed walking

Figure 25 displays, for descriptive purposes, the ensemble average of the joint angles of the participants post-ACLR across the hip (sagittal and frontal), knee (sagittal) and ankle (sagittal) during obstructed walking conditions on the crossing leg. No statistical analyses were conducted on these data. For sections and figures to follow, CL

is an abbreviation for crossing leg, and Inj and Non-Inj are abbreviations for injured and non-injured, respectively.

The patterns observed for the obstacle conditions seemed to be similar in terms of joint angles during the initial 30 to 40% of the gait cycle (GC). As obstacle height increased, the hip appeared to flex more. Additionally, between the 30 to 40% period of the GC, there was seemingly an increase in hip adduction angles with higher obstacle heights. Following this, hip abduction angles looked to decrease for obstacle heights of 10 to 40 cm, whereas abduction angles increased for heights of 50 and 60 cm. At the knee, there seemed to be an increase in flexion angles after 40% of the GC. At the ankle, dorsiflexion seemed to increase between the 40 to 50% period of the GC, followed by a decrease in plantar flexion from 50 to 60%, and finally an increase in dorsiflexion angles from the 60 to 80% period of the GC.

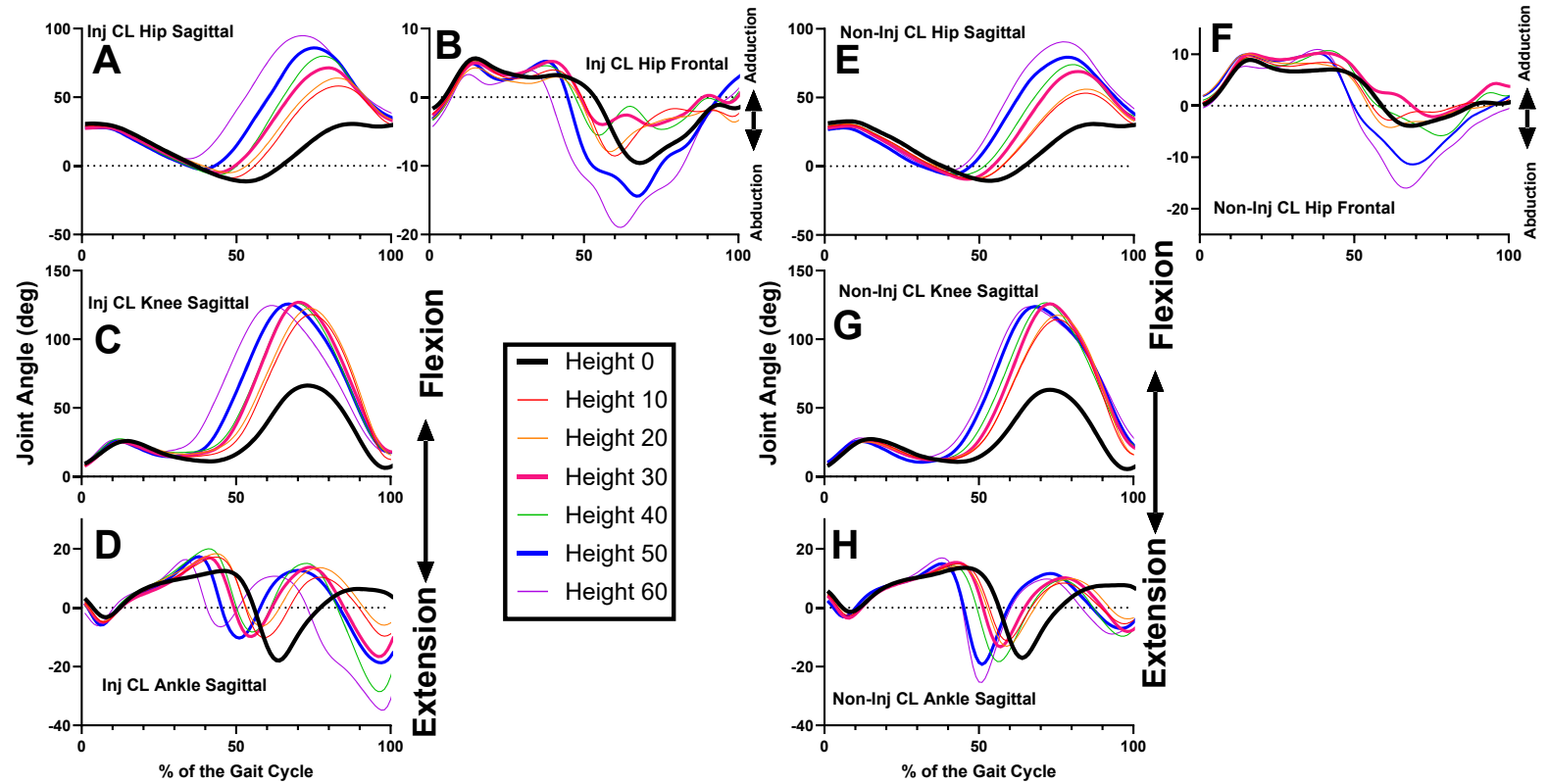


Figure 25. The ensemble average of the joint angles of the crossing legs of the participants post-ACLR during unobstructed and obstructed walking conditions. Positive Y angles: hip flexion, hip adduction, knee flexion and ankle dorsiflexion. Inj: injured, Non-Inj: non-injured, CL: crossing leg.

Section 4.2.3 Crossing leg lower limb joint moments during obstructed walking

Figure 26 displays, for descriptive purposes, the ensemble average of the net joint moments of the participants post-ACLR across the hip (sagittal and frontal), knee (sagittal) and ankle (sagittal) during obstructed walking conditions on the crossing leg. No statistical analyses were conducted on these data.

As obstacle height increased, the hip extension moment between the 0 to 10% period of the GC seemed to decrease. Hip flexion moments seemingly increased with higher obstacle heights from the 10 to 40% period of the GC, but these moments looked to decrease after 40% of the GC. In the frontal plane, hip abduction moments seemingly decreased as obstacle height increased. Additionally, while the typical transition from abductor to adductor moments around 55% of the GC occurred for obstacle heights less than 40 cm, this transition looked delayed for heights of 50 and 60 cm. For the higher obstacles, a new abductor moment emerged, which later transitioned into the usual adductor moment around the 60 to 65% period of the GC. At the knee, there seemed to be an increase in extension moment between the 5 to 10% period of the GC, followed by a decrease in knee extension moment between the 15 to 25% period of the GC. From the 30 to 45% period of the GC, knee extension moments seemed to increase again. A transition from extensor to flexor moments occurred between the 50% and 70% period of the GC, which was seen only during the obstacle conditions. At the ankle, dorsiflexion moments appeared to decrease between the 10 and 15% period of the GC. The plantar flexion moment followed a similar pattern across obstacle conditions; however, the peak plantar flexion moment was seemingly reduced only for the 60 cm obstacle height, and this decrease was observed exclusively on the injured leg.

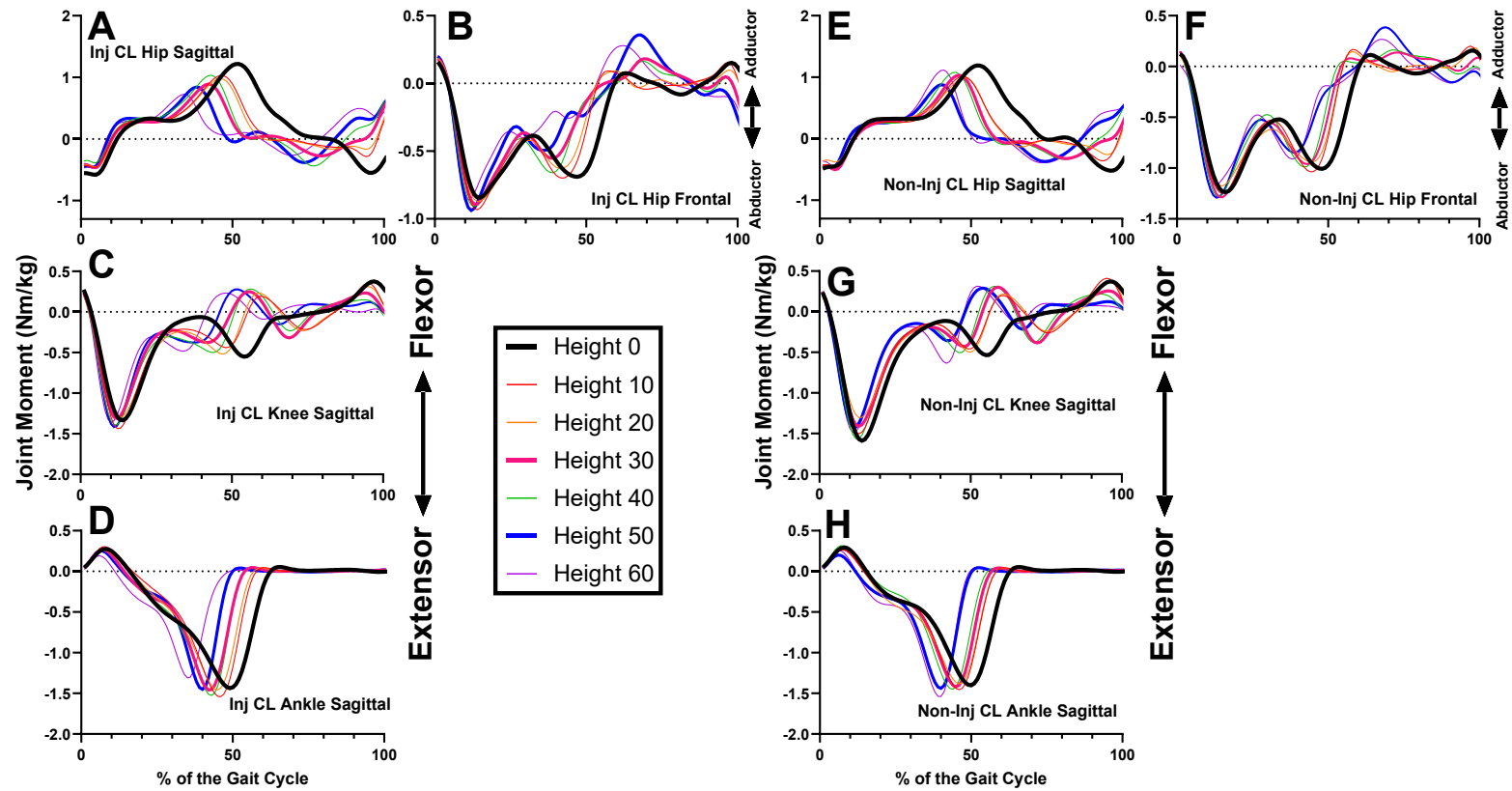


Figure 26. The ensemble average of the net joint moments of the crossing legs of the participants post-ACLR during unobstructed and obstructed walking conditions. Positive Y moments: hip flexion, hip adduction, knee flexion and ankle dorsiflexion. Inj: injured, Non-Inj: non-injured, CL: crossing leg.

Section 4.2.4 Crossing leg lower limb joint powers during obstructed walking

Figure 27 displays, for descriptive purposes, the ensemble average of the net joint powers of the participants post-ACLR across the hip (sagittal and frontal), knee (sagittal) and ankle (sagittal) during obstructed walking conditions on the crossing leg. This section focuses on the net joint power time history curves, whereas more information is provided in the next section regarding muscle power bursts.

At the hip in the sagittal plane, there seemed to be a decrease in power generation during the swing phase. In the frontal plane, there seemed to be similar power absorption by the hips between the 5 and 15% period of the GC, except for heights 50 and 60 cm, which seemed to increase. Moreover, the emergence of a new generation phase was seen for heights 40 to 60 cm, which was an absorption phase at the other remaining heights. At the knee, there seemed to be an increase in absorption of power from the 5 to 15% period of the GC. Additionally, power absorption seemed to decrease between the 40 and 50% period of the GC, while an emergence of a generation phase from the 50 to 70% period of the GC was seen only for the obstacle conditions. Absorption seemed to increase in the end swing only for heights 10 and 20 cm. At the ankle, prior to push off, absorption seemed to increase as obstacle height increased, accompanied by an increase in the subsequent generation phase for heights 30 to 60 cm.

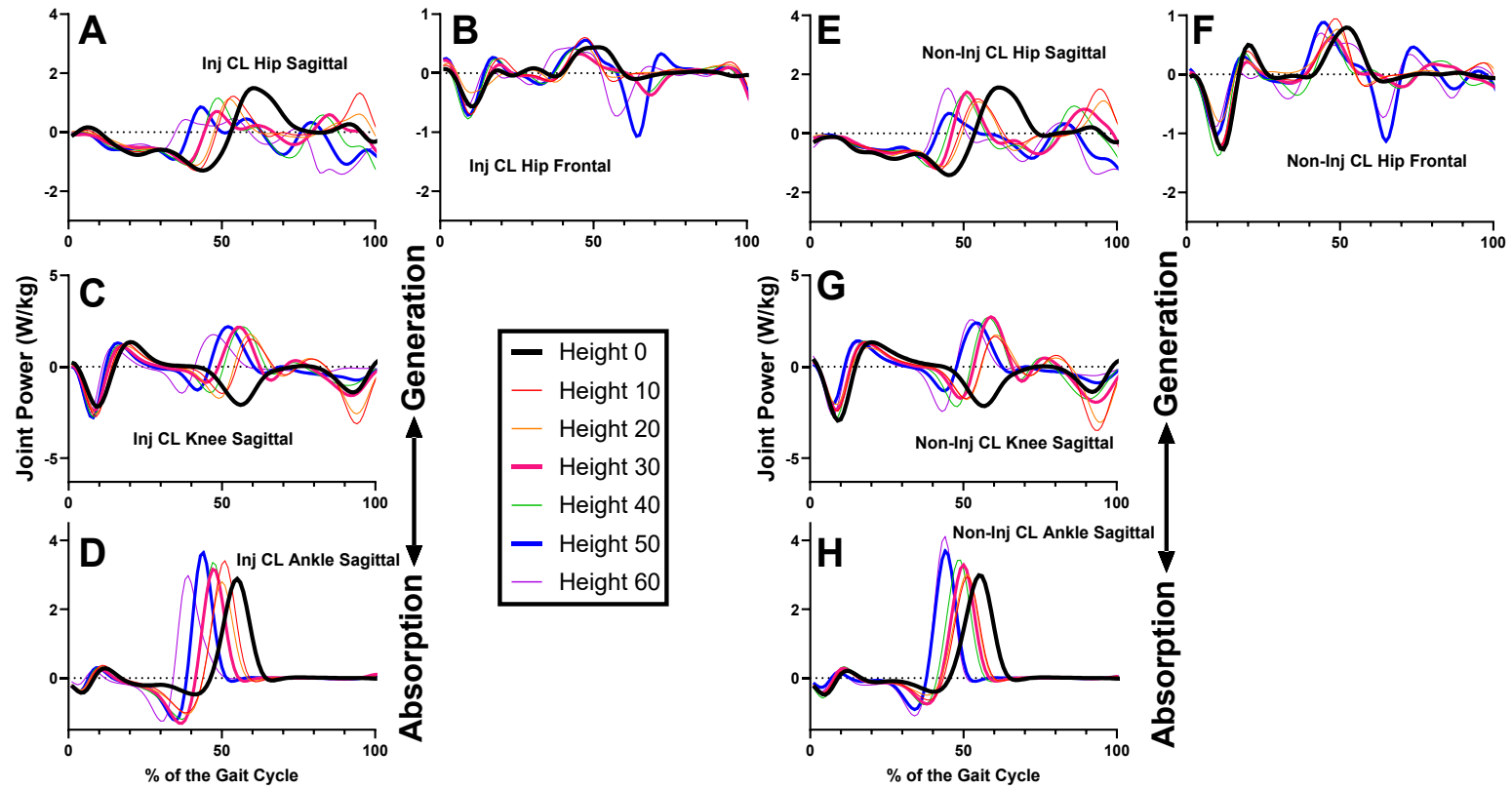


Figure 27. The ensemble average of the net joint powers of the crossing legs of the participants post-ACLR during unobstructed and obstructed walking conditions. Positive Y: energy generation. Inj: injured, Non-Inj: non-injured, CL: crossing leg.

Section 4.2.5 Crossing leg anticipatory locomotor adjustments

Figure 28 displays, for descriptive purposes, the ensemble average of the selective muscle power bursts as a function of obstacle height for the crossing leg.

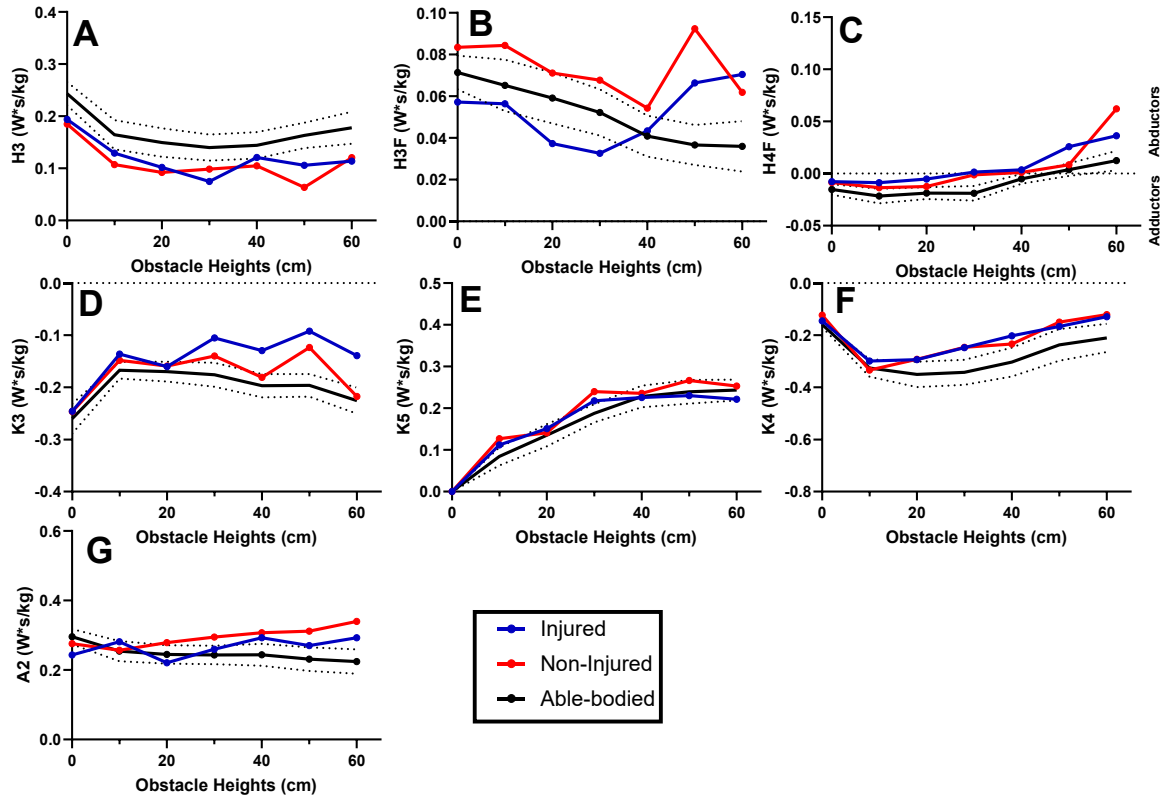


Figure 28. Mean selected muscle power bursts of the crossing legs of the participants post-ACLR as a function of obstacle height (cm) (Mean \pm 1SD). Positive power for the injured leg (blue), non-injured leg (red) and averaged able-bodied (black) leg indicates energy generation. H3: hip flexor energy generation, H3F: hip abductor energy generation, H4F: transition of hip adductor energy absorption to hip abductor energy generation, K3: knee extensors energy absorption, K5: knee flexors energy generation, K4: knee flexors energy absorption, A2: ankle plantar flexors energy generation.

The hip power energy phase generation by the hip flexors (H3, Figure 28A) was outside the able-bodied 95% CI for all the heights, except for height 40 cm for the injured leg. There did not appear to be differences between injured and non-injured legs. For the injured leg, the hip power generation by the hip abductors (H3F, Figure 28B) was less than the able-bodied for heights 0 to 30 cm but was greater for heights 40 to 60 cm (H3F for the injured leg was within the able-bodied 95% CI for heights 10 and 40 cm). For the non-injured leg, the hip abductors energy generation (H3F) was greater than the able-bodied for all the heights and was also outside the able-bodied 95% CI for all the heights. The muscle power burst H4F, which corresponded to the transition of energy absorption by the hip adductors to energy generation by the hip abductors (Figure 28C), for the injured and non-injured legs, was less in the absorption phase for both, but also greater in the energy generation phase.

The knee energy absorption by the knee extensors (K3, Figure 28D) was less in the injured and non-injured legs compared to the able-bodied participants. Moreover, the knee extensors energy absorption (K3) for the injured leg was inside of the able-bodied 95% CI for heights 0 and 20 cm, while the non-injured leg was inside the able-bodied 95% CI for heights 0, 20, 40 and 60 cm. The knee power generation by the knee flexors (K5, Figure 28E) was greater in the injured leg compared to the able-bodied until height 40 cm but was less for heights 50 and 60 cm. Moreover, the knee flexors energy generation (K5) for the injured leg was outside the able-bodied 95% CI for heights 10 and 30 cm only. For the non-injured leg, the knee flexors energy generation (K5) was greater compared to the able-bodied for all obstacles heights but was outside the able-bodied 95% CI for heights 10 and 30 cm only. The knee energy absorption by the knee

flexors (K4, Figure 28F) was less on the on the injured leg for all the heights and was outside the able-bodied 95% CI for all heights except for 0 and 10 cm. Compared to the able-bodied, the knee flexors energy absorption (K4) for the non-injured leg was only higher for height 10 cm and lower for the remaining heights. The knee flexors energy absorption (K4) was also within the able-bodied 95% CI for heights 0 and 10 cm only.

For the ankle power generation by the plantar flexors (A2, Figure 28G), both injured and non-injured legs were lower compared to the able-bodied at height 0. However, the injured leg was greater for the remaining heights except for height 20. The ankle plantar flexors energy generation (A2) on the injured leg was outside of the able-bodied 95% CI for heights 0, 40, 50 and 60 cm. The ankle plantar flexors energy generation (A2) in the non-injured leg was greater than the able-bodied ankle plantar flexors energy generation (A2) for all the heights after 0 and was within the able-bodied 95% only for height 10 cm.

Section 4.3 Supporting leg adaptations to obstructed walking

Section 4.3.1 Supporting leg average duration

The supporting leg gait cycle average duration was calculated and plotted as a function of obstacle height (Figure 29).

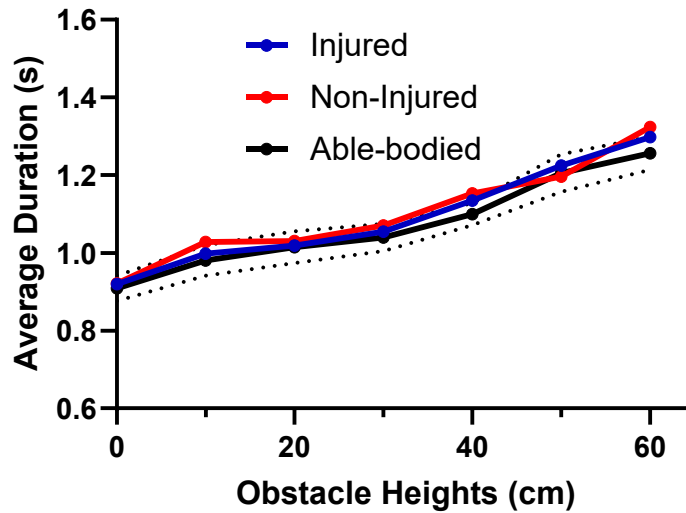


Figure 29. Average duration of the crossing leg gait cycle for participants post-ACLR supporting legs as a function of unilateral obstacle height (cm).

Statistical analysis was not performed; however, it was seen that the crossing leg average duration of the injured and non-injured legs of the participants post-ACLR were within the able-bodied 95% CI across all obstacle heights.

Section 4.3.2 Supporting leg lower limb joint angles during obstructed walking

Figure 30 displays, for descriptive purposes, the ensemble average of the joint angles of the participants post-ACLR across the hip (sagittal and frontal), knee (sagittal) and ankle (sagittal) during obstructed walking conditions of the supporting leg. No statistical analyses were conducted on these data. For sections and figures to follow, SL is an abbreviation for supporting leg, and Inj and Non-Inj are abbreviations for injured and non-injured, respectively.

At the hip, there seemed to be less hip flexion during the obstacle conditions up until around 40% of the gait cycle (GC). For obstacle heights between 10 and 40 cm, the hip appeared more extended between the 40 to 65% period of the GC. In the frontal

plane, the hip seemed to be less adducted for heights 10 and 20 cm and more abducted for the remaining heights during the stance phase. There also seemed to be less hip adduction between the 55 to 75% period of the GC for obstacle heights of 50 and 60 cm. The knee seemed to adopt a stiffer pattern, showing less flexion between the 10 to 45% period of the GC for the obstacle conditions. At the ankle, injured and non-injured legs showed different kinematic adaptations. For the injured leg, the pattern seemed to follow a similar trajectory to the unobstructed leg at heel strike for heights 10, 20, and 40 cm, followed by dorsiflexion during the stance phase. For the remaining heights, the ankle seemed to be plantar flexed from the beginning, dorsiflexing during midstance for height 30 cm, compared to dorsiflexion around 45% of the GC for heights 50 and 60 cm. For the non-injured leg, heights 10 and 20 cm seemed to adopt a similar pattern to the unobstructed leg, but with less dorsiflexion during the second half of the stance phase. For heights 30 and 40 cm, an initial dorsiflexion (0 to 5% period of the GC) seemed to occur, followed by plantar flexion, which transitioned to dorsiflexion around 40% of the GC. For heights 50 and 60 cm, a similar transition from plantar flexion to dorsiflexion seemed to occur at 40% of the GC, but the ankle was plantar flexed from the beginning.

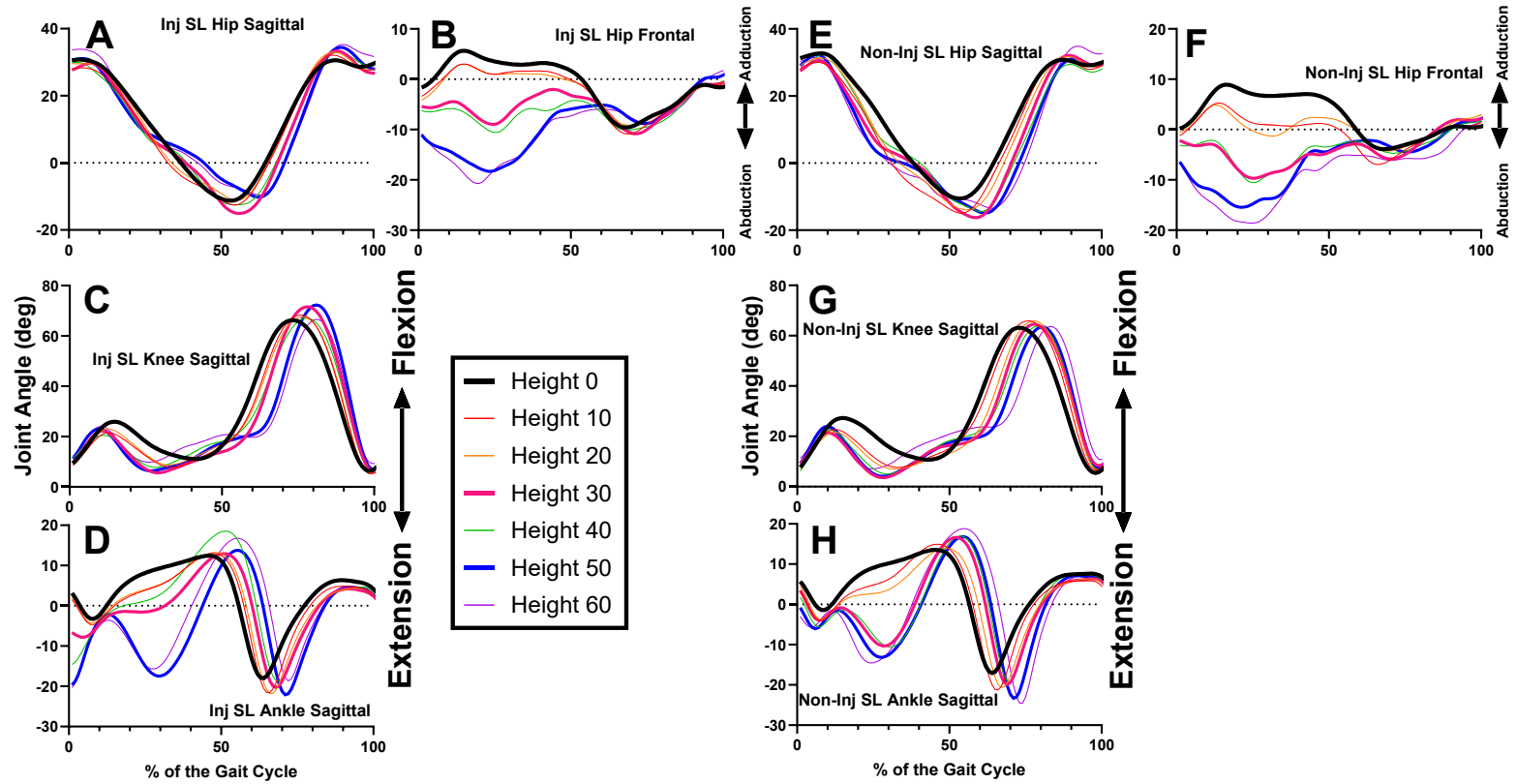


Figure 30. The ensemble average of the joint angles of the supporting legs of the participants post-ACLR during unobstructed and obstructed walking conditions. Positive Y angles: hip flexion, hip adduction, knee flexion and ankle dorsiflexion. Inj: injured, Non-Inj: non-injured, SL: supporting leg.

Section 4.3.3 Supporting leg lower limb joint moments during obstructed walking

Figure 31 displays, for descriptive purposes, the ensemble average of the net joint moments of the participants post-ACLR across the hip (sagittal and frontal), knee (sagittal) and ankle (sagittal) during obstructed walking conditions on the supporting leg.

There seemed to be an increase in the hip extension moment during early stance as obstacle height increased, followed by a decrease in hip flexion moments during the rest of the stance phase. In the frontal plane, heights 10 and 20 cm seemed to follow a similar pattern to unobstructed walking, with an abduction moment during the stance phase. However, the remaining heights appeared to adopt a different strategy, with a transition from abduction to adduction and back to abduction during mid-stance.

At the knee of the injured leg, the extension moment seemed to decrease as obstacle height increased between the 5 to 20% period of the gait cycle (GC). For heights 50 and 60 cm, there appeared to be a transition from extension to flexion, followed by extension again, around the 20 to 30% period of the GC. In contrast, the other heights only showed an extension moment. For the non-injured leg, the knee extension moment for heights 50 and 60 cm seemed to increase between the 5 to 15% period, followed by a decrease in extension between the 15 to 50% period of the GC. Similar to the injured leg, but with a slight variation, heights 30 to 60 cm on the non-injured leg showed a transition from extension to flexion, and then back to extension, between the 20 to 30% period of the GC.

At the ankle of the injured leg, heights 10 to 40 cm seemed to adopt similar patterns to the unobstructed condition, with a dorsiflexion moment between the 0 to 15%

period of the GC, followed by a plantar flexion moment. However, for heights 50 and 60 cm, a plantar flexor moment appeared throughout the entirety of the stance phase. For heights 10 and 20 cm, the plantar flexor moment seemed to increase linearly, resembling the unobstructed pattern. Heights 30 and 40 cm showed a constant plantar flexion moment between the 20 to 35% period of the GC, which then appeared to increase linearly. For heights 50 and 60 cm, the plantar flexor moment seemed to decrease between the 10 to 30% period of the GC, followed by a linear increase.

For the non-injured leg, all obstacle heights except for 60 cm seemed to adopt an initial dorsiflexor moment, followed by a plantar flexion moment. Heights 10 and 20 cm appeared similar to the unobstructed condition. However, for heights 30 to 60 cm, the non-injured leg adapted similarly to the injured leg's pattern for heights 50 and 60 cm. Specifically, a plantar flexor moment seemed to decrease during part of the stance phase and then increase linearly.

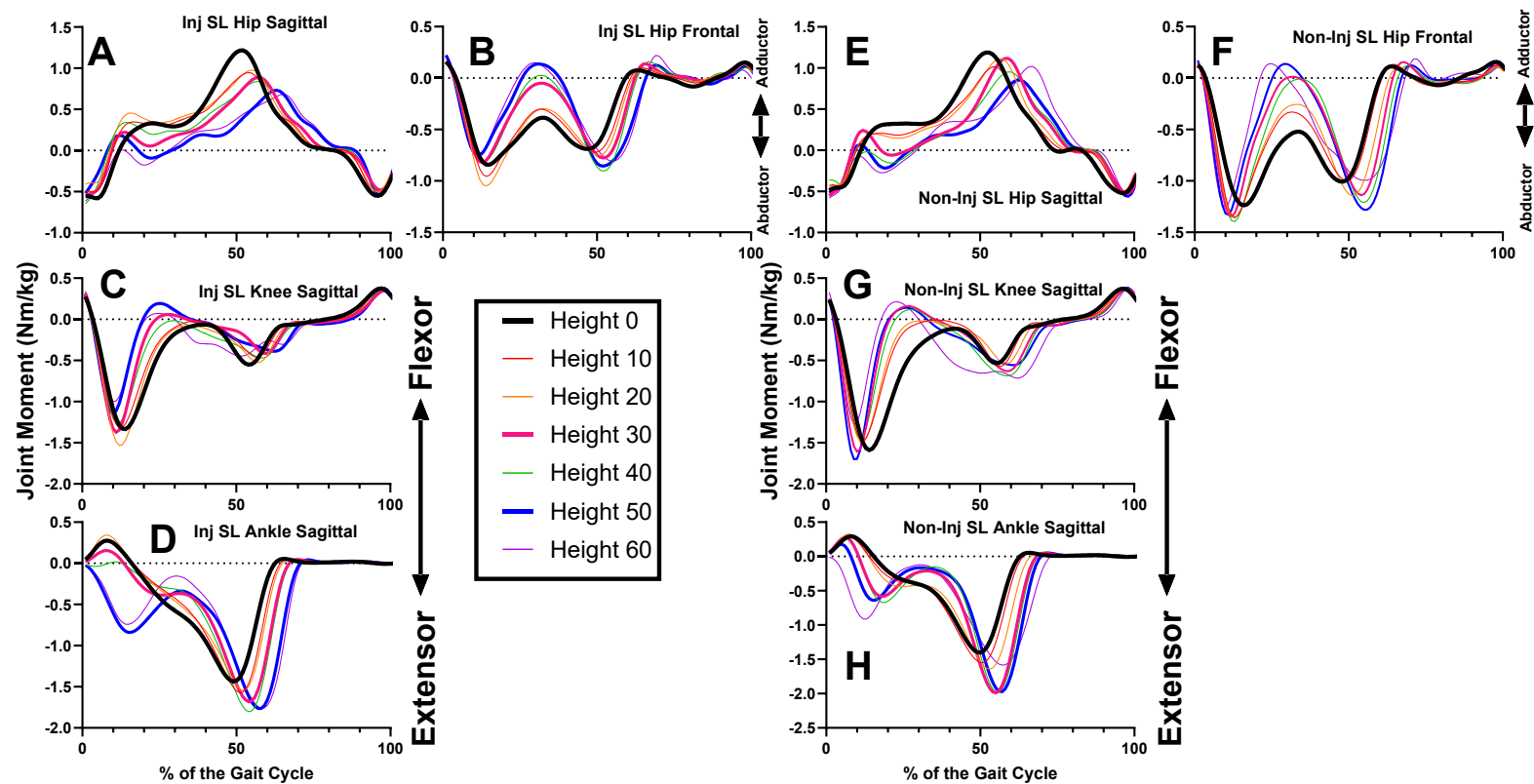


Figure 31. The ensemble average of the net joint moments of the supporting legs of the participants post-ACLR during unobstructed and obstructed walking conditions. Positive Y moments: hip flexion, hip adduction, knee flexion and ankle dorsiflexion. Inj: injured, Non-Inj: non-injured, SL: supporting leg.

Section 4.3.4 Supporting leg lower limb joint power during obstructed walking

Figure 32 displays the ensemble average of the net joint powers of participants post-ACLR across the hip, knee, and ankle during obstructed walking conditions on the supporting leg. This section focuses on the net joint power time history curves, while more information regarding muscle power bursts is provided in the next section. At the hip, there seemed to be increased power generation during early to mid-stance as obstacle height increased, followed by a decrease in power absorption leading into the swing phase. In the frontal plane, power absorption during early stance seemed to decrease, except for at 20 cm, followed by an increase in power generation during early to mid-stance. At the knee, both the injured and non-injured legs seemed to experience a decrease in power absorption during early stance as obstacle height increased, with power generation seeming to increase with higher obstacle heights, followed by a decrease in power absorption during the swing phase. At the ankle, for the injured leg, heights 10 to 40 cm seemed to adopt a similar pattern of increased power absorption (which increased with obstacle height) from the 10 to 45% period of the gait cycle (GC), followed by power generation. For heights 50 and 60 cm, energy generation seemed to occur from the 10 to 30% period of the GC, followed by absorption until push-off, with power generation around push-off seeming to increase with higher obstacle heights. For the non-injured leg, heights 10 and 20 cm seemed to follow a pattern similar to unobstructed walking, but with greater absorption during mid to late stance, while heights 30 to 60 cm seemed to follow a pattern similar to the injured leg's heights 50 and 60 cm, with power generation during early to mid-stance, followed by seemingly increased power absorption during mid to late stance..

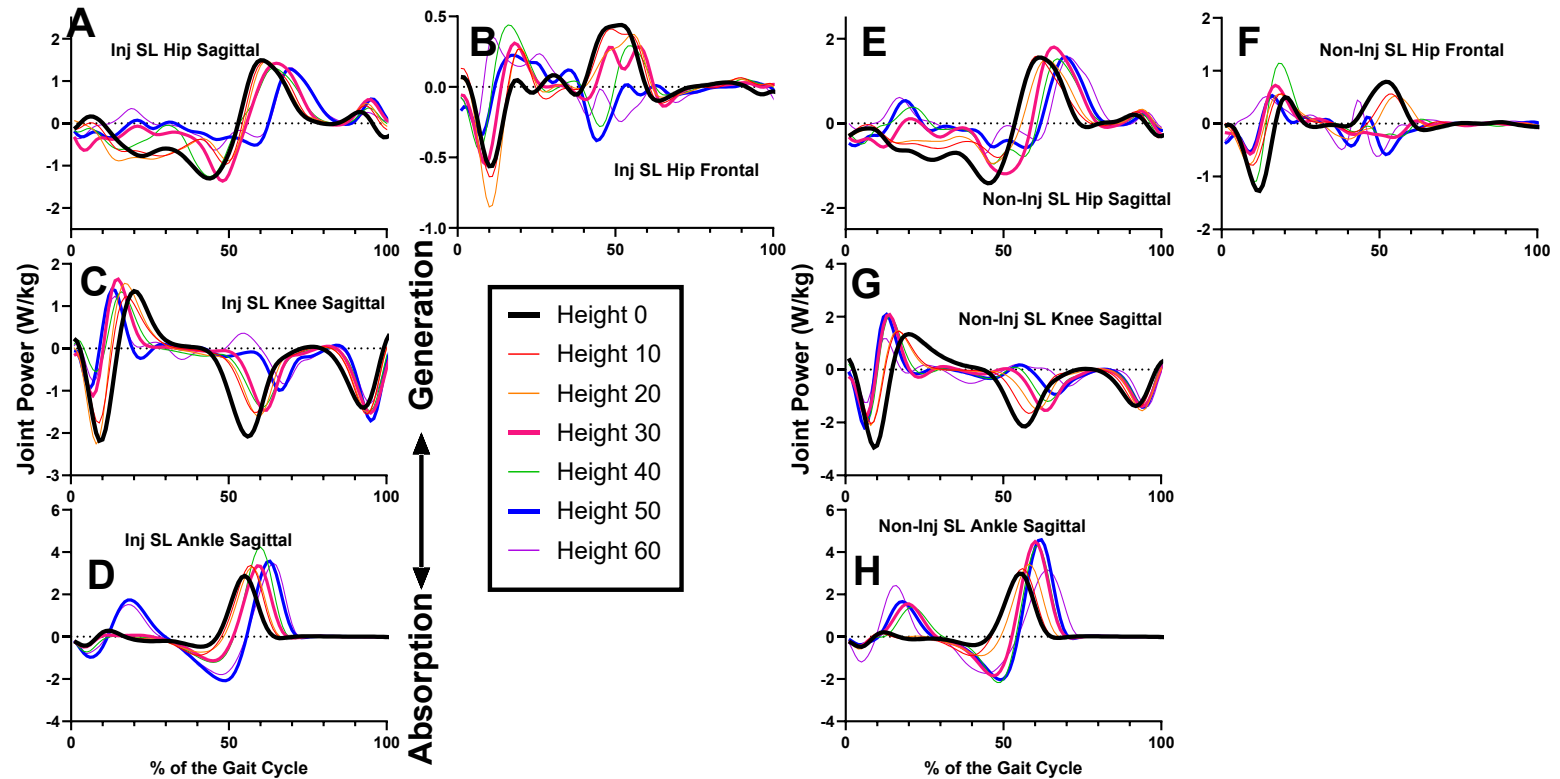


Figure 32. The ensemble average of the net joint power of the supporting legs of the participants post-ACLR during unobstructed and obstructed walking conditions. Positive Y: energy generation. Inj: injured, Non-Inj: non-injured, SL: supporting leg.

Section 4.3.5 Supporting leg anticipatory locomotor adjustments

Section 4.3.5.1 Supporting leg ALAs at the hip, knee and ankle

Figure 33 displays, for descriptive purposes, the ensemble average of the selective muscle power bursts as a function of obstacle height of the participants post-ACLR for the supporting leg.

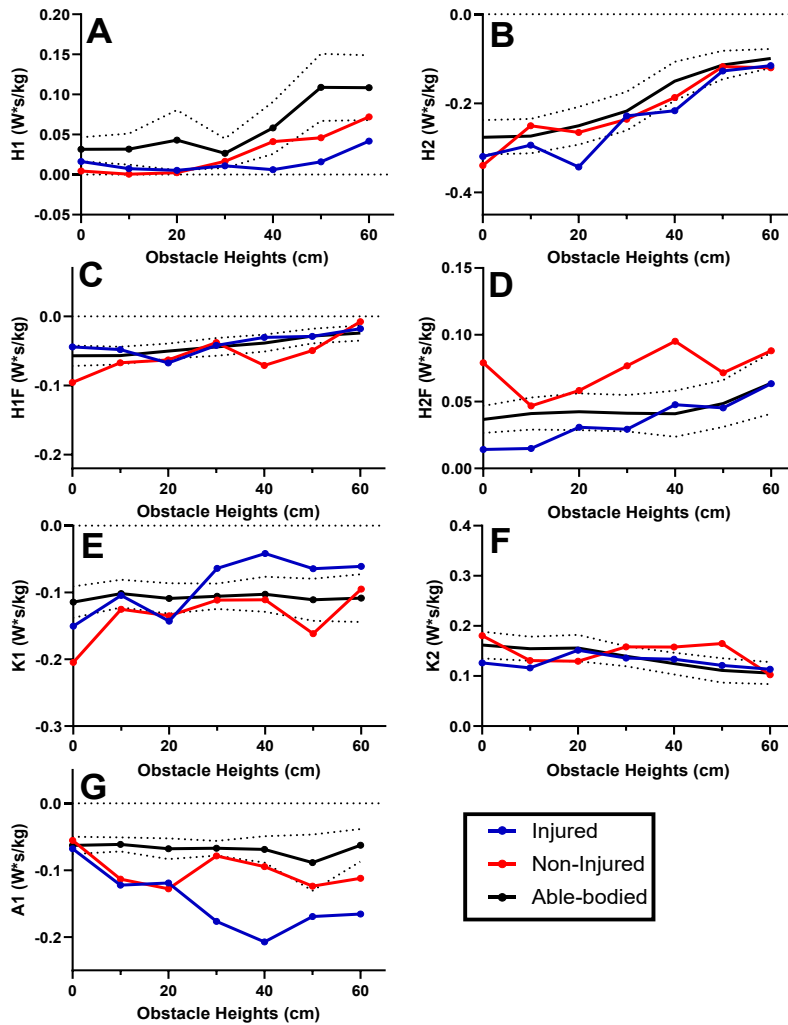


Figure 33. Selected muscle power bursts of the supporting legs of the participants post-ACLR as a function of obstacle height (cm) (Mean \pm 1SD). Positive power for the injured leg (blue), non-injured leg (red) and averaged able-bodied (black) leg indicates energy generation. H1: hip extensors energy generation, H2: hip flexors energy absorption, H1F: hip abductors energy absorption, H2F: hip abductors energy generation, K1: knee extensors energy absorption, K2: knee extensors energy generation, A1: ankle plantar flexors energy absorption.

The hip extensors energy generation (H1, Figure 33A) was lower across all heights for the injured and non-injured legs compared to the able-bodied hip extensors energy generation (H1). For the injured leg, the hip extensors energy generation (H1) was outside the able-bodied 95% CI for all heights except for height 30 cm. In contrast, the H1 muscle power burst of the non-injured leg was outside the able-bodied 95% CI for heights 0, 10, 20 and 50 cm. The hip energy absorption by the hip flexors (H2, Figure 33B) was higher for both legs compared to the able-bodied hip flexors energy absorption (H2), except for height 10 cm on the non-injured leg. On the injured leg, the hip flexors energy absorption (H2) was outside the able-bodied 95% CI for heights 20 and 40 cm only. On the non-injured leg, the hip flexors energy absorption (H2) was outside the able-bodied 95% CI for height 0 cm only. The hip energy absorption by the hip abductors (H1F, Figure 33C) was lower on the injured leg compared to the able-bodied for all heights except for height 20 cm, which was also the only height outside the able-bodied 95% CI. For the non-injured leg, the hip abductors energy absorption (H1F) was higher than the able-bodied for all heights except for 30 and 60 cm. Moreover, the hip abductors energy absorption (H1F) on the non-injured leg was outside the able-bodied 95% CI for all heights except for 10 and 30 cm. The hip abductors energy generation (H2F, Figure 33D) was lower on the injured leg for all heights except for height 40 cm. The hip abductors energy generation (H2F) was also inside the able-bodied 95% CI for all heights except for 0 and 10 cm on the injured leg. For the non-injured leg, the hip abductors energy absorption (H1F) was higher than the able-bodied for all heights and was outside the able-bodied 95% CI for all heights except for height 10 cm.

The knee energy absorption by the knee extensors (K1, Figure 33E) was higher in absorption for both legs until height 20 cm. Injured leg was lower in absorption compared to the able-bodied from height 30 to 60 cm. For the injured leg, the knee extensors energy absorption (K1) was outside the able-bodied 95% CI for all heights except 20 cm. For the non-injured leg, the knee extensors energy absorption (K1) remained higher in absorption compared to the able-bodied for all the heights except for 60 cm. For the non-injured leg, the knee extensors energy absorption (K1) was outside the able-bodied 95% CI for heights 0, 10, 20 and 50 cm. The knee extensors energy generation (K2, Figure 33F) was initially lower for the injured leg until height 30 cm. It then generated more power for heights 40 to 60 cm. For the injured leg, the knee extensors energy generation (K2) was outside the able-bodied 95% CI for all heights except 0 and 10. For the non-injured leg, the knee extensors energy generation (K2) was higher than the able-bodied for heights 0, 30, 40 and 50 cm, and lower for the rest. For the non-injured leg, the knee extensors energy generation (K2) was outside the able-bodied 95% CI for all heights except for 40 and 50 cm.

The energy absorption by the plantar flexors (A1) was higher for the injured leg for all the heights and was also outside the able-bodied 95% CI for all heights except 0 cm. For the non-injured leg, the ankle plantar flexor energy absorption (A1) was higher than the able-bodied for all heights except 0 cm. It was also within the able-bodied 95% CI for heights 0, 30 and 50 cm.

Section 4.3.5.2 Supporting leg ALAs at the ankle

Figure 34 displays, for descriptive purposes, the ensemble average of the ALAs that occurred at the net ankle joint of the participants post-ACLR for the supporting leg.

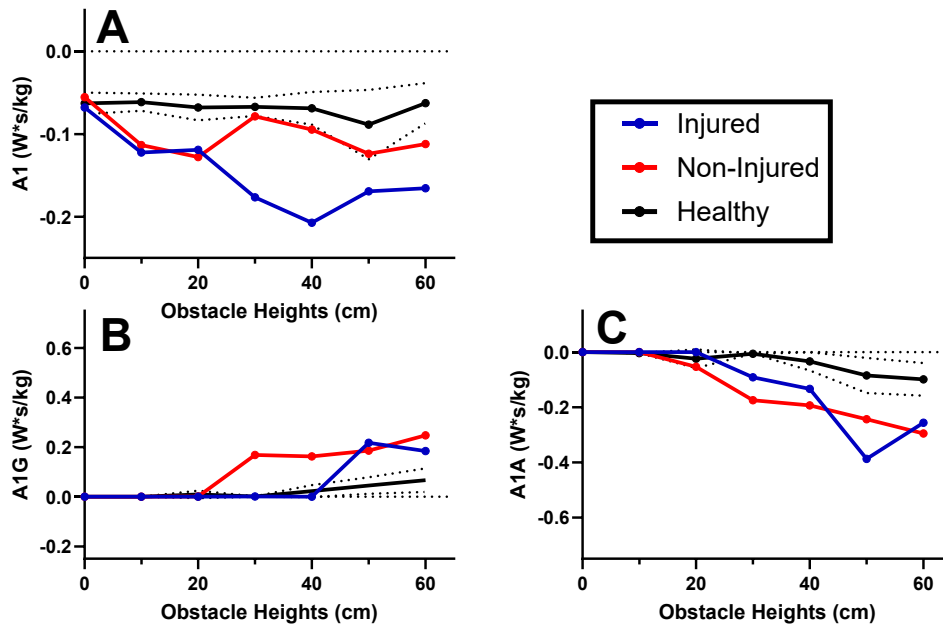


Figure 34. Selected ankle muscle power bursts of the supporting legs of the participants post-ACLR as a function of obstacle height (cm) (Mean \pm 1SD). Plots on top left, bottom left, and bottom right represent left and right selective muscle power burst as a function of obstacle height. Positive power for the injured leg (blue), non-injured leg (red) and averaged able-bodied (black) leg indicates energy generation. A1G: Plantar flexors energy generation, A1A: Plantar flexors energy absorption.

Similar to the able-bodied participants, there was the emergence of plantar flexors generation (A1G) followed by an energy absorption (A1A) during the stance for obstacle heights higher than 20 cm. The plantar flexors energy generation (A1G) was higher for the injured leg for heights 50 and 60 cm, which were also the only heights outside the able-bodied 95% CI. For the non-injured leg, the ankle plantar flexors energy generation (A1G) was higher than the able-bodied for heights 30 to 60 cm, which were also the heights that were outside the able-bodied 95% CI. The energy absorption by the ankle plantar flexors (A1A) was higher for the injured leg for heights 30 to 60 cm and heights 20 to 60 cm for the non-injured leg. The ankle plantar flexors energy absorption (A1A) for both legs was outside the able-bodied 95% CI for heights 30 to 60 cm.

Section 5: Discussion

Extensive research has been conducted in populations post-ACLR during unobstructed walking (Davis-Wilson et al., 2020; DeVita et al., 1997, 1998; Roewer et al., 2011); however, no study has examined kinetic adaptations during obstructed walking. The present study only includes two participants compared to eight from Devita et al (1998). As such, the discussion is thought to be preliminary. The first section focused on the unobstructed walking condition during the stance phase (Figure 33, values at height 0) and contrasted the results of this study with the literature. The second section focused on the adaptations during obstructed walking conditions on the crossing and supporting legs.

Section 5.1 Unobstructed walking mechanisms during the stance phase

In our sample of two participants post-ACLR, there seems to be a greater generation of energy by the hip extensor (H1) in the injured leg (0.016 W*s/kg) in comparison to the non-injured leg (0.004 W*s/kg). However, both were lower than in the able-bodied group (0.031 W*s/kg) and outside the able-bodied 95% CI (Figure 33A). Since no statistical analysis was conducted between the legs of the participants post-ACLR, we cannot ascertain whether the injured leg was significantly different from the non-injured leg. The reduction in hip joint muscle generation of power seems to be compensated by an increase in the absorption of energy by the knee extensors (K1) for both legs compared to the able-bodied group. This finding is different from previous studies suggesting that a protective mechanism developed by participants post-ACLR would generate at least the same amount of positive work at the hip (Roewer et al., 2011), if not more (DeVita et al., 1998), during the early stance phase of gait, thereby absorbing

less power compared to the knee (Davis-Wilson et al., 2020; Roewer et al., 2011). This might be attributed to the possible increased activation of the quadriceps muscle. Though sometimes absent during early stance, the rectus femoris, a bi-articular muscle, could be contributing to greater energy for hip flexion and knee extension. The increase in hip flexion power could decrease hip extension power, as observed in the participants post-ACLR. This possible greater involvement of the rectus femoris contrasts with literature reporting decreased quadriceps activation months and years after ACLR (Andriacchi and Birac, 1993; Rudolph et al., 2001). However, this finding is speculative as EMG was not captured for the present study.

Furthermore, the injured leg seems to have a smaller generation of energy by the knee extensors in comparison to the able-bodied, while the non-injured leg generates knee power that is comparable to the able-bodied group (K2, Figure 33F). This decrease in knee extensor energy generation (K2) is somewhat in line with what Devita et al. (1998) reported in terms of a decrease in negative work during the stance phase at six months post-ACLR compared to their able-bodied control group.

During early stance, there appeared to be greater energy absorption by the hip abductors (H1F) of the non-injured leg compared to the able-bodied group, while the injured leg appeared to absorb sufficient work (Figure 33C). Additionally, both legs of the participants post-ACLR appear to have a greater absorption of energy by the hip flexor muscles when compared to able-bodied participants (H2, Figure 33B). Furthermore, the subsequent energy generation by the hip abductors (H2F) of the non-injured leg was higher than that of the able-bodied group and the injured leg. In contrast, the former was lower than that of the able-bodied group (Figure 33D).

The hip abductors energy absorption (H1F) stabilizes the pelvis through isometric contraction of the hip abductors, while the hip abductors energy generation (H2F) elevates the pelvis due to isometric contraction by the same group of muscles (Eng and Winter, 1995). Such findings suggest a greater demand on the hip abductors to stabilize the pelvis during early stance and further elevate it during mid-stance on the non-injured leg, in contrast to the energy dissipation by the abductors of the injured leg, which may indicate weakness or insufficient activation to stabilize and elevate the pelvis. Insufficient activation or strength of the hip abductors could lead to altered knee mechanics. In fact, studies have indicated that decreased hip abduction strength is associated with increased knee valgus moments and a loss of frontal plane stability (Claiborne et al., 2006; Dashti Rostami et al., 2019; Lawrence et al., 2008; Lee and Powers, 2014). Moreover, increased knee valgus motion and moments are predictors of non-contact ACL injuries during landing tasks (Hewett et al., 2006). These findings suggest that individuals with inadequate activation of the hip abductors may be at a higher risk of further injury. The lack of sufficient control from the hip abductors can result in excessive knee valgus, which increases the potential for additional damage to the knee joint (Hewett et al., 2006).

In summary, for the supporting leg during the stance phase of unobstructed walking, no changes or adaptations were seen at the ankle during unobstructed walking, suggesting that the main alterations occurred at the knee and hip levels. This is in line with Devita et al. (1998), who reported that positive work at the knee and hip levels and negative work at the knee were significantly different at six months post-ACLR

compared to the able-bodied group, while the ankle positive and negative work was restored and not different from the control group.

Section 5.2 ACLR and obstructed walking ALA

The findings of the study and its association with the hypotheses of participants post-ACLR and able-bodied can be found in Tables 9 and 10.

Table 9. Summary of the energy bursts differences between the legs of participants post-ACLR during unobstructed and obstructed walking conditions.

Outcome measure	Hypothesized outcome	Observed outcome	Hypothesis supported?
Knee flexor energy generation (K5)	No difference between legs	No difference between legs	Yes
Knee extensor energy absorption (K3)	No difference between legs	No difference between the legs	Yes
Hip flexor energy generation (H3)	No difference between legs	No difference between legs	Yes
Hip abductor energy generation (H3F)	No difference between legs	Difference between the legs	No
Hip abductor energy generation (H1F)	No difference between legs	No difference between legs	Yes

Table 10. Summary of the energy bursts differences between the legs of participants post-ACLR and able-bodied participants during unobstructed and obstructed walking conditions

Outcome measure	Hypothesized outcome	Observed outcome	Hypothesis supported?
Knee flexor energy generation (K5)	Difference between groups	No difference between groups	No
Knee extensor energy absorption (K3)	Difference between groups	Difference between groups	Yes
Hip flexor energy generation (H3)	Difference between groups	Difference between groups	Yes

Hip abductor energy generation (H3F)	Difference between groups	Difference between groups	Yes
Hip abductor energy generation (H1F)	Difference between groups	No difference between groups	No

Both the injured and non-injured legs showed kinematic changes during obstructed walking by increasing the flexion of the lower body joints to achieve higher foot elevation and clear the obstacle. This mechanism aligns with the obstructed walking literature, highlighting the increased demand for the crossing leg to flex its joints and elevate the foot (McFadyen and Carnahan, 1997; Patla and Rietdyk, 1993; Winter et al., 1990).

However, during the supporting leg stance phase, the knees of both (injured and non-injured legs) appeared less flexed as obstacle height increased (Figure 30C, 30G). This suggests that participants post-ACLR adopted a stiffened knee pattern (also referred to as underloading (Herrington et al., 2017)), characterized by decreased knee flexion angles, reduced knee extensor moment, and lower absorption during the stance phase (Roewer et al., 2011; Rudolph et al., 1998). Such a pattern has been associated in the literature with the development of knee OA (Andriacchi and Dyrby, 2005). Furthermore, similar to the able-bodied group, participants post-ACLR adopted a forefoot strike at higher heights (30 to 60 cm) on the non-injured leg, and at heights 30, 50, and 60 cm on the injured leg (Figure 30D, 30H).

Section 5.2.1 Mechanism of higher foot elevation

Consistent with the literature on obstructed walking, participants post-ACLR on the crossing leg exhibited a new knee flexor strategy (K5), which was associated with

decreases in the knee extensors energy absorption (K3) and the hip flexors energy generation (H3) (see Figures 28E, 28D, and 28A). The knee flexors energy generation (K5) appeared to generate power similar to that of able-bodied participants up to the height 50 cm. Even though this has not been reviewed in the ACLR field, research looking into bilateral obstructed walking related to knee pathologies such as knee OA and knee replacements reveal that individuals with knee replacements display a reduced knee flexors energy generation (K5) compared to able-bodied participants (Byrne and Prentice, 2003). Additionally, it was revealed that knee OA and the able-bodied group displayed similar patterns in terms of kinematic adaptations (Wang et al., 2009). Moreover, it was also found that using a bandage wrapped around the knee during bilateral obstructed walking for knee OA participants improved GRF, decreased loading during weight acceptance, facilitated the accomplishment of the task, and provided better estimates of impulse required for propulsion of the CoM (Pegoretti et al., 2015). In addition to the increased knee flexors energy generation (K5) in the current study, there were reductions in the hip flexors energy generation (H3) and the knee extensors energy absorption (K3) in both the injured and non-injured legs in comparison to the able-bodied participants during the late stance/early swing phase. The reductions in the hip flexor energy generation (H3) and the knee extensors energy absorption (K3) may result from hip flexor and knee extensor moment reductions, respectively. It may be possible that an increase in hamstring activation, coupled with no changes in quadriceps activation, could lead to a higher level of co-contraction of the muscles at the knee joint. This may act as a protective mechanism to enhance joint stiffness (Solomonow et al., 1987). This finding is speculative as EMG study was not captured in the present study. Moreover, the knee

flexors energy generation (K5) could be related to the increased hamstring activation to ensure proper foot elevation and prevent tripping. Interestingly, at height 60 cm, while there was a slight increase in the knee flexors energy generation (K5) for the able-bodied group, the injured and non-injured legs of the participants post-ACLR seemed to decrease. Furthermore, the knee extensors energy absorption (K3) appeared to increase in both the injured and non-injured legs (indicating an increase in absorption) and the hip flexor energy generation (H3) (suggesting an increase in the energy generation) in the participants post-ACLR.

On the crossing leg, similar to the able-bodied group, participants post-ACLR exhibited a decrease in the hip abductors energy generation (H3F) up to a height of 40 cm. However, while the hip abductors energy generation (H3F) continued to decline in the able-bodied group, the participants post-ACLR increased their hip abductor generation of power during the late stance. This hip abductors energy generation (H3F) may lead to an elevation of the pelvis for the higher obstacles (50-60 cm). This suggests hip abductors may be more engaged in the participants post-ACLR at 50 and 60 cm heights to ensure the proper pelvis elevation. Furthermore, H4F, which signifies the transition from hip adductor energy absorption to hip abductor energy generation, occurred between heights 40 and 50 cm in the able-bodied group. In contrast, this transition occurred earlier for the participants post-ACLR, from heights 20 to 30 cm, with height 60 cm being noticeably higher in the participants post-ACLR compared to the able-bodied group. This, along with the finding of increased hip abductors energy generation (H3F) for heights 40 cm and beyond, indicates that the participants post-

ACLR depend more on their hip abductors to provide sufficient pelvis height during the crossing leg, further elevating shank height and ensuring toe clearance.

Unlike the decrease in energy generation by the plantar flexors (A2) observed in the able-bodied group, the ankle plantar flexors energy generation (A2) among participants post-ACLR appeared to be increasing on the crossing leg. This can be characterized by the seemingly rising plantar flexor moment noted during obstructed conditions (Figure 26D, 26H). This indicates increasing propulsion on the crossing leg to ensure adequate toe clearance.

In summary, for the crossing leg adaptations, ACLR adopted comparable patterns to the able-bodied participants, consisting of increased knee flexors energy generation (K5) coupled with a decrease in knee extensors energy absorption (K3) and hip flexor energy generation (H3). However, the participants post-ACLR exhibited an increased knee flexors energy generation (K5) for some obstacle heights coupled with decreased knee extensors energy absorption (K3) compared to the able-bodied participants, suggesting that co-contraction of the hamstring and quadriceps muscles might have occurred to increase joint stiffness. Additionally, participants post-ACLR adapted by increasing their hip abductors energy generation (H3F) during late stance for heights 50 and 60 cm, coupled with the hip circumduction like movement provided by the H4F muscle power burst transition. Lastly, added propulsion to the crossing leg was provided by the increase in ankle plantar flexor energy generation (A2) compared to the decrease in able-bodied as a function of obstacle height.

Section 5.2.2 Mechanism of upward bias of the swing limb

Section 5.2.2.1 Early stance adaptations

Participants post-ACLR appeared to increase the supporting leg hip extensors energy generation (H1, Figure 33A) as obstacle height increased, similar to the behaviour observed in the able-bodied group. However, each leg of the participants post-ACLR displayed distinct characteristics. Notably, the non-injured leg generated energy comparable to that of the able-bodied participants, remaining within the able-bodied 95% CI (only deviating at height 50 cm). This indicates that the hip extensors most likely contributed to elevating the pelvis, ensuring adequate height for obstacle clearance by the crossing leg. Conversely, the injured leg, while increasing, generated less hip power during the early stance compared to both the able-bodied and the non-injured leg. This suggests that weakness or inefficient activation of the hip extensors, most likely the gluteal muscles, may account for this reduced power generation. Consequently, this could result in forward trunk flexion over the femur and an ineffective provision of body support, as the gluteal muscles are responsible for these actions (Neumann, 2016). This lack of hip extensors energy generation (H1) in comparison to the able-bodied group contrasts with the ACLR literature regarding unobstructed walking, which demonstrates adequate and comparable activation of the hip extensors to provide vertical support during walking (DeVita et al., 1998).

During the early stance phase of the supporting leg, there seemed to be altered patterns in knee extensors energy absorption (K1) as obstacle height increased (Figure 33E). This contrasts with the able-bodied participants, who showed no such effect. Furthermore, the injured leg seemed to absorb less energy at the knee than the able-

bodied. Lastly, the non-injured leg appeared to contribute similar energy absorption levels to those of the able-bodied. The quadriceps are active during the early stance of gait to control knee flexion (Neumann, 2016). The present study showed a detectable decrease in the knee extensors energy absorption (K1) for the injured leg, supported by a decline in knee extension moment (Figure 31C). Additionally, as obstacle height increased, there appeared to be less knee flexion during the early stance phase (Figure 30C). These findings suggest that the injured leg adopted a stiffened knee pattern characterized by reduced knee flexion angles, knee extension moments, and, consequently, knee absorption power (Roewer et al., 2011; Rudolph et al., 1998), which may be linked to the development of knee OA (Andriacchi and Dyrby, 2005). This decrease in knee extensor energy absorption (K1) and the reduced hip extensors energy generation (H1) observed in the injured leg may indicate weakness or inefficient activation of the quadriceps and gluteal muscles, potentially leading to decreased control during gait initiation due to insufficient vertical support from the glutes and inadequate control of knee flexion and thigh impact by the quadriceps. Adopting a stiffened knee pattern is also evident in the non-injured leg, though not as pronounced as in the injured leg, likely due to better activation of the glutes and quadriceps under obstacle conditions. This finding is speculative as EMG was not captured in the present study.

In the frontal plane, the supporting leg hip abductor energy absorption (H1F) in the participants post-ACLR appeared to follow a similar trend to that of the able-bodied group (Figure 33C). The decrease in the hip abductors energy absorption (H1F) as a function of obstacle height increase is supported by a study that examined hip contributions in the frontal plane during slope walking, revealing that as the slope

increased, the hip abductors energy absorption (H1F) decreased significantly at 20° (approximately 30 cm of obstacle height) (Yang et al., 2018). This decrease in the hip abductors energy absorption (H1F) may be attributed to the prevention of pelvic drop.

In summary, for the supporting leg adaptations during the early stance, the injured leg of the participants post-ACLR would adopt a decreased hip extensors energy generation (H1) compared to the non-injured leg and the able-bodied participants. However, participants post-ACLR seemed to adopt a stiffened knee pattern that is characterized by decreased knee flexion angles, moments and power absorption.

Section 5.2.2.2 Early mid stance adaptations

The supporting leg hip flexor energy absorption (H2, Figure 33B) in both legs appeared to follow a decreasing trend, similar to the able-bodied group. Additionally, knee extensor energy generation (K2, Figure 33F) showed similar patterns in each leg of the ACLR group compared to the able-bodied group. The observed decrease in the hip flexors energy absorption (H2) and the knee extensor energy generation (K2) suggests that similar to the adaptations discussed in section 5.1.2 for the able-bodied participants, the participants post-ACLR adopted a pattern that would involve reducing the knee extensors energy generation to decelerate the forward progression of the trunk, coupled with the decrease in hip flexors energy absorption (H2) to ensure the trunk stays upright, rather than leaned over during obstructed walking (Zajac et al., 2003).

The supporting leg ankle plantar flexors energy absorption (A1) at the ankle did not seem to change for the able-bodied group, but it appeared to be altered in the participants post-ACLR. It looks like greater absorption occurred at the ankle as the

obstacle height increased, particularly on the injured leg. A stiffened knee pattern that would carry forward from the early stance could result in knee instability, which explains why the plantar flexors tended to increase their absorption to provide knee stability and prevent ATT (Rudolph et al., 1998). However, this could increase the compressive and shear forces at the knee, further leading to degenerative damage to the cartilage over time (Setton et al., 1999; Strickland et al., 1992). Additionally, the ankle plantar flexors energy absorption (A1) is responsible for controlling the speed and rotation of the shank over the foot. Despite the average duration of the crossing leg increasing for obstacle conditions and being within the able-bodied 95% CI of the able-bodied group (Figure 24), another explanation for the increase in the ankle plantar flexors energy absorption (A1) in participants post-ACLR could be due to them approaching the obstacle at a slower speed than the one seen with the able-bodied participants (could be by shortening their stride length) as a safety mechanism.

The emergence of energy generation by the plantar flexors (A1G, Figure 34B) on the supporting leg was also observed in the participants post-ACLR. However, it was significantly present at height 50 cm for the injured leg (minimal for heights 20 to 40 cm), in contrast to height 30 cm for the non-injured leg (minimal at height 20 cm). Furthermore, the ankle plantar flexors energy absorption (A1A, Figure 34C) appeared to increase as obstacle height increased. The ankle plantar flexors energy absorption (A1A) and ankle plantar flexors energy generation (A1G) in the non-injured leg were higher than those in the injured leg and the able-bodied group at heights 20, 30, 40, and 60 cm, while the injured leg was only higher at height 50 cm. This finding indicates that participants post-ACLR relied more on pelvic elevation through positive work at the

ankle joint (through the ankle plantar flexors energy generation (A1G) on the supporting leg) for obstructed walking adaptations compared to able-bodied participants.

Additionally, energy generation by the hip abductors (H2F) on the supporting leg was higher in the non-injured leg compared to both the able-bodied and injured legs. The latter two showed comparable values under obstacle conditions that required sufficient pelvic elevation to allow the crossing leg to safely clear the obstacle. Additionally, the knee extensors energy absorption (K3) of the injured leg appeared significantly lower when compared to the able-bodied and non-injured legs. This decrease in the knee extensors energy absorption (K3) in the injured leg, along with the increase in the hip abductors energy generation (H2F) in the non-injured leg, may indicate a mechanism of providing adequate pelvic elevation through increased activation of the hip abductors in the non-injured leg due to weakness or inefficient activation of the quadriceps in the injured leg.

In summary, for the supporting leg during early mid stance, the participants post-ACLR would have a similar adaptation to the able-bodied participants by decreasing the knee flexor energy generation (K2) to decelerate forward trunk acceleration, coupled with a decrease in hip flexor energy absorption (H2) to keep the trunk upright. Moreover, the ankle plantar flexor energy absorption (A1) seemed to be higher in the participants post-ACLR, which could be a mechanism to counteract knee instability by the stiffened knee pattern adopted during early stance. Additionally, the emergence of the ankle plantar flexor energy generation (A1G) and its visible increase compared to the able-bodied participants was a needed mechanism adopted by the participants post-ACLR to provide positive work through the ankle to lift the CoM.

Section 5.3 Limitations and future directions

The primary limitation of this study is that the behaviour of participants post-ACLR cannot be generalized due to an insufficient number of participants, resulting in underpowering that part of the study. In this study, two participants post-ACLR were recruited, in comparison to the eight participants in the Devita et al (1998) study that compared the behaviour of participants post-ACLR at three weeks and six months post-ACLR to a control group of able-bodied participants.

Furthermore, examining sex differences could have yielded valuable insights regarding existing alterations. This information could be significant in the ACLR field because females are more susceptible to ACLR injuries than males due to anatomical, neuromuscular and hormonal factors. (Gould et al., 2016; Hewett et al., 1999, 2006; Marieswaran et al., 2018; Skouras et al., 2022; Slauterbeck et al., 2002; Wojtys et al., 2002).

Section 6: Conclusion

The study explored several novel aspects of walking control in able-bodied and participants post-ACLR. It is the first study to conduct kinematic and kinetic analysis on the supporting leg of able-bodied participants during unilateral obstructed walking for obstacle heights as high as 60 cm and the first to analyze kinematics and kinetics in participants post-ACLR during unilateral obstructed walking.

The participants post-ACLR exhibited altered movement patterns during unobstructed walking. Adaptations in the supporting leg were primarily observed at the hip and knee joints, specifically through reduced hip extensors energy generation (H1), altered hip abductors energy absorption (H1F), and increased knee extensors energy absorption (K1).

During unilateral obstructed walking, for the crossing leg ALAs, the participants post-ACLR displayed a re-organization of lower limb kinetics by the emergence of the knee flexors energy generation (K5) coupled with a decrease in the hip flexors energy generation (H3) and the knee extensors energy absorption (K3). However, it is suggested that co-contraction of the hamstring and quadriceps muscle groups may be a protective mechanism that occurred during unilateral obstructed walking (evident with the decreased knee extensors energy absorption (K3) and increased knee flexors energy generation (K5)) to increase joint stiffness. Moreover, the hip abductors' energy generation (H3F) during the late stance was increased for higher obstacle heights, corroborated with the hip abduction provided by the H4F muscle power burst.

During the early stance of going over unilateral obstacles, the supporting leg of the participants post-ACLR adopted a stiffened knee pattern during unilateral obstructed walking. This was characterized by decreased knee flexion angles, moments and power absorption. Moreover, the ankle plantar flexor energy absorption (A1) seemed to increase as a function of obstacle height, which can be suggested to counteract the stiffened knee pattern. Moreover, the emergence of the ankle plantar flexor energy generation (A1G) was a crucial mechanism to provide positive work to lift the CoM. Lastly, consistent with the able-bodied participants, participants post-ACLR decreased their knee extensor energy generation (K2) to decelerate forward trunk acceleration, as well as decreased hip flexor energy absorption (H2) to provide upright posture.

References

- Amis, A. A., Bull, A. M., and Lie, D. T. (2005). Biomechanics of rotational instability and anatomic anterior cruciate ligament reconstruction. *Operative Techniques in Orthopaedics*, 15(1), 29–35. <https://doi.org/10.1053/j.oto.2004.10.009>
- Andriacchi, T. P., and Birac, D. (1993). Functional testing in the anterior cruciate ligament-deficient knee. *Clinical Orthopaedics and Related Research*, 288(288), 40–47. <https://doi.org/10.1097/00003086-199303000-00006>
- Andriacchi, T. P., and Dyrby, C. O. (2005). Interactions between kinematics and loading during walking for the normal and ACL deficient knee. *Journal of Biomechanics*, 38(2), 293–298. <https://doi.org/10.1016/j.jbiomech.2004.02.010>
- Arhos, E. K., Capin, J. J., Buchanan, T. S., and Snyder-Mackler, L. (2021). Quadriceps strength symmetry does not modify gait mechanics after anterior cruciate ligament reconstruction, rehabilitation, and return-to-sport training. *The American Journal of Sports Medicine*, 49(2), 417–425. <https://doi.org/10.1177/0363546520980079>
- Arundale, A. J., Capin, J. J., Zarzycki, R., Smith, A., and Snyder-Mackler, L. (2018). Functional and patient-reported outcomes improve over the course of rehabilitation: A secondary analysis of the ACL-SPORTS trial. *Sports Health*, 10(5), 441–452. <https://doi.org/10.1177/1941738118779023>
- Barber-Westin, S., and Noyes, F. R. (2020). One in 5 athletes sustain reinjury upon return to high-risk sports after ACL reconstruction: A systematic review in 1239 athletes younger than 20 years. *Sports Health*, 12(6), 587–597. <https://doi.org/10.1177/1941738120912846>
- Baumeister, J., Reinecke, K., and Weiss, M. (2008). Changed cortical activity after anterior cruciate ligament reconstruction in a joint position paradigm: An EEG study. *Scandinavian Journal of Medicine and Science in Sports*, 18(4), 473–484. <https://doi.org/10.1111/j.1600-0838.2007.00702.x>
- Bicer, E. K., Lustig, S., Servien, E., Selmi, T. A. S., and Neyret, P. (2010). Current knowledge in the anatomy of the human anterior cruciate ligament. *Knee Surgery, Sports Traumatology, Arthroscopy*, 18(8), 1075–1084. <https://doi.org/10.1007/s00167-009-0993-8>
- Boden, B. P., Dean, G. S., Feagin, J. A., and Garrett, W. E. (2000). Mechanisms of anterior cruciate ligament injury. *Orthopedics*, 23(6), 573–578.
- Bohn, M. B., Petersen, A. K., Nielsen, D. B., Sørensen, H., and Lind, M. (2016). Three-dimensional kinematic and kinetic analysis of knee rotational stability in ACL-deficient patients during walking, running and pivoting. *Journal of Experimental Orthopaedics*, 3(1), 27. <https://doi.org/10.1186/s40634-016-0062-4>

- Brophy, R. H., Schmitz, L., Wright, R. W., Dunn, W. R., Parker, R. D., Andrich, J. T., McCarty, E. C., and Spindler, K. P. (2012). Return to play and future ACL injury risk after ACL reconstruction in soccer athletes from the multicenter orthopaedic outcomes network (MOON) group. *The American Journal of Sports Medicine*, 40(11), 2517–2522. <https://doi.org/10.1177/0363546512459476>
- Butler, D. L., Noyes, F. R., and Grood, E. S. (1980). Ligamentous restraints to anterior-posterior drawer in the human knee. A biomechanical study. *The Journal of Bone and Joint Surgery. American Volume*, 62(2), 259–270.
- Butler, R. J., Marchesi, S., Royer, T., and Davis, I. S. (2007). The effect of a subject-specific amount of lateral wedge on knee mechanics in patients with medial knee osteoarthritis. *Journal of Orthopaedic Research*, 25(9), 1121–1127. <https://doi.org/10.1002/jor.20423>
- Butler, R. J., Minick, K. I., Ferber, R., and Underwood, F. (2009). Gait mechanics after ACL reconstruction: Implications for the early onset of knee osteoarthritis. *British Journal of Sports Medicine*, 43(5), 366–370. <https://doi.org/10.1136/bjism.2008.052522>
- Byrne, J. M., and Prentice, S. D. (2003). Swing phase kinetics and kinematics of knee replacement patients during obstacle avoidance. *Gait and Posture*, 18(1), 95–104. [https://doi.org/10.1016/s0966-6362\(02\)00164-9](https://doi.org/10.1016/s0966-6362(02)00164-9)
- Capin, J. J., Khandha, A., Zarzycki, R., Arundale, A. J. H., Ziegler, M. L., Manal, K., Buchanan, T. S., and Snyder-Mackler, L. (2018). Gait mechanics and tibiofemoral loading in men of the ACL-SPORTS randomized control trial. *Journal of Orthopaedic Research*, 36(9), 2364–2372. <https://doi.org/10.1002/jor.23895>
- Ciccotti, M. G., Kerlan, R. K., Perry, J., and Pink, M. (1994). An electromyographic analysis of the knee during functional activities: II. The anterior cruciate ligament-deficient and -reconstructed profiles. *The American Journal of Sports Medicine*, 22(5), 651–658. <https://doi.org/10.1177/036354659402200513>
- Claiborne, T. L., Armstrong, C. W., Gandhi, V., and Pincivero, D. M. (2006). Relationship between hip and knee strength and knee valgus during a single leg squat. *Journal of Applied Biomechanics*, 22(1), 41–50. <https://doi.org/10.1123/jab.22.1.41>
- Courtney, C. A., Durr, R. K., Emerson-Kavchak, A. J., Witte, E. O., and Santos, M. J. (2011). Heightened flexor withdrawal responses following ACL rupture are enhanced by passive tibial translation. *Clinical Neurophysiology*, 122(5), 1005–1010. <https://doi.org/10.1016/j.clinph.2010.07.029>

- Culvenor, A. G., Alexander, B. C., Clark, R. A., Collins, N. J., Ageberg, E., Morris, H. G., Whitehead, T. S., and Crossley, K. M. (2016). Dynamic single-leg postural control is impaired bilaterally following anterior cruciate ligament reconstruction: Implications for reinjury risk. *The Journal of Orthopaedic and Sports Physical Therapy*, 46(5), 357–364. <https://doi.org/10.2519/jospt.2016.6305>
- Daniel, D. M., Stone, M. L., Dobson, B. E., Fithian, D. C., Rossman, D. J., and Kaufman, K. R. (1994). Fate of the ACL-injured patient: A prospective outcome study. *American Journal of Sports Medicine*, 22(5), 632–644. <https://doi.org/10.1177/036354659402200511>
- Dashti Rostami, K., Naderi, A., and Thomas, A. (2019). Hip abductor and adductor muscles activity patterns during landing after anterior cruciate ligament injury. *Journal of Sport Rehabilitation*, 28(8), 871–876. <https://doi.org/10.1123/jsr.2018-0189>
- Dault, M. C., Frank, J. S., and Allard, F. (2001). Influence of a visuo-spatial, verbal and central executive working memory task on postural control. *Gait and Posture*, 14(2), 110–116. [https://doi.org/10.1016/s0966-6362\(01\)00113-8](https://doi.org/10.1016/s0966-6362(01)00113-8)
- Davis, H. C., Luc-Harkey, B. A., Seeley, M. K., Troy Blackburn, J., and Pietrosimone, B. (2019). Sagittal plane walking biomechanics in individuals with knee osteoarthritis after quadriceps strengthening. *Osteoarthritis and Cartilage*, 27(5), 771–780. <https://doi.org/10.1016/j.joca.2018.12.026>
- Davis, I. S., Tenforde, A. S., Neal, B. S., Roper, J. L., and Willy, R. W. (2020). Gait retraining as an intervention for patellofemoral pain. *Current Reviews in Musculoskeletal Medicine*, 13(1), 103–114. <https://doi.org/10.1007/s12178-020-09605-3>
- Davis-Wilson, H. C., Pfeiffer, S. J., Johnston, C. D., Seeley, M. K., Harkey, M. S., Blackburn, J. T., Fockler, R. P., Spang, J. T., and Pietrosimone, B. (2020). Bilateral gait 6 and 12 months post–anterior cruciate ligament reconstruction compared with controls. *Medicine and Science in Sports and Exercise*, 52(4), 785–794. <https://doi.org/10.1249/MSS.0000000000002208>
- DeVita, P., Aaboe, J., Bartholdy, C., Leonardis, J. M., Bliddal, H., and Henriksen, M. (2018). Quadriceps-strengthening exercise and quadriceps and knee biomechanics during walking in knee osteoarthritis: A two-centre randomized controlled trial. *Clinical Biomechanics*, 59, 199–206. <https://doi.org/10.1016/j.clinbiomech.2018.09.016>
- DeVita, P., Hortobagyi, T., and Barrier, J. (1998). Gait biomechanics are not normal after anterior cruciate ligament reconstruction and accelerated rehabilitation. *Medicine and Science in Sports and Exercise*, 30(10), 1481–1488. <https://doi.org/10.1097/00005768-199810000-00003>

- DeVita, P., Hortobagyi, T., Barrier, J., Torry, M., Glover, K. L., Speroni, D. L., Money, J., and Mahar, M. T. (1997). Gait adaptations before and after anterior cruciate ligament reconstruction surgery. *Medicine and Science in Sports and Exercise*, 29(7), 853–859. <https://doi.org/10.1097/00005768-199707000-00003>
- Di Stasi, S., Hartigan, E. H., and Snyder-Mackler, L. (2015). Sex-specific gait adaptations prior to and up to 6 months after anterior cruciate ligament reconstruction. *The Journal of Orthopaedic and Sports Physical Therapy*, 45(3), 207–214. <https://doi.org/10.2519/jospt.2015.5062>
- Eng, J. J., and Winter, D. A. (1995). Kinetic analysis of the lower limbs during walking: What information can be gained from a three-dimensional model? *Journal of Biomechanics*, 28(6), 753–758.
- Fleming, B. C., Renstrom, P. A., Ohlen, G., Johnson, R. J., Peura, G. D., Beynon, B. D., and Badger, G. J. (2001). The gastrocnemius muscle is an antagonist of the anterior cruciate ligament. *Journal of Orthopaedic Research*, 19(6), 1178–1184. [https://doi.org/10.1016/S0736-0266\(01\)00057-2](https://doi.org/10.1016/S0736-0266(01)00057-2)
- Gilchrist, J., Mandelbaum, B. R., Melancon, H., Ryan, G. W., Silvers, H. J., Griffin, L. Y., Watanabe, D. S., Dick, R. W., and Dvorak, J. (2008). A randomized controlled trial to prevent noncontact anterior cruciate ligament injury in female collegiate soccer players. *The American Journal of Sports Medicine*, 36(8), 1476–1483. <https://doi.org/10.1177/0363546508318188>
- Gokeler, A., Neuhaus, D., Benjaminse, A., Grooms, D. R., and Baumeister, J. (2019). Principles of motor learning to support neuroplasticity after ACL injury: Implications for optimizing performance and reducing risk of second ACL injury. *Sports Medicine (Auckland, N.Z.)*, 49(6), 853–865. <https://doi.org/10.1007/s40279-019-01058-0>
- Gould, S., Hooper, J., and Strauss, E. (2016). Anterior cruciate ligament injuries in females: Risk factors, prevention, and outcomes. *Bulletin of the NYU Hospital for Joint Diseases*, 74(1), 46–51.
- Harrington, I. J. (1976). A bioengineering analysis of force actions at the knee in normal and pathological gait. *Biomedical Engineering*, 11(5), 167–172.
- Haus, J., and Halata, Z. (1990). Innervation of the anterior cruciate ligament. *International Orthopaedics*, 14(3), 293–296. <https://doi.org/10.1007/BF00178762>
- Herrington, L., Alarifi, S., and Jones, R. (2017). Patellofemoral joint loads during running at the time of return to sport in elite athletes with ACL reconstruction. *The American Journal of Sports Medicine*, 45(12), 2812–2816. <https://doi.org/10.1177/0363546517716632>

- Hewett, T. E., Lindenfeld, T. N., Riccobene, J. V., and Noyes, F. R. (1999). The effect of neuromuscular training on the incidence of knee injury in female athletes. A prospective study. *The American Journal of Sports Medicine*, 27(6), 699–706. <https://doi.org/10.1177/03635465990270060301>
- Hewett, T. E., Myer, G. D., and Ford, K. R. (2006). Anterior cruciate ligament injuries in female athletes: Part 1, mechanisms and risk factors. *The American Journal of Sports Medicine*, 34(2), 299–311. <https://doi.org/10.1177/0363546505284183>
- Hewett, T. E., Myer, G. D., Ford, K. R., Heidt, R. S., Colosimo, A. J., McLean, S. G., van den Bogert, A. J., Paterno, M. V., and Succop, P. (2005). Biomechanical measures of neuromuscular control and valgus loading of the knee predict anterior cruciate ligament injury risk in female athletes: a prospective study. *The American Journal of Sports Medicine*, 33(4), Article 4. <https://doi.org/10.1177/0363546504269591>
- Holm, I., Oiestad, B. E., Risberg, M. A., Gunderson, R., and Aune, A. K. (2012). No differences in prevalence of osteoarthritis or function after open versus endoscopic technique for anterior cruciate ligament reconstruction: 12-year follow-up report of a randomized controlled trial. *The American Journal of Sports Medicine*, 40(11), 2492–2498. <https://doi.org/10.1177/0363546512458766>
- Hooper, D. M., Morrissey, M. C., Drechsler, W. I., Clark, N. C., Coutts, F. J., and McAuliffe, T. B. (2002). Gait analysis 6 and 12 months after anterior cruciate ligament reconstruction surgery. *Clinical Orthopaedics and Related Research*, 403, 168–178. <https://doi.org/10.1097/00003086-200210000-00025>
- Kapreli, E., Athanasopoulos, S., Gliatis, J., Papathanasiou, M., Peeters, R., Strimpakos, N., Van Hecke, P., Gouliamos, A., and Sunaert, S. (2009). Anterior cruciate ligament deficiency causes brain plasticity: A functional MRI study. *The American Journal of Sports Medicine*, 37(12), 2419–2426. <https://doi.org/10.1177/0363546509343201>
- Kaufman, K. R., Hughes, C., Morrey, B. F., Morrey, M., and An, K.N. (2001). Gait characteristics of patients with knee osteoarthritis. *Journal of Biomechanics*, 34(7), 907–915. [https://doi.org/10.1016/S0021-9290\(01\)00036-7](https://doi.org/10.1016/S0021-9290(01)00036-7)
- Kennedy, J. C., Alexander, I. J., and Hayes, K. C. (1982). Nerve supply of the human knee and its functional importance. *The American Journal of Sports Medicine*, 10(6), 329–335. <https://doi.org/10.1177/036354658201000601>
- Kielė, D., Masiulis, N., Aleknavičiūtė, V., Solianik, R., Dargevičiūtė, G., and Skurvydas, A. (2020). Balance alterations before ACL surgery and after rehabilitation. *Reabilitacijos Mokslai : Slauga, Kineziterapija, Ergoterapija*, 2(5). <https://doi.org/10.33607/rmske.v2i5.868>

- Komdeur, P., Pollo, F. E., and Jackson, R. W. (2002). Dynamic knee motion in anterior cruciate impairment: A report and case study. *Proceedings - Baylor University Medical Center*, 15(3), 257–259.
<https://doi.org/10.1080/08998280.2002.11927850>
- Konishi, Y., Fukubayashi, T., and Takeshita, D. (2002). Possible mechanism of quadriceps femoris weakness in patients with ruptured anterior cruciate ligament. *Medicine and Science in Sports and Exercise*, 34(9), 1414–1418.
<https://doi.org/10.1097/00005768-200209000-00003>
- Kowalk, D. L., Duncan, J. A., McCue, F. C., and Vaughan, C. L. (1997). Anterior cruciate ligament reconstruction and joint dynamics during stair climbing. *Medicine and Science in Sports and Exercise*, 29(11), 1406–1413.
<https://doi.org/10.1097/00005768-199711000-00003>
- Lawrence, R. K., Kernozek, T. W., Miller, E. J., Torry, M. R., and Reuteman, P. (2008). Influences of hip external rotation strength on knee mechanics during single-leg drop landings in females. *Clinical Biomechanics (Bristol, Avon)*, 23(6), 806–813.
<https://doi.org/10.1016/j.clinbiomech.2008.02.009>
- Lee, S.P., and Powers, C. M. (2014). Individuals with diminished hip abductor muscle strength exhibit altered ankle biomechanics and neuromuscular activation during unipedal balance tasks. *Gait and Posture*, 39(3), 933–938.
<https://doi.org/10.1016/j.gaitpost.2013.12.004>
- Lewek, M., Rudolph, K., Axe, M., and Snyder-Mackler, L. (2002). The effect of insufficient quadriceps strength on gait after anterior cruciate ligament reconstruction. *Clinical Biomechanics*, 17(1), 56–63.
[https://doi.org/10.1016/S0268-0033\(01\)00097-3](https://doi.org/10.1016/S0268-0033(01)00097-3)
- Lisee, C., Davis-Wilson, H. C., Evans-Pickett, A., Horton, W. Z., Blackburn, J. T., Franz, J. R., Thoma, L. M., Spang, J. T., and Pietrosimone, B. G. (2022). Linking gait biomechanics and daily steps after ACL reconstruction. *Medicine and Science in Sports and Exercise*, 54(5), 709–716.
<https://doi.org/10.1249/MSS.0000000000002860>
- Mall, N. A., Lee, A. S., Cole, B. J., and Verma, N. N. (2013). The functional and surgical anatomy of the anterior cruciate ligament. *Operative Techniques in Sports Medicine*, 21(1), 2–9. <https://doi.org/10.1053/j.otsm.2012.10.007>
- Marieswaran, M., Jain, I., Garg, B., Sharma, V., and Kalyanasundaram, D. (2018). A review on biomechanics of anterior cruciate ligament and materials for reconstruction. *Applied Bionics and Biomechanics*, 2018, 4657824.
<https://doi.org/10.1155/2018/4657824>

- Markolf, K. L., Burchfield, D. M., Shapiro, M. M., Shepard, M. F., Finerman, G. A., and Slauterbeck, J. L. (1995). Combined knee loading states that generate high anterior cruciate ligament forces. *Journal of Orthopaedic Research*, *13*(6), 930–935. <https://doi.org/10.1002/jor.1100130618>
- McFadyen, B. J., and Carnahan, H. (1997). Anticipatory locomotor adjustments for accommodating versus avoiding level changes in humans. *Experimental Brain Research*, *114*(3), 500–506. <https://doi.org/10.1007/pl00005659>
- Morrison, J. B. (1970). The mechanics of the knee joint in relation to normal walking. *Journal of Biomechanics*, *3*(1), 51–61. [https://doi.org/10.1016/0021-9290\(70\)90050-3](https://doi.org/10.1016/0021-9290(70)90050-3)
- Neto, T., Sayer, T., Theisen, D., and Mierau, A. (2019). Functional brain plasticity associated with ACL injury: A scoping review of current evidence. *Neural Plasticity*, *2019*, 3480512. <https://doi.org/10.1155/2019/3480512>
- Neumann, D. A. (2016). *Kinesiology of the musculoskeletal system*. Elsevier Health Sciences.
- Parus, K., Lisiński, P., and Huber, J. (2015). Body balance control deficiencies following ACL reconstruction combined with medial meniscus suture. A preliminary report. *Orthopaedics and Traumatology: Surgery and Research*, *101*(7), 807–810. <https://doi.org/10.1016/j.otsr.2015.07.015>
- Paterno, M. V. (2015). Incidence and predictors of second anterior cruciate ligament injury after primary reconstruction and return to sport. *Journal of Athletic Training*, *50*(10), 1097–1099. <https://doi.org/10.4085/1062-6050-50.10.07>
- Paterno, M. V., Rauh, M. J., Schmitt, L. C., Ford, K. R., and Hewett, T. E. (2012). Incidence of contralateral and ipsilateral anterior cruciate ligament (ACL) injury after primary ACL reconstruction and return to sport. *Clinical Journal of Sport Medicine*, *22*(2), 116–121. <https://doi.org/10.1097/JSM.0b013e318246ef9e>
- Patla, A., and Rietdyk, S. (1993). Visual control of limb trajectory over obstacles during locomotion: Effect of obstacle height and width. *Gait and Posture*, *1*(1), 45–60. [https://doi.org/10.1016/0966-6362\(93\)90042-Y](https://doi.org/10.1016/0966-6362(93)90042-Y)
- Pegoretti, K. S., Moraes, R., Masullo, C. L., Chagas-Neto, F. A., Miranda, A., Kfuri, M., and Bevilaqua-Grossi, D. (2015). Additional sensory input improves the strategy of stepping over obstacle in individuals with knee osteoarthritis. *Journal of Back and Musculoskeletal Rehabilitation*, *28*(4), 689–697. <https://doi.org/10.3233/BMR-140570>

- Pfeiffer, S. J., Spang, J., Nissman, D., Lalush, D., Wallace, K., Harkey, M. S., Pietrosimone, L. S., Schmitz, R., Schwartz, T., Blackburn, T., and Pietrosimone, B. (2019). Gait mechanics and T1 ρ MRI of tibiofemoral cartilage 6 months after ACL reconstruction. *Medicine and Science in Sports and Exercise*, 51(4), 630–639. <https://doi.org/10.1249/MSS.0000000000001834>
- Pietrosimone, B., Loeser, R. F., Blackburn, J. T., Padua, D. A., Harkey, M. S., Stanley, L. E., Luc-Harkey, B. A., Ulici, V., Marshall, S. W., Jordan, J. M., and Spang, J. T. (2017). Biochemical markers of cartilage metabolism are associated with walking biomechanics 6-months following anterior cruciate ligament reconstruction. *Journal of Orthopaedic Research*, 35(10), 2288–2297. <https://doi.org/10.1002/jor.23534>
- Pollard, C. D., Sigward, S. M., and Powers, C. M. (2017). ACL injury prevention training results in modification of hip and knee mechanics during a drop-landing task. *Orthopaedic Journal of Sports Medicine*, 5(9), Article 9. <https://doi.org/10.1177/2325967117726267>
- Pratt, D. J. (1994). Some aspects of modern orthotics. *Physiological Measurement*, 15(1), 1–27. <https://doi.org/10.1088/0967-3334/15/1/001>
- Roewer, B. D., Di Stasi, S. L., and Snyder-Mackler, L. (2011). Quadriceps strength and weight acceptance strategies continue to improve two years after anterior cruciate ligament reconstruction. *Journal of Biomechanics*, 44(10), 1948–1953. <https://doi.org/10.1016/j.jbiomech.2011.04.037>
- Rudolph, K. S., Axe, M. J., Buchanan, T. S., Scholz, J. P., and Snyder-Mackler, L. (2001). Dynamic stability in the anterior cruciate ligament deficient knee. *Knee Surgery, Sports Traumatology, Arthroscopy*, 9(2), 62–71. <https://doi.org/10.1007/s001670000166>
- Rudolph, K. S., Eastlack, M. E., Axe, M. J., and Snyder-Mackler, L. (1998). 1998 Basmajian student award paper. *Journal of Electromyography and Kinesiology*, 8(6), 349–362. [https://doi.org/10.1016/S1050-6411\(97\)00042-4](https://doi.org/10.1016/S1050-6411(97)00042-4)
- Sadeghi, H., Allard, P., Prince, F., and Labelle, H. (2000). Symmetry and limb dominance in able-bodied gait: A review. *Gait and Posture*, 12(1), 34–45. [https://doi.org/10.1016/S0966-6362\(00\)00070-9](https://doi.org/10.1016/S0966-6362(00)00070-9)
- Salmon, L., Russell, V., Musgrove, T., Pinczewski, L., and Refshauge, K. (2005). Incidence and risk factors for graft rupture and contralateral rupture after anterior cruciate ligament reconstruction. *Arthroscopy: The Journal of Arthroscopic and Related Surgery*, 21(8), 948–957. <https://doi.org/10.1016/j.arthro.2005.04.110>
- Schutte, M. J., Dabezies, E. J., Zimny, M. L., and Happel, L. T. (1987). Neural anatomy of the human anterior cruciate ligament. *The Journal of Bone and Joint Surgery. American Volume*, 69(2), 243–247.

- Setton, L. A., Elliott, D. M., and Mow, V. C. (1999). Altered mechanics of cartilage with osteoarthritis: Human osteoarthritis and an experimental model of joint degeneration. *Osteoarthritis and Cartilage*, 7(1), 2–14. <https://doi.org/10.1053/joca.1998.0170>
- Shelburne, K. B., Pandy, M. G., Anderson, F. C., and Torry, M. R. (2004). Pattern of anterior cruciate ligament force in normal walking. *Journal of Biomechanics*, 37(6), 797–805. <https://doi.org/10.1016/j.jbiomech.2003.10.010>
- Simon, D., Mascarenhas, R., Saltzman, B. M., Rollins, M., Bach, B. R., and MacDonald, P. (2015). The relationship between anterior cruciate ligament injury and osteoarthritis of the knee. *Advances in Orthopedics*, 2015, 928301. <https://doi.org/10.1155/2015/928301>
- Skouras, A. Z., Kanellopoulos, A. K., Stasi, S., Triantafyllou, A., Koulouvaris, P., Papagiannis, G., and Papathanasiou, G. (2022). Clinical significance of the static and dynamic Q-angle. *Cureus*, 14(5), e24911. <https://doi.org/10.7759/cureus.24911>
- Slater, L. V., Hart, J. M., Kelly, A. R., and Kuenze, C. M. (2017). Progressive changes in walking kinematics and kinetics after anterior cruciate ligament injury and reconstruction: A review and meta-analysis. *Journal of Athletic Training*, 52(9), 847–860. <https://doi.org/10.4085/1062-6050-52.6.06>
- Slauterbeck, J. R., Fuzie, S. F., Smith, M. P., Clark, R. J., Xu, K. T., Starch, D. W., and Hardy, D. M. (2002). The menstrual cycle, sex hormones, and anterior cruciate ligament injury. *Journal of Athletic Training*, 37(3), 275–278.
- Snyder-Mackler, L., Ladin, Z., Schepsis, A. A., and Young, J. C. (1991). Electrical stimulation of the thigh muscles after reconstruction of the anterior cruciate ligament. Effects of electrically elicited contraction of the quadriceps femoris and hamstring muscles on gait and on strength of the thigh muscles. *The Journal of Bone and Joint Surgery. American Volume*, 73(7), 1025–1036.
- Solomonow, M., Baratta, R., Zhou, B. H., Shoji, H., Bose, W., Beck, C., and D'Ambrosia, R. (1987). The synergistic action of the anterior cruciate ligament and thigh muscles in maintaining joint stability. *The American Journal of Sports Medicine*, 15(3), 207–213. <https://doi.org/10.1177/036354658701500302>
- Strickland, E. M., Fares, M., Krebs, D. E., Riley, P. O., Givens-Heiss, D. L., Hodge, W. A., and Mann, R. W. (1992). In vivo acetabular contact pressures during rehabilitation, Part I: Acute phase. *Physical Therapy*, 72(10), 691–699. <https://doi.org/10.1093/ptj/72.10.691>

- Swanik, C. B., Covassin, T., Stearne, D. J., and Schatz, P. (2007). The relationship between neurocognitive function and noncontact anterior cruciate ligament injuries. *The American Journal of Sports Medicine*, 35(6), 943–948. <https://doi.org/10.1177/0363546507299532>
- Timoney, J. M., Inman, W. S., Quesada, P. M., Sharkey, P. F., Barrack, R. L., Skinner, H. B., and Alexander, A. H. (1993). Return of normal gait patterns after anterior cruciate ligament reconstruction. *The American Journal of Sports Medicine*, 21(6), 887–889. <https://doi.org/10.1177/036354659302100623>
- Tinetti, M. E. (2003). Preventing falls in elderly persons. *The New England Journal of Medicine*, 348(1), 42–49.
- Uchio, Y. (2016). Mechanoreceptors in the ACL. In M. Ochi, K. Shino, K. Yasuda, and M. Kurosaka (Eds.), *ACL Injury and Its Treatment* (pp. 51–65). Springer Japan. https://doi.org/10.1007/978-4-431-55858-3_5
- Wang, T.M., Yen, H.C., Lu, T.W., Chen, H.L., Chang, C.F., Liu, Y.H., and Tsai, W.C. (2009). Bilateral knee osteoarthritis does not affect inter-joint coordination in older adults with gait deviations during obstacle-crossing. *Journal of Biomechanics*, 42(14), 2349–2356. <https://doi.org/10.1016/j.jbiomech.2009.06.029>
- Winter, D. A., Patla, A. E., and Frank, J. S. (1990). Assessment of balance control in humans. *Medical Progress Through Technology*, 16(1–2), 31–51.
- Wojtys, E. M., Huston, L. J., Boynton, M. D., Spindler, K. P., and Lindenfeld, T. N. (2002). The effect of the menstrual cycle on anterior cruciate ligament injuries in women as determined by hormone levels. *The American Journal of Sports Medicine*, 30(2), 182–188. <https://doi.org/10.1177/03635465020300020601>
- Yang, Z., Qu, F., Cui, C., and Rietdyk, S. (2018). The Contribution of Frontal Hip Power to Slope Walking. <https://www.semanticscholar.org/paper/The-Contribution-of-Frontal-Hip-Power-to-Slope-Yang-Qu/df6f5bd9863b8858f0289cd8a01ec7e7dfc9e228>
- Zajac, F. E., Neptune, R. R., and Kautz, S. A. (2003). Biomechanics and muscle coordination of human walking: Part II: Lessons from dynamical simulations and clinical implications. *Gait and Posture*, 17(1), 1–17. [https://doi.org/10.1016/S0966-6362\(02\)00069-3](https://doi.org/10.1016/S0966-6362(02)00069-3)
- Zantop, T., Petersen, W., and Fu, F. H. (2005). Anatomy of the anterior cruciate ligament. *Operative Techniques in Orthopaedics*, 15(1), 20–28. <https://doi.org/10.1053/j.oto.2004.11.011>